The applications of fluidized bed drying to pulse proteins: experiments, mathematical modelling, and techno economic analysis

A thesis submitted in fulfilment of the requirements for the degree of Doctor of Philosophy

By

Shu Cheng

Supervisor: Professor Timothy Langrish

March 2025

School of Chemical and Biomolecular Engineering

The University of Sydney

Statement of originality

This is to certify that, to the best of my knowledge, the content of this thesis is my own work. This thesis has not been submitted for any degree or other purpose.

I certify that the intellectual content of this thesis is the product of my own work and that all the assistance received in preparing this thesis and sources has been acknowledged.

During the preparation of this thesis, ChatGPT was used for the purposes of text enhancement, including grammar checking and sentence structure. Where any text was modified by generative AI, the author then reviewed the resulting content for any errors, inaccuracies or biases, and modified it as required. The author takes full responsibility for the submitted thesis and ensures the work is their own and has used generative AI within the parameters of use, see University of Sydney generative AI guide for researchers.

Acknowledgment

I would like to express my deepest gratitude to my supervisor, Professor Timothy Langrish, for his invaluable guidance, unwavering support, and profound expertise throughout my whole Master's and PhD journey. Over the past five years, his mentorship has been instrumental in shaping my academic and research endeavors. It has been a privilege to work under his supervision.

I extend my sincere appreciation to my research groupmates, Daisy (Yongmei) Sun and Jingying Cheng, Jacky Zhou, Chao Zhong and Zexin Lei for their camaraderie and encouragement. Their support has not only enriched my academic experience but also made daily interactions more enjoyable.

This research was financially supported by a Postgraduate Research Scholarship in *Transitioning Australian Pulses into Protein-based Food Industries* under the Global Innovation Linkages (GIL) program. I sincerely appreciate the support provided by Professor Brent Kaiser, Dr. Daniel Skylas, Chris Whiteway, Dr. Valeria Messina and Dr. Peter Valtchev, as well as all those involved in the GIL program. Their contributions have significantly enhanced the scope and impact of my research.

I am profoundly grateful to my parents, Jinxia Wu and Bin Cheng, for their unwavering love and support, which have been the foundation of my academic pursuits. Additionally, the emotional support from Coconut and Chickpea has been a source of strength and motivation throughout this journey. I would also like to express my gratitude to Dr. Lizhuo Wang for his valuable assistance and companionship, which have made this experience more fulfilling.

I am deeply thankful to everyone who has contributed to this journey in various ways.

During the preparation of this thesis, ChatGPT was used for the purposes of text enhancement, including grammar checking and sentence structure. Where any text was modified by generative AI, the author then reviewed the resulting content for any errors, inaccuracies or biases, and modified it as required. The author takes full responsibility for the submitted thesis and ensures the work is their own and has used generative AI within the parameters of use, see University of Sydney generative AI guide for researchers.

Abstract

This thesis investigates the application of fluidized bed drying (FBD) to the processing of pulses, specifically chickpeas and dehulled faba beans, with a focus on reducing anti-nutritional factors (ANFs) and improving nutritional quality. The research is divided into eight chapters. It begins with an introduction and literature review to establish the research context and identify gaps in the current knowledge. Detailed materials and methods are provided to outline the experimental framework.

This study addresses the challenge of preserving protein structure and removing antinutritional factors during the fluidized bed drying of chickpeas. By using a drying schedule, the denaturation of the pulse protein secondary structure was reduced. 86% of the trypsin inhibitor was also removed at the target moisture content. The drying s chedule used an initial inlet air temperature of 80°C, and after 30minutes the temperature was reduced to 60 °C.

Technico-economic analysis for the costs of dryng chickpeas has been studied in this thesis. The processing cost per unit mass of chickpeas is predicted to decrease with increasing recycle ratio, from over A$1.32/kg of chickpeas with no recycle down to A$0.0885/kg of chickpeas at a ratio of 99%. With no air recycle, the lowest inlet air temperature (40^{o}C) gives the lowest cost, but near the optimum recycle ratio, the highest inlet air temperature (80^{o}C) is best. This pattern is followed when considering equivalent carbon dioxide emissions, with the lowest emissions (over 0.259 kg CO_2 (kg chickpeas)$^{-1}$) corresponding to high recycle ratios and high inlet air temperatures. The use of air recycle should cause no significant challenges when implementing a drying schedule for trypsin-inhibitor reduction in chickpeas.

In parallel, the processing of dehulled faba beans has been examined, with an emphasis on phytic acid reduction through a combination of soaking, microwaving, and FBD techniques. Phytic acid is thermally stable, and drying did not lead to any significant reduction in

concentration. Soaking the dehulled faba beans in 0.1% citric acid for 12 hours at 37ºC removed 50% of the phytic acid. After soaking for 12 hours, microwaving the faba beans for two minutes removed over 70% phytic acid, including soaking in water or soaking in 0.1% citric acid solution. This thesis addresses the challenge of removing phytic acid, which is one of the major anti-nutritional factors present in faba beans.

A comprehensive techno-economic analysis evaluates the implications of these processes on the cost of drying faba beans, focusing on the comparison between boiling and microwave-based processing. Specifically, microwaving with air recycling has a lower COM (AU$/kg) at $2.85/kg compared with $2.96/kg for the open-loop system. Similarly, boiling with air recycling results in a lower COM (AU$/kg) of $2.72/kg compared with $2.90/kg for the open-loop system. These findings suggest that implementing an air recycle system in fluidized bed drying can lead to significant cost savings in pulse protein processing while maintaining process efficiency, and that boiling with air recycling used in drying is an optimal processing technique to remove phytic acid from dehulled faba beans.

The findings demonstrate the potential of FBD to effectively reduce ANFs while maintaining the quality of pulse proteins. Furthermore, the integration of air recycle systems and advanced processing technologies offers significant economic and environmental benefits, reducing both operational costs and carbon dioxide emissions. This research provides valuable insights into sustainable and efficient pulse processing and offers a foundation for future studies in this area.

List of Publications:

The following works have been published or submitted to international journals or conference during my PhD research. I was responsible for designing the studies, analyzing the data, and drafting the manuscripts under the supervision of Professor Timothy Langrish. Co-authors contributed to experimental design, data collection, and manuscript revision.

The publications are listed in chronological order based on their date of publication. I am the first author of the publications / international conference listed below.

Cheng, S., Zhong, C., Langrish, T.A., Sun, Y., Zhou, Z. and Lei, Z., 2022. The relative importance of internal and external physical resistances to mass transfer for caffeine release from apple pectin tablets. *Current Research in Food Science*, *5*, pp.634-641. https://doi.org/10.1016/j.crfs.2022.03.014.

Cheng, S., Sun, Y., Langrish, T.A., 2022. The Mass Transfer Resistance of Sausage Casings as Examples of Real Gut Systems. 12th Australasian Heat and Mass Transfer Conference.

Cheng, S. and Langrish, T.A., 2023. Fluidized bed drying of chickpeas: Developing a new drying schedule to reduce protein denaturation and remove trypsin inhibitors. *Journal of Food Engineering*, *351*, p.111515. https://doi.org/10.1016/j.jfoodeng.2023.111515.

Cheng, S., Skylas, D.J., Whiteway, C., Messina, V. and Langrish, T.A., 2023. The effects of fluidized bed drying, soaking, and microwaving on the phytic acid content, protein structure, and digestibility of dehulled faba beans. *Processes*, *11*(12), p.3401. https://doi.org/10.3390/pr11123401

Cheng, S., Sun, Y., Thorburn, M. Cheng. J., Lei. Z, Langrish, T.A., 2024. In-vitro starch digestibility from different types of starch and the effect of phytic acid on starch digestion. 17th International Hydrocolloids Conference.

Cheng, S. and Langrish, T.A., 2025. A Review of the Treatments to Reduce Anti-Nutritional Factors and Fluidized Bed Drying of Pulses. *Foods*, *14*(4), p.681. https://doi.org/10.3390/foods14040681.

Additionally, I have co-authored the following publications, which were published in international refereed journals during my PhD research.

Skylas, D.J., Whiteway, C., Johnson, J.B., Messina, V., Kalitsis, J., **Cheng, S.**, Langrish, T.A. and Quail, K.J., 2024. Dry fractionation of Australian mungbean for sustainable production of value-added protein concentrate ingredients. *Cereal Chemistry*, *101*(4), pp.720-738. https://doi.org/10.1002/cche.10774.

Li, Z., Messina, V., Skylas, D.J., Valtchev, P., Whiteway, C., **Cheng, S.**, Langrish, T.A., Quail, K.J. and Dehghani, F., 2024. Effect of Dry and Wet Fractionation on Nutritional and Physicochemical Properties of Faba Bean and Yellow Pea Protein. *Legume Science*, *6*(2), p.e244. https://doi.org/10.1002/leg3.244.

Sun, Y., **Cheng, S.**, Cheng, J. and Langrish, T.A., 2024. Mass Transfer Resistance and Reaction Rate Kinetics for Carbohydrate Digestion with Cell Wall Degradation by Cellulase. *Foods*, *13*(18), p.2881. https://doi.org/10.3390/foods13182881.

Sun, Y., Cheng, J., **Cheng, S.** and Langrish, T.A., 2025. Multifilm Mass Transfer and Reaction Rate Kinetics in a Newly Developed In Vitro Digestion System for Carbohydrate Digestion. *Foods*, *14*(4), p.580. https://doi.org/10.3390/foods14040580

Langrish, T.A.G. and **Cheng, S.**, 2024. Technico-Economic Analysis for the Costs of Drying Chickpeas: An Example Showing the Trade-off between Capital and Operating Costs for Different Inlet Air Temperatures. 23rd International Drying Symposium.

Permission to include the published material in this chapter has been granted by my supervisor, Professor Timothy Langrish. Additionally, in cases where I am not the corresponding author of a published work, permission for inclusion has been obtained from the corresponding author.

Shu Cheng

As the supervisor for the candidature upon which this thesis is based, I confirm that the authorship attribution statements above are accurate.

Professor Timothy Langrish

Abbreviations

Abbreviations	Full name
FBD	Fluizied bed drying
ANFs	Anti-nutritional factors
mmt	Million metric tonnes
TEA	Technico-Economic Analysis
TI	Trypsin inhibitor
BBTI	Bowman-Birk trypsin inhibitors
KTI	Kunitz trypsin inhibitors
CTI	Chymotrypsin inhibitors
HAs	Haemagglutinins
CMFD	Combined microwave and fluidized bed drying
FTIR	Fourier transform infrared spectroscopy
ATR	Attenuated total reflectance spectra
SEM	Scanning electron microscopy
PEC	Purchased equipment cost
PPC	Process plant cost
CRF	Capital recovery factor
COL	Cost of operational labor
COM	Cost of manufacturing
DMC	Direct manufacturing cost
FMC	Fixed manufacturing cost
GE	General expense
CUT	Cost of utilities
CWT	Cost of waste treatment
CRM	Cost of raw material
FCI	Fixed capital investment

Table of Contents

List of Figures

List of Tables

Chapter 1. Introduction

1. Overview

This chapter outlines the foundational background and the primary motivation driving the research presented in this thesis. It highlights the relevance of the research problem and its significance within the broader context of scientific inquiry and industrial application. Furthermore, the overall aim of the study is articulated, accompanied by an overview of the structure of the thesis to provide a roadmap for the reader.

The content of this chapter incorporates material published in the following peer-reviewed journal articles and conference paper:

- Cheng, S. and Langrish, T.A.G., 2023. Fluidized bed drying of chickpeas: Developing a new drying schedule to reduce protein denaturation and remove trypsin inhibitors. *Journal of Food Engineering*, *351*, p.111515. https://doi.org/10.1016/j.jfoodeng.2023.111515
- Cheng, S., Skylas, D.J., Whiteway, C., Messina, V. and Langrish, T.A.G., 2023. The Effects of Fluidized Bed Drying, Soaking, and Microwaving on the Phytic Acid Content, Protein Structure, and Digestibility of Dehulled Faba Beans. Processes, 11(12), p.3401. https://doi.org/10.3390/pr11123401
- Langrish, T.A.G. and Cheng, S., 2024. Technico-Economic Analysis for the Costs of Drying Chickpeas: An Example Showing the Trade-off between Capital and Operating Costs for Different Inlet Air Temperatures. 23rd International Drying Symposium.
- Cheng, S. and Langrish, T.A., 2025. A Review of the Treatments to Reduce Anti-Nutritional Factors and Fluidized Bed Drying of Pulses. Foods, 14(4), p.681. https://doi.org/10.3390/foods14040681.

As the first author of first two publications, I played a central role in the conception and execution of the research. Specifically, I was responsible for designing the studies, performing detailed data analysis, and drafting the majority of the manuscripts. As a co-author of the conference paper, I played an important role in the success of this work. My contributions included designing the experiments, collecting and analyzing data, formatting the manuscript, and delivering the presentation at the conference. These activities were conducted under the expert guidance of my supervisor, Professor Timothy Langrish, who provided invaluable feedback on manuscript structure, academic clarity, and overall editing.

The inclusion of published materials in this thesis has been authorized by my supervisor, Professor Timothy Langrish, in accordance with the policies and ethical standards of the University of Sydney. These published works provide a robust foundation for the discussions presented in this thesis and underscore the collaborative and multidisciplinary nature of the research.

By presenting a synthesis of these publications, this chapter establishes the context for the research questions addressed in subsequent chapters. It emphasizes the originality and significance of the work, setting the stage for an in-depth exploration of the methodologies, findings, and implications of the study.

1.1 Pulses and the Need for Processing Them

Pulses are a grain legume produced for human consumption and include lentil, faba bean, mung bean, field pea, chickpea and lupin. Pulses are an essential dietary component for millions of people across the world due to their high protein content [1]. In the context of this study, *pulses* refer specifically to dry edible seeds of certain leguminous crops, such as chickpeas (*Cicer*

arietinum) and faba beans (*Vicia faba*). While all pulses are legumes, not all legumes are classified as pulses. Pulses are recognised as an important component of the human diet, primarily due to their high protein content—typically containing two to three times more protein per serving compared to common cereal grains such as rice, oats, barley, and wheat. Given their nutritional significance, this research focuses on assessing protein denaturation in pulses using Fourier-transform infrared (FTIR) spectroscopy.

Australia's diverse agroclimatic zones produce a wide array of high-quality pulse grains. According to the data from Australia Export Grains Innovation Central [2], Australia produces an average of 2.2 million metric tonnes (mmt) of pulses from more than 1.8 million hectares. In Australia, pulses average just under 10 per cent of the total area planted to crop. In favourable production areas they can occupy as much as 25% of the total crop area. Pulses are grown in crop rotations, with cereals and oilseeds, given their ability to fix nitrogen into the soil and their contribution to sustainable and profitable farming practices [2].

As shown in Figure 1, pulse production in Australia is dominated by Australian white lupin, which constitutes approximately 30-40% of the total production. Chickpea production follows, contributing 20-35% to the overall pulse yield. Field pea, lentil, and faba and broad bean each represent 10-15% of the production share. In contrast, mung bean accounts for less than 5% of the total pulse production in the country.

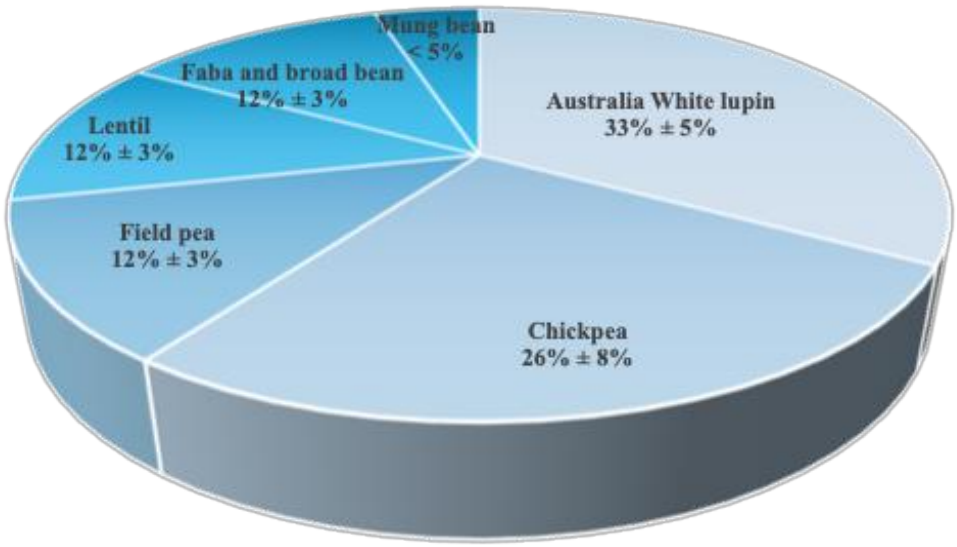

Figure 1. *Pulse production in Australian. (Data from AEGIC [2])*

Studying pulses is important to optimize their utilization and maximize the value of these essential resources. This thesis focuses on investigating the drying processes of pulses, with particular emphasis on faba beans and chickpeas. Drying techniques play a critical role in post-harvest processing, as they not only extend the shelf life of pulses by reducing moisture content and preventing spoilage but also have the potential to enhance their nutritional value by minimizing anti-nutritional factors and improving functional properties. This research aims to contribute to the development of advanced drying methods that promote the effective use of pulse resources and support the growing demand for sustainable and nutritious food products.

Anti-nutritional factors (ANFs) in pulses, such as phytic acid, tannins, and trypsin inhibitors, can interfere with nutrient absorption and reduce the bioavailability of essential minerals like iron and zinc [3]. These compounds pose challenges for the nutritional quality of pulse-based foods, particularly in plant-based diets [4]. To address this, hydrolysis reactions are often employed to break down or reduce the levels of ANFs. However, these reactions require the pulses to be wetted or soaked beforehand, as the presence of moisture is essential for enzymatic or chemical activity [5]. Once the ANFs are mitigated, the pulses need to be dried to restore

their low moisture content, which is critical for long-term storage and maintaining product quality. This necessity underscores the importance of drying processes in pulse processing, particularly in ensuring nutritional enhancement while maintaining the physical and functional properties of the product.

1.2 Drying Process

1.2.1 Fluidized Bed Drying

Numerous studies highlight the complexity of the fluidized bed drying process, as it is influenced by a variety of factors, including gas temperature, humidity, flow rate, and particle size. Each of these variables plays a critical role in determining the drying efficiency and product quality. For instance, Kozanoglu et al. investigated the effect of particle size on the fluidized bed drying of pepper seeds [6]. Their findings revealed that smaller particles exhibited higher mass transfer coefficients and a faster drying rate. Interestingly, during different stages of the drying process, the drying rate varied even for particles of the same size, highlighting the dynamic nature of fluidized bed drying.

In addition to particle size, the particle size distribution has been shown to significantly influence the drying process. Grace and Sun [7] demonstrated that the distribution of particle sizes impacts the uniformity of drying and the overall process efficiency. Furthermore, the heat transfer coefficient, a key parameter in fluidized bed drying, is predominantly determined by the gas flow rate and the geometry of the system, including particle size.

The fluidized bed drying of soybeans has also been extensively studied by several researchers. Workers such as Darvishi, Prachayawarakorn, and Dondee have explored different methods of drying soybeans in fluidized beds [8-10]. From these works, the most common method involves storing the soybeans at a constant temperature of 3–10°C for a week, followed by

conditioning under ambient conditions until the grain temperature reaches room temperature. For soybeans, five common physical quality assessments are typically performed: cracking and breakage [8, 9], color analysis using a color meter [9], protein solubility [8-10], urease activity [10, 11], and moisture content [8-11]. Operating temperatures in fluidized beds often exceed 135°C, which can effectively inactivate the urease enzyme [10]. Additionally, Darvishi et al. observed that at a constant air velocity, higher temperatures led to increased shrinkage and bulk density of the soybeans [8].

Tirawanichakul et al. explored the effect of varying inlet air temperatures on fluidized bed drying performance [12]. Their study found that an increase in the inlet drying air temperature led to a slight reduction in the drying rate for samples with the same initial moisture content. However, the influence of elevated temperature became more pronounced with higher initial moisture content, resulting in notable improvements in drying performance. These findings emphasize the interplay between temperature and moisture content in optimizing fluidized bed drying conditions.

Overall, these studies underscore the intricate nature of fluidized bed drying, where multiple interdependent variables must be carefully controlled to achieve efficient drying and maintain product quality.

1.2.2 Spray Drying

Spray drying is predominantly used for drying liquid dispersions and is a well-established technique in the food and pharmaceutical industries. It enables the production of solid dispersions from liquid suspensions, improving solubility by dispersing poorly water-soluble components into an amorphous matrix carrier [13]. However, spray drying is less effective for

larger particles or extrudates exceeding 1 mm, making fluidized bed drying a more suitable alternative in such cases.

Lan et al. investigated the use of spray drying to reduce the beany flavor of soybean dispersions by modifying the solubility of pea protein under acidic conditions (pH = 4.5) before drying [14]. They demonstrated that incorporating gum arabic and maltodextrin as carriers significantly reduced concentrations of flavor markers, such as 1-octen-3-ol and 1-pentanol [14]. Despite its advantages, lipid oxidation during the high-temperature process remains a significant challenge.

1.2.3. Other Drying Methods

Alternative drying methods have also been explored to optimize pulse protein processing. For instance, hydro-drying, also known as Refractance Window (RW) drying, has been studied for its application in drying suspensions and particulate materials. This method uses conductive hydraulic drying, where suspensions are distributed onto a conveyor belt and scraped off after drying [15]. Preethi et al. conducted a comparative analysis of hydro-drying and freeze-drying, finding no significant differences in the particle characteristics of pulse proteins [16]. RW drying has shown promise for maintaining the physicochemical and functional properties of proteins [17].

1.3 Thesis Aim

The aim of this thesis is to investigate the effectiveness of advanced drying technologies, particularly fluidized bed drying, for improving the processing of pulse proteins. The research focuses on enhancing product quality by minimizing protein denaturation and improving the removal of key anti-nutritional factors (ANFs), such as trypsin inhibitors and phytic acid.

Additionally, the study assesses the techno-economic feasibility of these processing methods, with an emphasis on reducing energy consumption, operational costs, and carbon dioxide emissions.

To achieve this aim, the following specific objectives were established:

- To evaluate the impact of different pretreatments (soaking, boiling, and microwaving) on the removal of ANFs and the structural integrity of pulse proteins.
- To optimize fluidized bed drying conditions for chickpeas and dehulled faba beans, targeting both product quality and ANF reduction.
- To analyze the effect of drying conditions on protein secondary structure using FTIR, and to assess microstructural changes via SEM.
- To conduct a techno-economic analysis of the drying processes, including the integration of air recycle systems, to quantify cost savings and environmental benefits.
- To identify processing configurations that offer the best trade-off between nutritional quality, energy efficiency, and sustainability.

This thesis contributes new insights into the integration of pretreatment and drying technologies for pulse processing and offers a novel techno-economic and environmental evaluation framework for their practical implementation.

1.4 Thesis Structure

To address the aims of the thesis, this thesis has been divided into eight chapters.

Chapter 1: Introduction

The first chapter introduces the research, outlining the general background, motivations, and objectives of the project in a concise manner.

Chapter 2: Literature Review

The second chapter is the literature review chapter. In this chapter, current developments in fields that are relevant to this thesis have been summarised, and the background of the research has been further explained. The research gaps that are aimed to be addressed in this thesis have been discussed.

Chapter 3: Material and Methods

This chapter provides a detailed discussion of the materials and methods used in this thesis.

Chapter 4: Fluidized Bed Drying of Chickpeas

This chapter focus on the fluidized bed drying of chickpeas. By involve the drying schedule to reduce the protein denaturation and remove trypsin inhibitors. Figure 2 presents the conceptual framework of the chapter.

Chapter 5: Technico-Economic Analysis for the Costs of Drying Chickpeas

The technico-economic analysis in the chapter is based on the fluidized bed drying process from chapter 4. There is an example showing the trade-off between capital and operating costs for different inlet air temperatures

Chapter 6: The Effects of Fluidized Bed Drying, Soaking and Microwaving on Phytic Acid Content, Protein Structure and Digestibility in Dehulled Faba Beans

This chapter focus on the faba beans. By using different methods (such as, fluidized bed drying, soaking and microwaving) to remove the phytic acid from faba beans. Figure 3 presents the conceptual framework of the chapter.

Chapter 7: Technico Economic Analysis: Microwave Processing to Remove Phytic Acid from Dehulled Faba Beans

The technico-economic analysis in the chapter is based on the fluidized bed drying and microwaving process from chapter 6.

Chapter 8: Overall Discussion and Conclusion

This chapter outlines the conclusions and recommendations, providing a summary of the findings from the preceding chapters and proposing directions for future research based on these outcomes.

Overall, the second chapters build upon the findings discussed in the introduction, applying fluidized bed drying (FBD) to the processing of chickpeas and dehulled faba beans, with a focus on reducing specific anti-nutritional factors. Chapter 3 investigates the application of FBD in the processing of chickpeas, specifically targeting the reduction of trypsin inhibitors. Chapter 4 addresses the processing of dehulled faba beans, with an emphasis on mitigating phytic acid content. Both chapters underscore the critical role of optimizing FBD parameters, such as inlet air temperature to ensure effective reduction of anti-nutritional factors while preserving the nutritional quality of the pulse proteins.

Chapter 5 presents a comprehensive techno-economic analysis of the processing of both chickpeas and dehulled faba beans. This analysis evaluates the economic feasibility of the FBD process, including the potential for air recycle systems to enhance energy efficiency and reduce both operational costs and carbon dioxide emissions. The results demonstrating that the integration of advanced technologies such as air recycle systems can significantly improve the sustainability and economic viability of pulse processing using FBD.

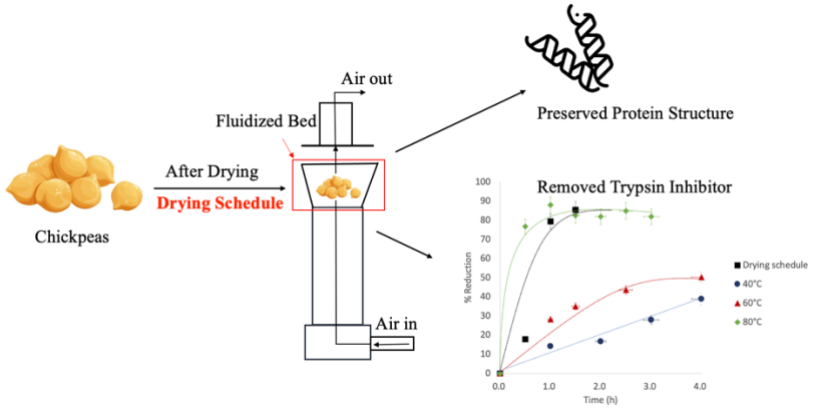

Figure 2. *Conceptual framework from Chapter 4 illustrating the development of a novel drying schedule for chickpeas.*

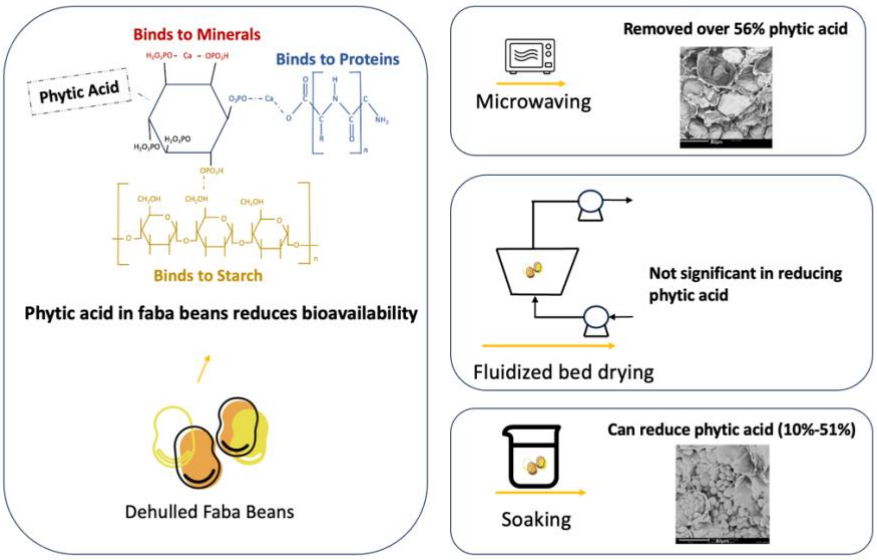

Figure 3. *Conceptual framework from Chapter 5 depicting the removal of phytic acid from dehulled faba beans.*

Chapter 2. Literature Review

This chapter provides a comprehensive summary of recent developments in fields relevant to this thesis, further elaborating on the background of the research. The key research gaps that this thesis aims to address have been critically analyzed and discussed in detail.

The content of this chapter is based on a peer-reviewed journal article, titled *"A Review of the Treatments to Reduce Anti-Nutritional Factors and Fluidized Bed Drying of Pulses,"* which was published in the *Journal of Foods*. As the first author of this article, I was responsible for designing the study, conducting data analysis, and drafting the manuscript, under the guidance of my supervisor, Professor Timothy Langrish. Professor Langrish contributed to the editing and structural refinement of the manuscript.

Permission to include the published material in this chapter has been granted by my supervisor, Professor Timothy Langrish.

1. Introduction

Pulses provide nutrients, such as proteins, dietary fibers, antioxidants and resistant starches, that are needed for human health [1]. Pulses are also excellent meat protein substitutes. For example, the plant protein in plant-based meat comes from pulses [18]. However, some of the chemicals naturally occurring in pulses are known to be "anti-nutritional factors" (ANFs) or "anti-nutritional compounds" (ANC). ANFs can reduce nutrient absorption, inhibit aspects of human metabolism, or affect protein digestibility. Therefore, ANFs are generally for human consumption [19]. It is important to control the concentration of ANFs in pulses during processing using different treatments, such as soaking, cooking, dehulling, microwaving and drying.

Fluidized bed drying (FBD) has been used in food processing due to its high thermal efficiency and relatively low operating costs [20]. Specifically, the application of FBD to pulses has been found to be effective in extending shelf life, reducing transportation costs, removing some ANFs, retaining key quality parameters, and maintaining nutritional values [21]. Current studies of pulse protein processing focus on nutrients and the quality of proteins. For example, the review by Mudryj et al. [22] reported that the saponins and tannins in pulses have antioxidant and anti-cancer effects. The protein, fiber, and vitamins provided in pulses are all important nutrients [22]. Shevkani et al. [23] studied the antioxidant properties of different types of pulses (including chickpeas, cowpeas, kidney beans, mung beans, lima beans, peas and lentils) and the relationship between amino acid composition and antioxidants. For instance, chickpea-derived peptides, especially those rich in hydrophobic amino acids, have demonstrated significant antioxidant potential [23].

Preserving or enhancing the protein structure during drying is of great importance, as the integrity of the proteins is critical for maintaining the nutritional quality and functional properties of the final product. Therefore, optimizing drying parameters to minimize ANFs

while safeguarding protein structure is essential for achieving both high product quality and efficient processing outcomes.

Moreover, fluidized bed drying is a widely utilized method in food processing that presents significant opportunities for optimizing energy and exergy efficiency. This thesis examines the advances in energy and exergy management within fluidized bed drying systems, particularly in the context of pulse processing. The energy demands of traditional open-loop systems are high, driven by substantial natural gas consumption for heating the fluidizing air. Emerging technologies, such as fluidized bed dryers with air recycle, offer promising solutions by recycling hot air and thereby reducing energy consumption and processing costs [24]. Recent studies highlight that air recycle systems not only lower operational costs but also improve exergy efficiency and reduce carbon emissions [25]. A comparative analysis of different fluidized bed dryers, including widely used models, has not been carried out yet to consider the possibility that pressure drops, and thermal energy use may significantly impact exergy efficiency. This review provides an in-depth evaluation of these energy and exergy dynamics, emphasizing their implications for enhancing the sustainability and effectiveness of fluidized bed drying processes for pulses.

Finally, despite these advantages, significant challenges remain, particularly regarding the effective removal of thermally resilient ANFs, such as phytic acid and tannins. Although FBD is effective at reducing enzyme inhibitors, its ability to eliminate these thermally resilient (and frequently non-enzymatic) ANFs is limited, which can negatively affect the nutritional value and digestibility of pulses.

Some scholars have surveyed the effects of various processing methods on anti-nutritional factors (ANFs), with a focus on dehulling, soaking, hydrothermal treatment, germination, fermentation, and irradiation [3, 26, 27]. However, there is a significant gap in this previous work in terms of the impact of drying processes. The perspective presented in this thesis may

contribute to the understanding of how drying can be employed to remove ANFs, as drying is an important step in pulse protein processing.

2. Pulse Proteins

Pulses are an important source of dietary protein and must provide the body with a balanced supply of essential amino acids. The functional properties of pulse proteins are used in the development of various products, such as those from baking, noodles and plant-based meat [23]. Nutritional imbalance due to the lack of protein is still a food problem faced by many countries. Pulses have the potential to become an alternative source of nutritional and functional proteins [28]. These proteins have multiple biological effects and provide sufficient essential amino acids and give good protein digestibility [29]. Technically, they provide suitable raw materials for the development of new products such as noodles, breads, and biscuits [29]. Although these pulses may be good sources of proteins, they contain a variety of ANFs that may cause nutritional limitations [30]. ANFs present in pulses are thought to impair protein digestibility and compromise the nutritional value of the pulses at high concentrations [31].

Table 1 shows the ANFs in the six major pulses. For example, according to Kumar's review [3], trypsin inhibitor, chymotrypsin inhibitor and phytic acid are three main ANFs for chickpeas. Trypsin and chymotrypsin inhibitors have high concentrations in chickpeas compared with the other five pulses, which are in the range (for chickpeas) between 8.1-20.9 TIU/mg and 6.1-8.8 IU/mg, respectively [32]. The contents of saponins, haemagglutinin activity and phytic acid are higher in faba beans than in chickpeas [3]. The content of phytic acid in faba beans can reach up to 98 mg/g [33]. For untreated faba beans, the saponin content

is 137 mg/g [33]. The content of trypsin inhibitor in faba beans is relatively lower than in other pulses, such as chickpeas, mung beans and lentils [34]. According to Table 1, the contents of ANFs in, lentils, mung beans and lupins are lower overall compared with the contents of trypsin inhibitor in chickpeas and phytic acid in faba beans. For field peas, the content of haemagglutinin can reach 80 HU/g, which is the highest content compared with the other five pulses [26]. Due to biological diversity, different types of pulses contain different types of ANFs, and the ANF contents vary significantly within each type of pulse.

Table 1. *The main anti-nutritional factors in chickpeas, faba bean, lentils, mung beans, lupins and field peas.*

Pulses	Trypsin inhibitors (TIU/mg protein)	Chymotrypsin inhibitor (IU/mg)	a-amylase inhibitor (IU/g)	Haemagglutinin (HU/g)	Phytic acid (mg/g)	Tannins (mg/g)	Saponins (mg/g)	References
Chickpeas	8.1-21	6.1-8.8	3.1-11	6.2	5.8-12	0.04-4.9		[27, 30]
Faba beans	2.3-7.2	3.6	19	49	32-98	0.3-21	31-137	[30, 31, 33]
Lentils	3.6-7.6	0	0	50	4.1-13	1.3-3.9	180-1595	[27, 34]
Mung beans	16			27	5.8-12	3.3		[35, 36]
Lupins	=< 0.1				0.41-14			[37-39]
Field peas	0.8-6.3	2.7-4.9	17	80	3.0-13	2.8-3.1		[27, 34]

3. Specific Anti-Nutritional Factors and Their Treatments

These antinutrients cause several biochemical pathways to be hindered. Pulses have been reported to have somewhat reduced digestibility compared with some protein sources because the presence of anti-nutrient enzymes involved in digestion reduces the bioavailability of nutrients [40]. ANFs in pulses can be divided into enzyme inhibitors, haemagglutinins, phytic acid, tannins and saponins, based on their chemical and physical properties [41]. This section discusses the impact of different treatments on reducing the concentrations of ANFs.

3.1 Enzyme Inhibitor

An enzyme is a substance that speeds up certain chemical reactions in the body, much like a catalyst does in a chemical reaction [41]. The main enzyme inhibitors in pulses include trypsin inhibitors, chymotrypsin inhibitors, and α-amylase inhibitors [32]. Both trypsin inhibitors and chymotrypsin inhibitors affect protein digestion in humans. For α-amylase inhibitors, they are related to starch digestion [26]. Addressing the removal of these inhibitors is important for improving the digestibility and nutritional value of pulse-based products.

- Trypsin Inhibitor (TI) and Chymotrypsin Inhibitor

Trypsin inhibitors (TI) are defined as proteolytic enzymes that affect protein digestion [26]. Paraphrasing [26], "*trypsin inhibitor is a group of serine protease enzymes. TI in pulses can be divided into Bowman-Birk trypsin inhibitors (BBTI) and Kunitz trypsin inhibitors (KTI) according to their molecular size*". The molecular weight of BBTI is smaller at about 8 kDa than KTI, which has a molecular weight of about 20 kDa [42]. Some pulses contain both types of trypsin inhibitors, such as soybean, while lentils contain only one kind of TI [42]. Both of TI have a negative effect on the biological activity of the digestive enzyme trypsin. Trypsin is called "trypsinogen" when it is in the pancreas and is present in an inactive form [43]. It is then

activated upon entry into the small intestine to produce the trypsin enzyme, which is a trypsin inhibitor complex. This reaction is irreversible [44], so trypsin in the intestines is reduced by the intake of TIs, resulting in reduced protein digestibility [45], and improving the digestibility of pulse proteins by removing TI is helpful in pulses.

Table 2 shows different treatments to reduce TI activity in pulses. According to Nielsen et al [46]. and Subbulakshmi et al. [47], 6 to 10 days germination can remove around 30-39% TI from pinto beans and french beans. Marquez et al [48]. tried different treatments to remove TI in chickpeas. Soaking overnight reduced 36% TI and boiling for 30 s removed 56%. TI activity increased with increasing boiling time [49]. At the target moisture content, higher drying temperatures reduced more TI. At the same time, the rate of TI removal was also related to the drying temperature. Overall, TIs are thermosensitive and can be effectively inactivated through thermal processing methods, such as boiling and fluidized bed drying. Germination and soaking treatments can remove 30-40% of TI.

Table 2. *Activity reduction for trypsin inhibitors in pulses under different treatment conditions.*

Pulses	Processing conditions	Trypsin inhibitor activity reduction (%)	References
French beans	10 days germination	30	[46]
Pinto beans	6 days germination	39	
Chickpeas	Soaked in water at room temperature for 16 hours	36	[50]
Chickpeas	Boiled in water at 96°C, 30 s	56	[49]
Chickpeas	Boiled in water at 96°C, 300 s	100	[49]
Soybeans	Autoclaved at 121°C, 60 min	96	[48]
Soybeans	Fluidized bed dried at 120°C, 10 min	85	[51]

The function of chymotrypsin inhibitors is similar to those of trypsin inhibitors, limiting protein digestibility. However, the site of activity for these inhibitors differs. While trypsin targets the amino acids lysine and arginine, chymotrypsin specifically acts on hydrophobic residues such as tyrosine, tryptophan, and phenylalanine [26]. According to the results from Baintner, the removal of chymotrypsin inhibitors shows similar trends to trypsin inhibitor removal during heating processing for soybeans [52]. The removal of chymotrypsin inhibitor required higher temperature than that for trypsin inhibitor. In other words, fluidized bed drying presents a potential processing technique for effectively removing TI and CTI in pulses.

- α-amylase Inhibitors

α-amylase inhibitors present in seeds can function as antinutritional factors for both human and animal nutrition [53]. These inhibitors reduce starch digestibility by inhibiting the activity of pancreatic and salivary α-amylase enzymes [27, 54]. According to Table 3 from [27, 54], the activity of α-amylase inhibitors is low in lentils, faba beans, and chickpeas. However, soybeans, black beans, pinto beans, and dark red kidney beans contain higher levels of α-amylase inhibitors, which is consistent with the results from [55]. Table 3 presents the changes in levels of α-amylase inhibitory activity in various types of beans. The results indicate that the soaking process does not significantly affect the α-amylase inhibitor activity in the pulses, as shown by the relatively small percentage reductions across the different types. In contrast, cooking results in a substantial reduction in α-amylase inhibitors activity for all pulse types, with reductions ranging from 80% to 100%. This situation suggests that cooking is far more effective than soaking in decreasing the α-amylase inhibitory activity in these beans.

Table 3. *Activity reduction for α-amylase inhibitors in pulses under different treatment conditions.*

Pulses	Processing conditions	α-amylase inhibitor activity reduction (%)	Reference
Dark red kidney bean	Soaked in room temperature, 4 h	11	[27]
Soybean		4	
Black bean		7	
Dark red kidney bean	Boiled in 95 °C, 1 h	90	
Soybean		100	
Black bean		91	
Sweet potato flour	Oven dried in 90 °C, 2 h	80	[56]
Taro tubers	Cooked 30 min	86 - 88	
Sweet potato flour	Microwaved 120 s	65 - 100	
Taro tubers	Microwaved 120 s	63 - 91	

According to Rekha and Padmaja, most thermal methods, including oven drying, cooking, and microwave baking, are effective in removing alpha-amylase inhibitors [56]. However, there is limited prior research that has thoroughly investigated the effectiveness of fluidized bed drying in removing these inhibitors from pulses. This represents a significant research gap.

3.2 Haemagglutinin

Haemagglutinins have been known to agglutinate red blood cells and impair various physiological and biochemical processes in mammals upon ingestion [57]. According to Bender, the amount and stability of haemagglutinin vary among different types of pulses. For example, whole yellow pea contains haemagglutinin, at 5.64 HU/mg dry matter [58]. Soybeans

contain high levels of haemagglutinin, at 693 HU/mg dry matter [43]. More than 89% of haemagglutinin can be removed by cooking at 100ºC for 2 minutes. Cooking for 20 minutes, 100% haemagglutinin can be removed from most varieties of pulses [58]. However, soaking does not significantly help to remove haemagglutinin, either from lentils [58] or from chickpeas [43]. According to Alajaji and El-Adawy, most kinds of heat treatment may effectively remove all of the HA from chickpea at high temperatures (over 100ºC) [59]. However, Bender founds that inadequate cooking can lead to food poisoning, as heating at 80 ºC for 15 min resulted in HA levels that were seven times higher than those in the raw beans. As the heating time increased, the HA content decreased correspondingly. Bender also found that HAs are removed at 90 °C. Overall, drying at high temperatures or for long times removes HA [58].

Table 4. *Activity reduction for haemagglutinin (HA) in pulses under different treatment conditions.*

Pulses	Processing conditions	Haemagglutinin activity reduction (%)	References
Red Lentils	Soaked overnight	22	[58]
Red Lentils	Cooked at 100°C for 2 min	97	[58]
Red Lentils	Cooked at 100°C for 20 min	100	[58]
Chickpeas	Soaked	1.7	[43]
Chickpeas	Cooked	94	[43]
Chickpea	Autoclaved	100	[59]
Chickpea	Microwaved	100	[59]

3.3 Phytic Acid

Phytic acid is found in most grains, legumes, nuts, oilseeds, pipes, pollen, spores and organic soil [4]. PA has been reported to be able to bind (indirectly or directly) to minerals, proteins, and starches [4]. As shown in Figure 4, reactions occur between phytic acid and minerals, proteins and starches. Due to the ability of phytic acid to bind to starch, it can reduce the conversion of starch into glucose. This may be helpful to a certain extent for low-glycemic index diets and diabetes control [60], but it may be undesirable at higher concentrations due to reduced availability of minerals in human digestion. The phosphate groups of phytic acid are negatively charged and can interact with positively charged components, such as many minerals and proteins. This combination affects the solubility, functionality, digestibility, and absorption processes for these minerals and proteins during digestion.

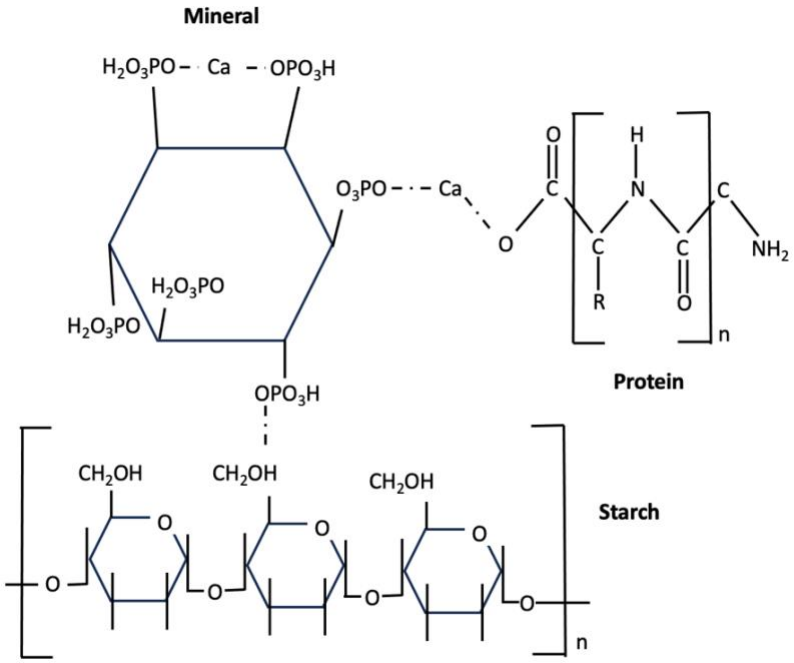

Figure 4. *The complex between phytic acid and a mineral, protein and starch. Adapted and modified from Oatway et al, [4].*

Paraphrasing [61], "*for those who follow a balanced diet, phytic acid is not a health concern, but for those at risk for iron or zinc deficiency as well as vegetarians, phytic-rich foods may cause potential health risks.*" This is particularly concerning in many developing countries, where whole grain cereals and legumes make up a large part of the diet [4]. There is a range of phytic acid concentrations in pulses, depending on the type of pulse and the processing involved [4]. Therefore, it is important to reduce the content of phytic acid during processing. Table 5 shows the different amounts of reduction for phytic acid under different treatment conditions.

From Table 5, the reduction of phytic acid increased with microwaving time. At the same time, the temperature of the dehulled faba beans increases with microwaving time as well. However, as the mass of faba beans increases, the reduction of phytic acid shows a downward trend at the same microwaving time.

The reduction of phytic acid during microwave processing is probably due to hydrolysis. Soaking before microwave treatment further enhances the potential for phytic acid hydrolysis. Phytic acid in dried grains is entirely in the form of a water-soluble salt. During processing, phytate is converted into pentaphosphate and tetraphosphate [60]. At the same time, high temperatures during microwaving may promote the hydrolysis reaction to a certain degree. Since phytic acid removal is caused by hydrolysis, boiling should remove phytic acid.

According to Alonso et al. [35], soaking and extrusion can reduce phytic acid levels by 30±3%. Germination for 72h can remove phytic acid by 59%. However, Shi et al. [43] found that there was no detectable decrease in phytic acid levels after soaking any of the seeds. Table 5 shows that environmental factors may affect the removal of phytic acid for different types of pulses under different soaking conditions (different temperatures, different pH values) [28, 61, 62]. Germination is an effective method for removing phytic acid. The amount of phytic acid removed is proportional to the duration of germination. Alonso et al. found that germination for 24, 48 and 72 h removed 54, 59 and 61% of phytic acid, respectively [35]. In addition, microwaving is a potential method to remove phytic acid. According to Sharif et al. [63] and Manez et al. [64], soaking and microwaving the pulses together can remove 49±4% of the phytic acid content. Daneluti et al. [65] found that phytic acid thermally decomposes at a temperature of 380°C, resulting in the reduction of carbon and hydrogen. This situation means that phytic acid is thermally stable during this microwaving, and increasing the temperature is not the optimal way to remove phytic acid. As a result, fluidized bed drying did not lead to a significant reduction in phytic acid concentration. In contrast, soaking reduced phytic acid levels to a certain extent, while microwaving had a more pronounced effect in reducing phytic acid levels in faba beans.

Table 5. *Phytic acid reduction in pulses under different treatment conditions.*

Pulse	Processing conditions	Phytic Acid Reduction (%)	References
Faba beans	Soaked	32.7	[35]
Faba beans	Germination 72 h	61	[35]
Goat peas	Soaked in room temperature	3.9	[66]
Lentils	Soaked in acidic condition	37	[67]
India tribal pulse	Soaked in alkaline condition	11	[68]
Lentils	Microwaved + soaked	45 - 52	[63]
Vicia faba	Extrusion	27	[35]
Lentils	Microwave + soaking	45	[64]

3.4 Tannins

Tannins are one of the most common antinutritional factors. They are present not only in pulses but also in most plants [69]. Tannins are defined as complex, amorphous and water-soluble polymeric phenolic substances [70, 71]. Tannins can be divided into three major types: hydrolysable tannins, phlorotannins, and condensed tannins [69, 72]. Phlorotannins are the simplest tannin group in terms of their structures [72] and can be detected in aquatic species such as brown algae [73]. Condensed tannins are more widely distributed than hydrolysable tannins. Tannins can precipitate proteins [69, 72]. This property of tannins is used to transform raw animal into leather [74], because tannin molecules cross-link proteins, making these proteins more resistant to bacterial and fungal attacks [72]. Tannins, on the other hand, may reduce the activity of many enzymes [72]. One of the main characteristics of tannins as digestive inhibitors or toxins in humans or animals is that they form chemical complexes with substances such as proteins, polysaccharides, alkaloids, nucleic acids, steroids and saponins, reducing the ability of the human body to absorb these nutrients [75]. Therefore, removing tannins from pulses is an important part of food processing for these materials.

The characteristics and amounts of tannins in pulses are affected by processing due to their high reactivity [71]. Alonso et al [35]. and Khandelwal et al. [71] have shown that germination can remove over 50% of any tannins present. The germination process in the work of Khandelwal et al [71]. was performed by soaking the pulses in tap water overnight at room temperature for 12 hours, then wrapping the sample pulses in a moist cloth and leaving them at room temperature for 24 hours. For lentils, after germination, the tannins could not be measured, suggesting that they are entirely removed by germination [71]. According to the results from Table 6, boiling for 90 minutes can remove 29% of tannins from lentils [59]. With increased boiling time, for example, boiling faba beans until they are soft, 76% tannins may be removed [33]. Cooking under high pressures has been reported to improve the removal of the

tannins [59]. Microwaving has also been reported to remove half of the tannin content in lentils [36]. Dehulling for faba beans has been reported to remove about 92% of the tannins [35]. Overall, most treatments, including cooking, microwaving, boiling, dehulling, germination and extrusion are helpful for removing tannins. Common to cooking and boiling, tannin reduction increases with an increase in the cooking temperature or pressure. Dehulling and germination are also both effective at removing tannins.

Table 6. *Tannin reductions in pulses under different treatment conditions.*

Pulses	Processing condition	Tannins reduction (%)	References
Chickpeas	Pressure cooked (15 psi) at 121°C, 35 min	84	[59]
Chickpeas	Microwaved	48	[59]
Lentils	Boiled at 100°C, 90 min	29	[36]
Lentils	Pressure cooked at 121°C,35 min	36	[36]
Faba beans	Boiled in water at 100°C, until soft	76	[33]
Faba beans	Dehulled	92	[35]
Faba beans	Germinated 24h	56	[35]
Faba beans	Extrusion	54	[35]
Green grams	Germinated for 24h	54	[71]
Lentils	Germinated for 24h	100	[71]

4. Drying Technologies for Pulses, and the Effects of Drying on Anti-Nutritional Factors

The fluidized bed drying of pulses has been studied by several researchers, such as Darvishi, Prachayawarakorn, and Dondee, who have focussed on different ways to dry pulses in fluidized beds [8-10]. For pulses, there are at least five common physical quality characteristics, such as cracking and breakage [8, 9], colour testing by colour meter [9], protein solubility [8-10], the concentration of ANFs [10], and moisture content [8-11]. According to the study from Darvishi et al. [8], fluidized drying at high temperatures can cause V-shaped cracks in pulses. During the drying process, the movement of water is limited by water diffusion in pulses, and the diffusion rate increases as the temperature rises. The drying of the surfaces causes the surface temperature of pulses to rise above the wet-bulb temperature. Therefore, at higher drying temperatures, the surfaces of the kernels become brittle and prone to cracking. Dondee et al. [9] showed that fluidized bed drying resulted in minor changes in the color of pulses.

The fluidized bed drying of pulses is relevant to reducing some ANFs in pulses and grains. As shown in Table 7, the fluidized bed drying process can remove some ANFs. According to the results of Osella et al. [51], the rate of trypsin inhibitor inactivation increases with higher fluidized bed drying temperatures.

For α-amylase inhibitors, drying at 90 ^{o}C for two hours has been reported to removed 80% of these inhibitors [56]. This suggests that fluidized bed drying is effective in removing enzyme inhibitors, such as trypsin inhibitors and α-amylase inhibitors. However, HAs are slightly different from enzyme inhibitor and cannot be removed at low temperatures or short drying times, and higher temperatures (over 90^{o}C) or long drying time is needed to remove them [58].

For thermally stable ANFs, such as phytic acid and tannins (non-enzymatic inhibitors), the fluidized bed drying process has limitations. Pande et al. [76] found that fluidized bed drying of green gram seeds at 50 to 70°C slightly reduced phytic acid content but did not completely remove it. The study by Muetzal and Becker indicated that tannin activity was not affected by the drying method [77]. Boiling and cooking for short processing times do not appear to be effective but microwaving and germination may be a reasonable way to remove tannins.

Overall, fluidized bed drying is a promising method for reducing certain enzyme inhibitors in pulses, such as trypsin and α-amylase inhibitors. However, its effectiveness is limited when dealing with thermally stable ANFs, such as phytic acid and tannins. To overcome these limitations, combined microwave and fluidized bed drying may be attempted in future work.

Table 7. *The removal of different ANFs by fluidized bed drying.*

Drying conditions	Pulses/Grains	ANFs	Finds	References
Drying at 120°C for 10min	Soybeans	Trypsin inhibitor	Reduce 90% trypsin inhibitors	[51]
Dried in 90°C for 2 h	Sweet potato flour	α-amylase inhibitors	Reduce 80% α-amylase inhibitors	[56]
Drying temperature from 50°C to 70°C	Green gram seed	Phytic acid	No significant effects, in the range of 600-630mg/100g	[76]
Drying temperature from 120°C to 140°C	Faba beans	Phytic acid	No significant effects	[78]

5. Modifications of the Fluidized Bed Drying Process in Pulses

There are two major challenges with for the fluidized bed drying of pulses. Firstly, the process is unable to eliminate all types of ANFs, such as non-enzymatic inhibitors, including phytic acid and tannins. Secondly, the fluidized bed drying process is associated with high energy consumption and processing costs. This is primarily due to the necessity for maintaining high temperatures and gas flow rates to achieve the desired drying efficiency, which further challenges the economic feasibility of the process. Consequently, these challenges necessitate ongoing research and development to optimize the ANFs removal process and enhance energy reuse and recovery during the fluidized bed drying for pulses.

5.1 Combined Microwave and Fluidized Bed Drying (CMFD).

For the first challenge, several studies have highlighted the effectiveness of microwaving in removing thermally stable ANFs, such as phytic acid [78, 79] and tannins [79], in a short amount of time. For example, Sharma et al. report that microwaving for 40-100 s could remove up to 77% tannins from sorghum [79]. Similarly, a previous study by Cheng et al. found that microwaving for two minutes could effectively remove most of the phytic acid from faba beans [78]. However, compared with fluidized bed drying, microwaving is less effective in removing trypsin inhibitors. For example, Sharma et al. found that microwaving 30 min removed only 12-13% of trypsin inhibitors from buckwheat [79]. Therefore, a combined microwave and fluidized bed dryer (CMFD) could be a promising process for effectively reducing a wide range of ANFs in pulses.

In previous studies, CMFD has been applied in grain processing, including peppercorns [80], carrots [81], soybeans [82] and brown rice [83]. As outlined in Table 8, CMFD significantly accelerates the drying rate of fresh peppercorns, leading to a more effective drying process [80].

Additionally, CMFD has proven to be effective in drying diced carrots, resulting in improved drying efficiency and uniform moisture content [81]. According to Khoshtaghaza et al., CMFD optimizes the quality of soybean kernels while simultaneously reducing the energy consumption and improving drying kinetics [82]. Chupawa et al. demonstrated that the CMFD approach, combined with stepwise microwave heating and bed height control, improves the performance in preparing instant brown rice [83]. Similarly, Zare and Ranjbaran found through doing simulations that CMFD effectively achieves uniform drying in soybeans, coupled with enhanced drying rates [84].

Table 8. *Summary of studies on the efficacy of combined microwave-fluidized bed drying (CMFD) in grain processing.*

Material	Processing	Findings	Reference
Peppercorns	CMFD	Good product quality, physical structure maintained shorter drying time	[80]
Carrot	CMFD	CMFD dryer is 2–5 times shorter than in the fluidized bed dryer	[81]
Soybean	CMFD	Drying time can be shortened by 30–150 times by using CMFD, energy saving	[82]
Brown rice	CMFD	Energy saving	[83]
Soybean	CMFD	Uniform drying, enhance drying rate	[84]

In summary, while CMFD has demonstrated its effectiveness in enhancing drying performance in grain processing, its application for the removal of anti-nutritional factors (ANFs) from pulses has not been extensively studied. The literature review indicates that CMFD holds considerable promise as a technique for reducing a broad spectrum of ANFs in pulses. However, the scarcity of research in this specific area underscores a significant gap, warranting further investigation to fully leverage the potential of CMFD in improving the nutritional quality of

pulses. Combined Microwave-Fluidized Bed Drying (CMFD) was not implemented in this study due to the specific focus and objectives of the research. This thesis provides a clearer assessment of its capabilities and limitations, forming a foundation for potential future research involving combined drying techniques like CMFD.

5.2 Energy and Exergy Saving During Fluidized Bed Drying

Drying is a process with substantial energy demands, necessitating the study of potential reductions in energy and exergy consumption [24, 25]. The adoption of emerging technologies is critical for advancing energy efficiency in this area.

5.3 Air Recycle Fluidized Bed Drying, Energy and Cost Saving

The operating costs of an open-loop, straight-through airflow system are very high, primarily due to the substantial energy expenses required to heat the fluidizing air. Consequently, incorporating some degree of air recycling emerges as a potential strategy for reducing energy consumption. As illustrated in Figure 5, an air-recycle fluidized bed dryer effectively recycles hot air during the drying process, thereby reducing processing costs. Moejes et al. demonstrated that an air recycle dryer system can significantly decreases the energy consumption during milk powder production [25]. Furthermore, Lei and Langrish [85] emphasized that closed-loop systems, where air recycle is similar to a closed-loop, not only enhance exergy efficiency but also contribute to a reduction in carbon dioxide emissions [24]. Exergy is energy availability, which is a measure of energy quality, and exergy is defined in the Chapter 8. Overall, air-recycle drying systems offer a good alternative to conventional methods due to their numerous potential advantages [86].

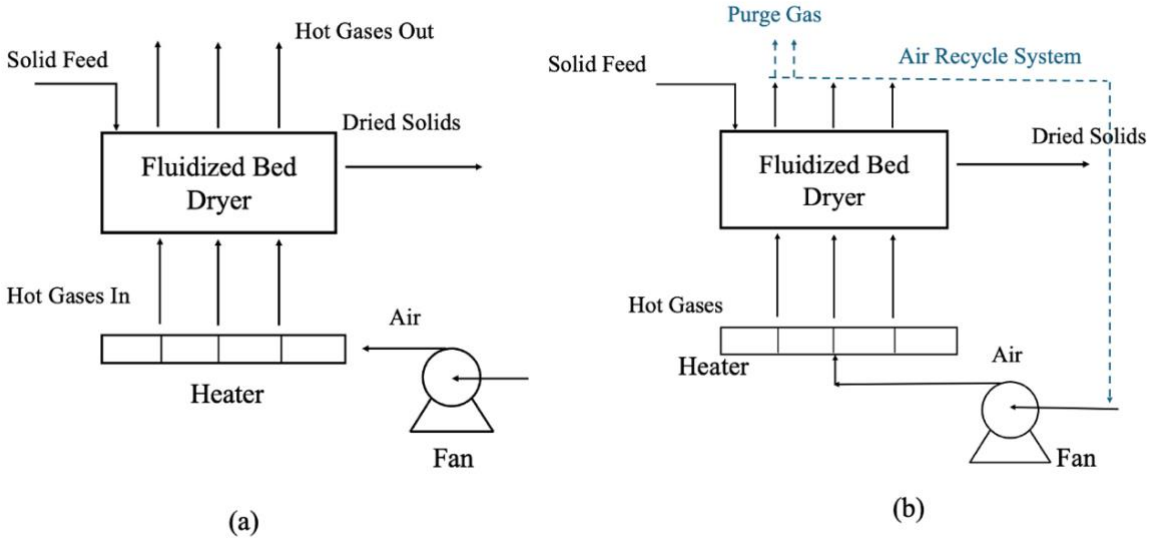

Figure 5. *Schematic diagram of a fluidized bed drying system with gas flow direction, (a) open-loop fluidized bed drying system; (b) air-recycle fluidized bed drying system.*

6. Conclusions

Fluidized bed drying (FBD) has been shown to be effective in removing certain enzyme inhibitors, such as trypsin inhibitors and α-amylase inhibitors. However, removing thermally-stable anti-nutritional factors (ANFs), such as phytic acid and tannins, presents challenges. While FBD alone is less effective for these stable ANFs, processes such as microwaving and germination offer promising alternatives for their removal. A potential solution to overcome the limitations of FBD is to optimize the system by combining microwave technology with fluidized bed drying (CMFD), which enhances the capability of fluidized beds in ANF removal.

The FBD process, despite its effectiveness, is associated with high energy consumption and operational costs. Strategies such as employing a fluidized bed system with air recycle and

optimizing exergy savings, for instance, by reducing pressure drops, can significantly improve the process's energy efficiency and lower costs. Further research into these optimization strategies could make FBD a more viable and sustainable method for pulse protein processing.

Chapter 3. Materials, Equipment and Methods

Following the research gaps identified in Chapter 2, this chapter details the materials, experimental setup, and analytical techniques used to explore the impact of fluidized bed drying and other treatments on pulses.

1.Materials

The dehulled faba bean (*Vicia faba*) seed material used in this study was provided by the Australia Export Grains Innovation Centre (AEGIC) in Sydney. And the McKenzie's Chickpeas from Coles were used in this study. The dimension of each whole chickpea with hulled is around 7.84 × 7.91 × 7.11 mm. The cotyledons of dehulled faba beans exhibit an oblong to oval shape with moderate curvature and a relatively smooth surface. For modeling and calculation purposes, the cotyledons were approximated as ellipsoids with average dimensions of 6.82 mm × 5.63 mm × 3.27 mm. According to the manufacturer, this product consists of pure chickpeas from Australia, with no additional additives.

2. Equipment

2.1 Sample Preparation

The chickpeas and dehulled faba beans were soaked with deionized water for 16 h at room temperature before the fluidized-bed drying process was started. The superficial water on the chickpeas and faba beans was gently wiped off with a kitchen towel before placing them in the fluidized bed dryer. The chickpeas and faba beans generally were found to have a moisture content of 49% – 60% after soaking. The target moisture content of chickperas and dehulled faba beans is 14%.

2.2 Fluidized Bed Drying

Chickpeas and dehulled faba beans were dried using a fluidized bed dryer as shown in Figure 6. Both fans 1 and 2 work in tandem to control the air flow rate through the fluidized bed. The flow velocity for chickpeas and dehulled faba beans were measured to be about 9.5 and 8.5 $m \cdot s^{-1}$ separately at the fluidized bed by using an orifice-plate flowmeter. The range of inlet air temperatures for the chickpeas was between 40 °C and 80 °C. The range of inlet air temperatures for faba beans was between 100 °C and 140 °C. A chickpea sample was taken every 30 min, and its moisture content was measured. The faba beans were fluidized and sub-samples collected at two-minute intervals for analysis of the moisture content (oven-drying method). After weighing, the faba beans and the chickpeas were placed in an 80 °C drying oven for a period of 24 hours.

$$MC_{wb} = \frac{m_0 - m_1}{m_0} \times 100\% \quad (1)$$

Where m_0 is the mass of the faba beans before drying, and m_1 is the mass of faba beans after drying. The drying curve was obtained from the moisture contents measured as functions of time. Then the drying curve was fitted by the following equation

$$X - C = A \exp(-Bt) \quad (2)$$

Where X is the fitted moisture content, A, B and C are fitted constants, and t is the drying time.

Moisture content was converted to a dry basis MC (db) using the following relationship:

$$MC_{db} = \frac{MC_{\mathrm{wb}}}{1 - MC_{\mathrm{wb}}} \times 100\% \quad (3)$$

At the same time, a dry and a wet bulb thermocouple were placed at the inlet of the fluidized bed, and the corresponding temperatures were measured, allowing the relative humidity in the inlet air to the fluidized bed to be calculated. This equipment provided data for the simulation modelling.

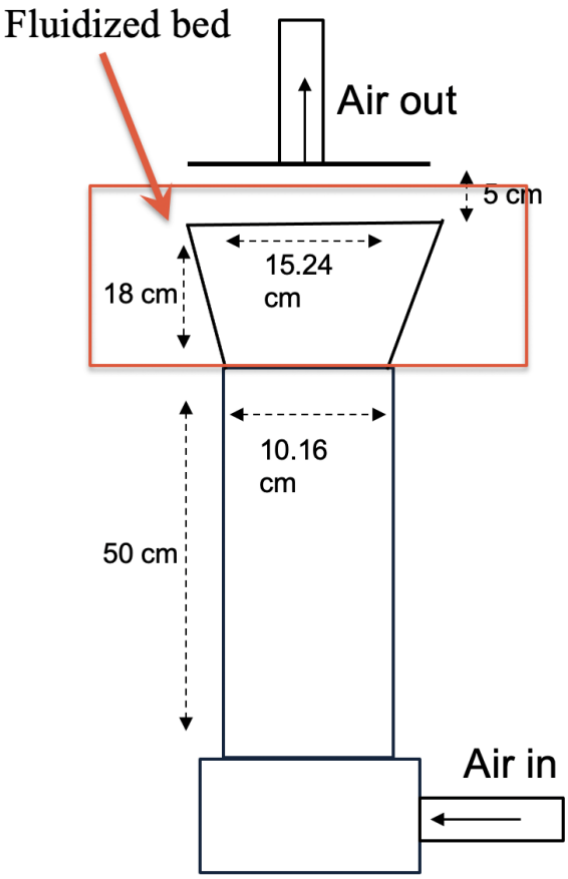

Figure 6. *The fluidized bed used in this study.*

2.3 Simulation Modelling

The modelling and simulation in this project are based on the Kemp and Oakley models. From the research of Kemp and Oakley [87], the drying modelling can be divided into approaches for fast drying material and for slow drying material. The difference between these two materials is that the drying rate of slow drying material was only affected by the air

temperatures, while the drying rate of fast drying material was affected by the air velocities, the air temperatures, and the bed depth [87].

In equations 3 and 4, Z is the normalization scaling factor, $\Delta\tau$ is the time required to remove a certain amount of moisture from the food materials, m_B is the bed weight, and A is the cross-sectional area of the fluidized bed. Hence (m_B/A) means the bed weight per unit area (A), sometimes called the bed loading, G is the air mass velocity, T_{GI} is the temperature of inlet air, and T_{wb} means the temperature of the bed. The normalized scaling factor Z may be used to predict the drying time under different operating conditions, such as different air flow rates and inlet air temperatures. By comparing the drying curve obtained from the modeling and experimental data, the type of material that best represents chickpeas (slow or fast drying) may be assessed.

Fast Drying Material: $$Z = \frac{\Delta\tau_2}{\Delta\tau_1} = \frac{(m_B/A)_2 G_1 (T_{GI} - T_{wb})_1}{(m_B/A)_1 G_2 (T_{GI} - T_{wb})_2} \quad (4)$$

Slow Drying Material: $$Z = \frac{\Delta\tau_2}{\Delta\tau_1} = \frac{(T_{GI} - T_{wb})_1}{(T_{GI} - T_{wb})_2} \quad (5)$$

The scaling equation approach developed by Kemp and Oakley [87] for fluidized-bed dryers utilizes a ratio or factor Z to scale the time coordinates of two drying curves (moisture content–time profiles). The moisture content at a given time t_1 under the first set of drying conditions (dry-bulb temperature, wet-bulb temperature, and air velocity) can be scaled to a corresponding time t_2 under a second set of drying conditions through a simple linear multiplication, defined as the constant ratio or factor $Z=t_2/t_1$. This factor Z is dependent on the differences between the

two sets of drying conditions. The linear nature of this scaling ensures that the shapes of the moisture content–time curves are preserved.

2.4 Microwaving

- Bench Top Microwave

A domestic bench top microwave oven was used in this study to establish the fundamental processing conditions for microwave processing. By testing different masses of pulses (10 g, 20 g, 50 g, 100 g, 200 g and 500 g) at different microwaving times (0.5 minutes, 1 minute, 2 minutes, 5 minutes and 10 minutes), the relationship between microwaving and phytic acid reduction was obtained.

The final temperature of the dehulled faba beans after microwaving was measured with an immersion thermometer. The microwave intensity (kJ g^{-1}) was estimated from the product of the microwave power and the time of microwaving divided by the mass of the beans.

- Industrial scale microwave

To scale up, a 20kW industrial microwave oven (MIP3 Batch Tempering & Drying Oven, Ferrite Microwave Technologies) was considered. Using the bench-top microwaving data, the amount of faba beans that can be treated to reduce their phytic acid contents by 96.5% in an industrial microwave oven system was determined. The annualized capital cost and the operating cost of the industrial microwave have been analysed.

For the reduction of phytic acid, it was hypothesized that the reduction of phytic acid during microwaving is related to the temperature and microwave intensity (microwave energy per unit mass of faba beans). This study have assumed the following relationship between the reduction of phytic acid and final temperature (T, K) and microwave intensity (I, kJ/kg):

$$\text{Reduction of phytic acid (\%)} = a^* I + b^* T \quad (6)$$

Where a and b are constant parameters. From basic reaction kinetic theory, all chemical reactions stop at zero degrees Kelvin [88]. This is the reason for using units of degrees Kelvin rather than degrees Celsius here.

3. Methods

3.1 Trypsin Inhibitors

A standard colorimetric method was used in this project. This method has been approved and reapproved by the American Oil Chemists Society (Method Ba 12-75) and the American Association of Cereal Chemists International (Method 22-40.01). The method was conducted as described by Liu [89].

3.2 Phytic Acid

A sensitive method from Haug et al. [90] was used in this study, as described in Bhinder et al. [91]. Briefly, 0.5 g of faba bean flour was stirred in a 0.2N solution in 25mL of HCl for three hours and then filtered. A ferric solution was prepared by dissolving 0.2 g of ammonium iron (III) sulphate in 100 mL of 2N HCl and diluting it to 1000 mL with distilled water. A 2,2′-bipyridine solution was prepared by dissolving 10 g of 2,2′-bipyridine and 10 mL of thioglycolic acid in 1000 mL distilled water. A sample extract (0.5 mL) and 1 mL of a ferric solution was mixed in a boiling water bath for 30 min. A 2,2′-bipyridine solution (2 mL) was added after the solution had cooled down, and the absorbance was measured at 519 nm by

using a UV-Vis spectrophotometer (Cary 60 Instrument, Agilent, Santa Clara, CA, USA) following a reaction time of 1 min. Samples were also analysed in triplicate.

3.3 In-vitro Protein Digestibility

The method was developed from Hsu et al., [92], which was previously used to measure the protein digestibility for lentils. In order to pass through an 80-mesh screen, all faba bean samples used for in vitro digestion study were ground to a fine flour. A 10 mL volume of aqueous protein suspension (6.25mg protein/mL) in distilled water was adjusted to a pH of 8 (with 0.1N HCl/NaOH). This process was performed while stirring the solution at 37^{o}C in a water bath. To initiate digestion, a pH-adjusted multi-enzyme solution (1.6 mg/mL trypsin, 3.1 mg/mL chymotrypsin, and 1.3 mg/mL peptidase) was added. An aliquot (1 mL) of this multi-enzyme solution was then added to the protein suspension whilst stirring at 37^{o}C. Samples were analysed in triplicates.

Protein digestibility was calculated as follows (Equation 7):

$$\text{Digestibility (\%)} = 210.46\text{-}18.1x \quad (7)$$

Where x is the pH at the time of 10 minutes.

The pH-drop method estimates protein digestibility by measuring the change in pH after a specified period (10 min) of hydrolysis. It is based on the principle that hydrolysis results in the release of carboxyl (-COO^{-}) and amino (-NH^{3+}) groups [92]. At neutral and alkali pHs, the free amino groups deionize and protons (H^{+}) are liberated. The free H+ groups released into the surrounding reaction medium cause a decrease in pH, and the drop in pH is recorded automatically over a 10-minute period using a recording pH meter.

3.4 Material Characterization

3.4.1 Fourier Transform Infrared (FTIR) Spectroscopy

Before scanning, chickpeas and dehulled faba beans were ground into powder and sieved through a mesh. This process makes the particle size of the chickpea and dehulled faba bean powder as uniform as possible. Attenuated total reflectance (ATR) spectra were used in this experiment. FTIR spectra were collected at a resolution of 4 cm^{-1} with 32 scans in the wavelength range 2000–400 cm^{-1}. The collected data were analyzed using the software OMNIC 8.2 for further data processing. The interference of water was first subtracted in the calculation process. Then, the curve was smoothed, and the Gaussian deconvolution was calculated. Further calculations quantified the secondary structure of the protein in the amide regions.

3.4.2 Scanning Electron Microscopy (SEM)

Faba bean samples were prepared by using double-sided carbon tape glued to an aluminum stub. Electron micrographs were obtained using a Zeiss ULTRA plus (Carl Zeiss SMT AG, Germany) Scanning Electron Microscope (SEM) in backscatter electron detector (BSD) mode with an operating vacuum of 1Pa (absolute). 200-30,000x magnification was used in all images.

3.5 Technico Ecoonomic Analysis

This study conducted a techno-economic analysis by evaluating both capital and operational costs in the processing, including drying of dehulled faba bean. The following key factors were included in the analysis:

- **Purchased Equipment Cost (PEC)**: The capital costs of each piece of equipment used in the processing chain, including dehuller, boiler, microwave, and fluidized bed dryer,

were evaluated. These individual equipment costs formed the foundation for determining the overall process plant cost.

- **Process Plant Cost (PPC)**: The total cost of setting up the processing plant was estimated using the Lang factor, which scales the purchased equipment cost (PEC) to reflect the full plant cost. According to Towler et al, [93] PPC is generally 3 to 4 times the PEC. This study uses a Lang factor of 4 to account for additional costs, including equipment installation, piping, electrical connections, and control systems.
- **Capital Recovery Factor (CRF)**: The capital recovery factor was applied to calculate the annualized capital expenditure. This factor accounts for the cost of recovering the initial capital investment over the equipment's lifespan and incorporating both interest rates. The CRF is a critical component for assessing the long-term financial sustainability and payback period of the processing facility.

$$CRF = \frac{i\,(1+i)^n}{(1+i)^n - 1} \tag{8}$$

Where i is the interest rate (fractional), and n is the number of repayments.

- **Energy Costs**: Energy consumption was calculated for each piece of equipment, including electricity, natural gas for heating, and water. The air recycle system fluidized bed drying system is expected to significantly reduce energy consumption, contributing to lower operational costs.
- **Cost of Operational Labor (COL) and Cost of Manufacturing (COM)**: The cost of operational labor (COL) and the overall cost of manufacturing (COM) were considered.

$$COM = Direct\ Manufacturing\ Costs\ (DMC) + Fixed\ Manufacturing\ Costs\ (FMC) + General\ Expense\ (GE) \quad (9)$$

According to Turton [94], direct manufacturing costs (DMC) includes the cost of raw material, waste treatment, utilities, operating labor, direct supervisory and clerical labor, maintenance and repairs, operating supplies, laboratory charges and patents and royalties.

$$DMC = CRM + CWT + CUT + 1.33COL + 0.069FCI + 0.03COM \quad (10)$$

For the fixed manufacturing costs includes depreciation, local taxes and insurance and the plant overhead costs [94].

$$FMC = 0.708COL + 0.168FCI \quad (11)$$

General expenses (GE) includes the cost of administration, distribution and selling costs, and the research and development expenses [94].

$$GE = 0.177COL + 0.009FCI + 0.16COM \quad (12)$$

By adding these three costs together, the total manufacturing cost could be obtained by follow [94].

$$COM = 0.304\,FCI + 2.73\,COL + 1.23\,(CUT + CWT + CRM) \quad (13)$$

Where FCI is the fixed capital investment, COL is the cost of operating labor, CUT is the cost of utilities and CWT is the cost of waste treatment and CRM is the cost of raw material. The factor (0.304) of FCI is the capital recovery factor (CRF). 0.304 means the interest rate is 16% and the number of repayments is 5 years. 0.304 as the CRF used in this study. When the interest rate is 10% and the number of repayments is 10 years, the CRF is 0.163. Both 0.163 and 0.304 were used in this work.

By integrating these critical factors (PEC, PPC, CRF, energy costs, COL and COM) this study delivers a technico-economic assessment of the faba bean drying processing. This analysis not only identifies areas for cost optimization but also underscores the importance of efficiency in both capital investment and ongoing operations.

3.5.1 Air Recycling System

- **The use of air recycling:** These considerations lead to a conceptual scheme for operating the fluidized bed with partial recycle of air, as shown in Figure 7. In this system, the air heater is required to heat the new make-up air, provide energy for evaporation, and compensate for heat losses from the whole system. Increasing the amount of recycle then increases the gas humidity, reducing the drying rate, thereby increasing the required bed cross-sectional area, increasing the capital cost. However, it also decreases the amount of air that must be heated, reducing the air heating costs. In addition, when air is recirculated, the increase in humidity raises both the wet-bulb temperature and the drying time relative to the original conditions.

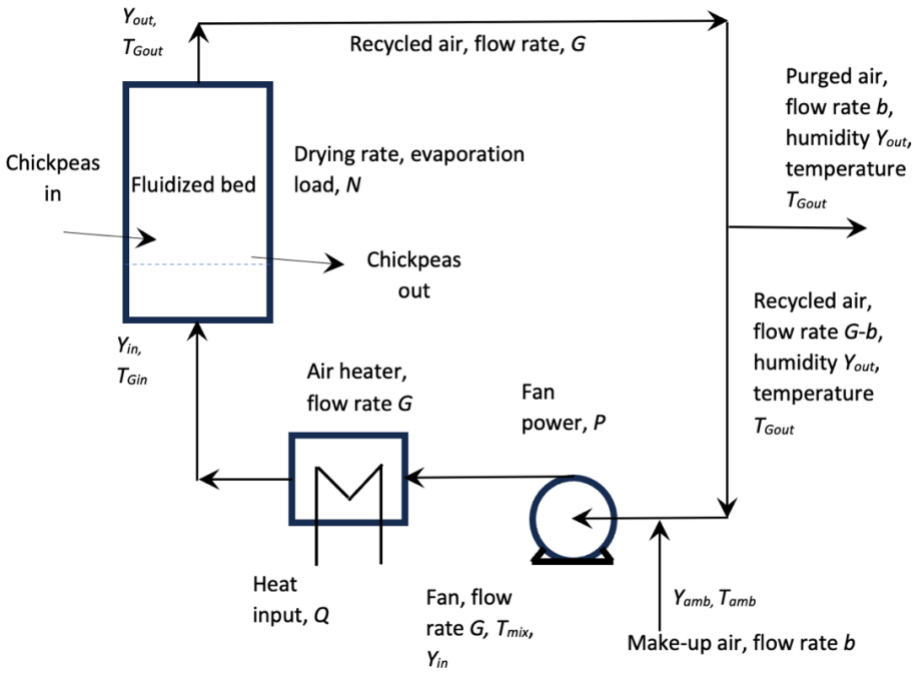

Figure 7. *Schematic diagram of air recycle system for fluidized bed drying (of chickpeas and other pulses)*

The configuration of the system includes the following features. The purged air is drawn out of the system after the dryer, with a temperature and humidity equal to the values of those variables leaving the dryer, T_{Gout} and Y_{out}, respectively. The make-up air comes from the ambient atmosphere at a temperature and humidity of T_{amb} and Y_{amb}, respectively.

3.5.2 Microwaving Drying Processing

The situation for domestic bench top and industrial scale microwave ovens analysed in the Chapter 7. The domestic bench top oven has been tested first, before scaling to the industrial oven. Dehulled faba beans from Australia Export Grains Innovation Centre were used in the study. The overall microwaving procedure is shown in the following flowchart (Figure 8).

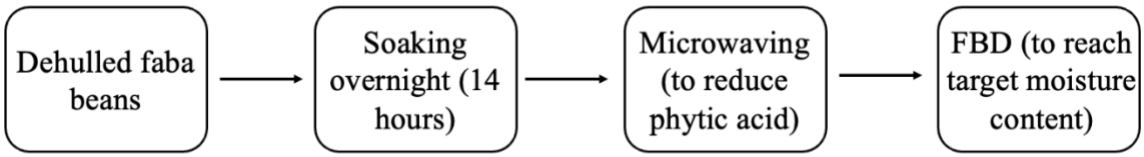

Figure 8. The flow chart of the microwave drying process.

The dehulled faba beans have been soaked in water for 14 hours, and the ratio of water and faba beans was 500 ml water soaking 100 g faba beans. After soaking, the water has been drained out and the microwaving has been done to reduce the content of phytic acid in the dehulled faba beans. Then the dehulled faba beans have been dried in the fluidised bed dryer need to reach the target moisture content (around 14%).

3.5.2 Boiling Process

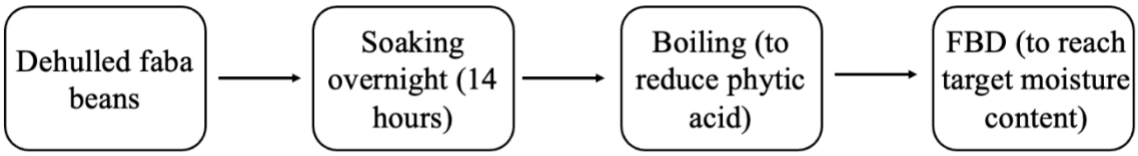

Figure 9. The flow chart of boiling process.

Similar to microwave drying, the dehulled faba beans were soaked in water for 14 hours, and the ratio of water to faba beans was 500 ml water soaking to 100 g faba beans. After soaking, the faba beans were boiled to reduce the content of phytic acid in the dehulled faba beans. Then the dehulled faba beans have been dried in the fluidised bed dryer need to reach the target moisture content (around 14%).

Chapter 4. Fluidized Bed Drying of Chickpeas - Developing a New Drying Schedule to Reduce Protein Denaturation and Remove Trypsin Inhibitors

1.Introduction

With the methodology established in Chapter 3, this chapter applies fluidized bed drying to chickpeas to evaluate its impact on drying performance, protein quality, and anti-nutritional factors. Pulse proteins are valuable ingredients for plant protein-based applications [95]. A new generation of consumers is more inclined towards the consumption of plant-based proteins due to dietary cultural factors and the high cost of animal-based proteins [96]. Among plant proteins, beans, peas, lentils and chickpeas have received significant attention, due to their sustainability and high nutritional value [1]. Chickpeas are a good source of carbohydrates and proteins, meeting adult requirements for all essential amino acids except methionine and cysteine, and they have low tryptophan contents. Therefore, this work studies the processing and drying of chickpeas.

Fluidized bed drying is an important operating technology in the pharmaceutical and food industries for solids processing [97]. For example, in the food industry, Nazghelichi studied the energy utilization of carrot cubes during fluidized bed drying process [98], the performance of industrial dryers has significant improved. Various scholars [99, 100] have argued that fluidized bed dryers have good temperature control and high heat-transfer efficiency. Relatively uniform product properties are found from using during the fluidized-bed drying process [101]. In fluidized-bed dryers, the heat and mass-transfer coefficients between solids and gases are high, and the products can be dried under relatively mild conditions [98, 102]. Hence fluidized bed drying technology may reduce product degradation

[99]. Therefore, fluidized bed drying technology is potentially suitable for the processing of pulse proteins.

In addition, some of these compounds in pulses protein are toxic, unpalatable or anti-nutritive for human consumption due to their tendency to block the absorption of nutrients, inhibit human metabolism or slow down digestive reactions. These materials are termed 'anti-nutritional factors' (ANFs) [3, 19]. According to Kumar's review, trypsin inhibitor, chymotrypsin inhibitor and phytic acid are three main ANFs for chickpeas. Trypsin is a proteolytic enzyme that is important for the digestion of proteins in living organisms [50]. Common methods for inactivating trypsin inhibitors include thermal treatments, soaking, germination and chemical treatments [50]. The thermal inactivation of trypsin inhibitor depends on the duration, temperature and moisture content of the sample [103]. Hence the content of trypsin inhibitor is likely to decrease during fluidized bed drying, and it may vary with drying temperature, time, and moisture content.

A drying schedule refers to a set of dry and wet-bulb temperatures that vary with time and moisture content of the product during the drying process. The concept of a drying schedule is commonly used in the drying of timber. There is significant literature outlining the application of drying schedules for reducing the distribution of moisture contents in a batch of timber [104, 105] developed and optimized a drying schedule for the drying of timber boards to reduce the number of small and medium-size cracks in the final dried timber. However, drying schedules have not been reported to any significant extent for the fluidized bed drying of most food products, particularly where the protein structures have been preserved while significantly reducing the concentrations of trypsin inhibitors. This development of a drying schedule for the processing of a pulse protein in a fluidized-bed dryer is a novel, original and innovative aspect of this work.

The challenge for the pulse-protein drying process is how to preserve the protein secondary structure and remove anti-nutritional factors at the same time. If the drying temperature is too high, the protein will be denatured, and conversely, if the drying temperature is too low, the ANFs will not be removed. The aim of this study is to improve the drying technology of pulse proteins and reduce the content of ANFs to the greatest extent while reducing the secondary structural changes of pulse protein as much as possible. This study demonstrates the feasibility of simulation modelling for the fluidized bed drying of pulse protein, which will assist in estimating drying times and production capacities for scale up. Overall, this study not only addresses the problem of ensuring the protein quality of chickpeas during the drying process, but also provides a basis for simulating the drying rate of this material. The drying conditions will be applicable to the scaled up drying operations for chickpeas.

2.Results and Discussion

2.1 Constant Drying Temperatures

This study has analyzed the drying of chickpeas under constant temperatures and drying schedule. This section has described the drying curves, simulation modelling, protein conformation modifications and trypsin inhibitor levels at constant drying temperature conditions of 40, 60 and 80^{o}C. The fluidized-bed drying equipment has been described in section 2.2 and Figure 10.

2.1.1 Drying Curves of Chickpeas

The drying curve is useful for estimating drying times and calculating drying rates. The moisture content-time curves in Figure 10 were obtained by measuring the moisture contents of chickpeas from samples taken every half an hour. Figure 10 shows the drying curves at three different temperatures. At an inlet air temperature of 40^{o}C, the process displayed the slowest

drying rate, requiring six hours to reach the target moisture content (14%). At 60°C, the process required three hours to achive the target moisture content (14%). The fastest drying rate was recorded at 80°C, reaching the target moisture content (14%) in 1.5 hours.

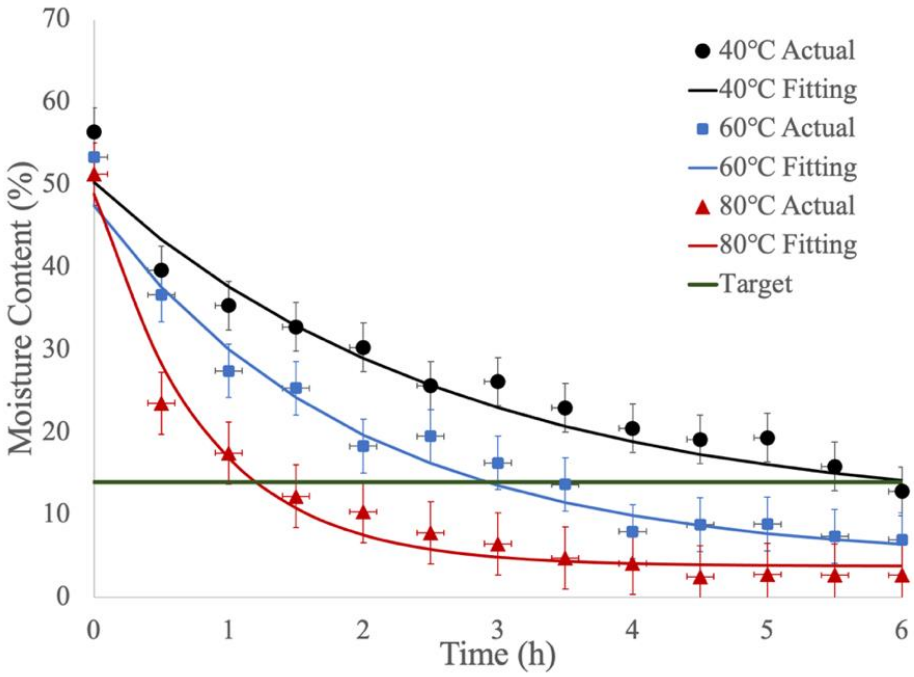

Figure 10. *Moisture content-time curves for the fluidized bed drying process of chickpeas at 40, 60 and 80°C*

During drying, both wet-bulb (T_{wb}) and dry-bulb (T_d) temperatures were measured in the ambient environment and within the fluidized bed. The corresponding air humidity (mixing ratio) was then calculated using the following psychrometric equation:

$$Y = 621.97 \times \frac{6.11 \times 10^{7.5 \times \frac{Twb}{237.7+Twb}}}{P - 6.11 \times 10^{7.5 \times \frac{Twb}{237.7+Twb}}} \quad (14)$$

where Y is the absolute humidity (g water/kg dry air), T_{wb} is the wet-bulb temperature (°C), and P is the atmospheric pressure (Pa).

The corresponding dry-bulb temperatures, wet-bulb temperatures, and relative humidity values for each of the constant inlet air temperatures are shown in Table 9.

***Table 9**. Dry-bulb temperatures, wet-bulb temperatures and relative humidities for each of the constant inlet air temperatures.*

	Average Humidity		
Dry- bulb	40.1	60.1	80.0
Wet-bulb	24.4	26.5	34.2
Relative Humidity	41%	17%	11%

As expected, the drying rate in Figure 10 increased with increasing temperature, as is generally expected for most materials, also for chickpeas from the work of Cil and Topuz [106].

2.1.2 The Scaling Technique for the Fluidized Bed Drying of Chickpeas

According to the Kemp and Oakley models [87], the difference between fast drying material models and slow drying material models is the bed weight per unit area. "Bed Loading" is the mass of material per unit of total fluidized bed area, in this case the dry mass of chickpeas. The total area of the fluidized bed was fixed, so changing the amount of chickpeas fed to the bed was required to change the bed loading. Even a relatively small change in mass was enough to change the bed load significantly. Changing the bed load helps to differentiate between "slow" and "fast" drying materials. According to equations 2 and 3, if changing the bed load has little or no effect on the drying curve (moisture content as a function of time), the material is a "slow" drying material. If changing the bed load has a large effect on the drying profile, then the material may be a "fast" drying material.

In this study, the bed mass was changed from 200g to 100g and 500g (by 50% and 150%) at 40^{o}C. Based on equations 2 and 3, fast-drying material and slow drying material modelling was used to predict the drying curves at 100g and 500g bed loading, respectively. According to

Figure 11, the drying curve obtained from the fast-drying material modelling was inconsistent with the drying curve obtained in the actual experiment. By contrast, the actual drying curve matched the slow-drying material curve closely. It can be concluded that chickpeas can be considered to be a slow-drying material, according to this definition.

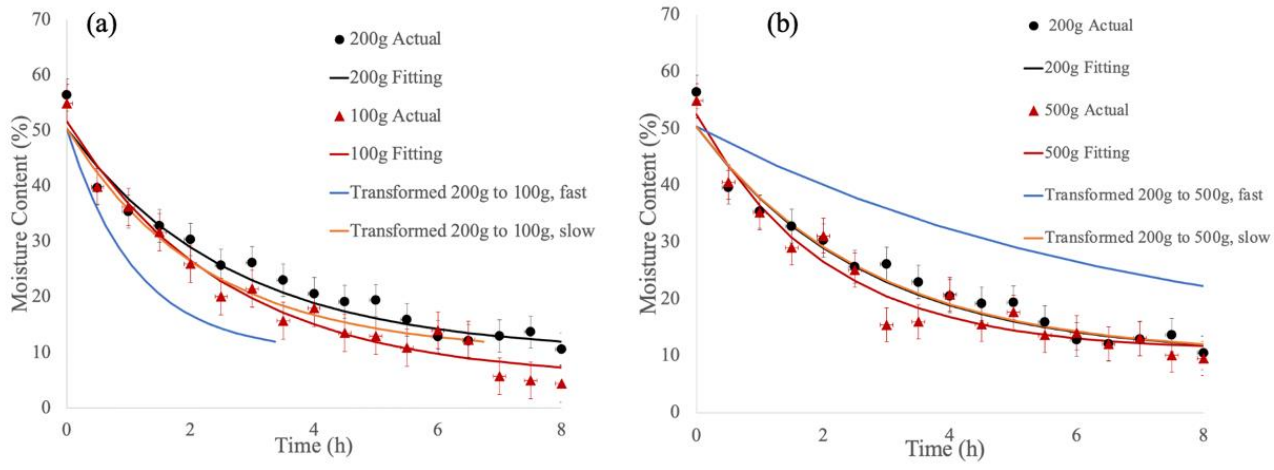

Figure 11. *Predicted drying curve for chickpeas (a) transformed from 200g to 100g, and (b) transformed from 200g to 500g at a constant inlet air temperature of 40°C.*

This study used equation 3 to predict the drying curve of chickpeas at different temperatures. In Figure 11, the solid line is the experimentally obtained drying curve. The dotted line is the predicted result. Figure 11(a) shows the predicted drying curve at 60°C derived from the drying curve at 40°C, and the predicted drying curve of 80°C derived from the drying curve of 60°C is shown in Figure 11(b). Figure 12 shows a slight deviation between the predicted results and the actual data, but most of the points fall within the range of the error bars. It can be concluded that the slow material drying model is suitable for describing the fluidized bed drying process of chickpeas within the temperature range from 40-80 °C.

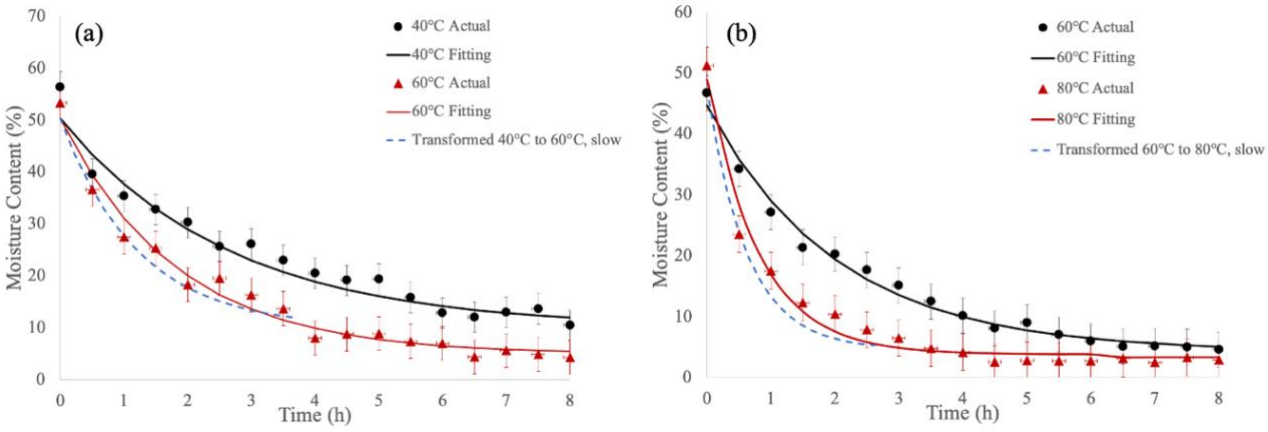

Figure 12. *Predicted drying curve for chickpeas (a) transformed from a constant inlet air temperature of 40 °C to 60 °C, and (b) transformed from a constant inlet air temperature of 60 °C to 80 °C.*

2.1.3 Protein Conformation Modification

Fourier transform infrared spectroscopy (FTIR) is a common method for estimating the secondary structure of proteins. This technique has been used for qualitative and quantitative estimation of protein secondary structure [23, 107, 108]. The following Figure 13 shows the FTIR results at the target moisture content for different inlet air temperatures.

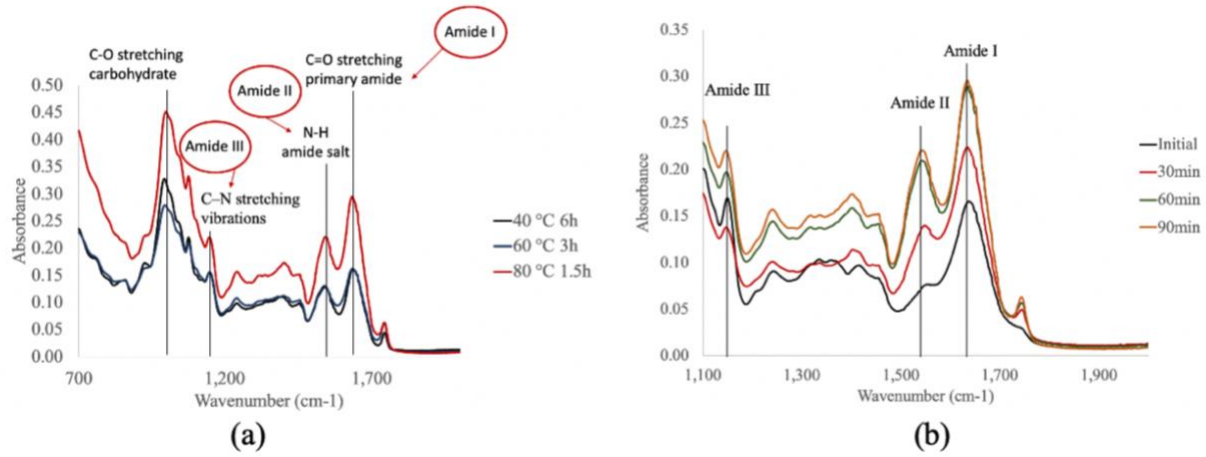

Figure 13. *FTIR results for chickpeas (a) Different constant inlet air temperatures at the target moisture content (14%) (i) 40°C drying for 6 hours, (ii) 60°C drying for 3 hours, and (iii) 80°C drying for 1.5 hours. (b) Different drying times at a constant inlet air temperature of 80°C.*

Figure 13(a) shows the FTIR comparison results at inlet air temperatures of 40, 60 and 80°C. After drying at 80 °C for 1.5 hours, there were obvious changes in the structures of the proteins in the amide I, II and III regions. At inlet air temperatures of 40°C and 60°C, the protein structures were more similar. The changes of protein secondary structure became more obvious with the increase in the inlet air temperature [23]. Heating can cause disorder in the protein secondary structure by affecting disulfide and hydrogen bonds. Heating of the plantglobulins leads to reorganization of the protein secondary structure [109]. Figure 13(b) shows the FTIR results for chickpeas at different drying times with an inlet air temperature of 80°C, indicating that the longer the drying time, the more the protein is denatured through the influence of its secondary structure. At 80 °C, the protein has begun to denature after drying for 30 minutes, but the protein structure was still close to that for the initial protein. After drying for 60 minutes, the protein has been obviously denatured, and there was a significant difference compared to the initial protein structure. There was little difference in protein structure between drying times of 60 minutes and 90 minutes.

2.1.4 *Trypsin Inhibitor*

Although chickpeas have many beneficial nutritional properties, they also contain a variety of ANFs. These compounds exhibit undesirable physiological effects that hinder nutrient absorption [50]. According to Kumar et al.'s review [3], trypsin inhibitor, chymotrypsin inhibitor and phytic acid are three main ANFs for chickpeas. The presence of trypsin inhibitors directly affects the digestibility of the pulse proteins consumed, so removing trypsin inhibitors in chickpeas during the drying process is an important consideration.

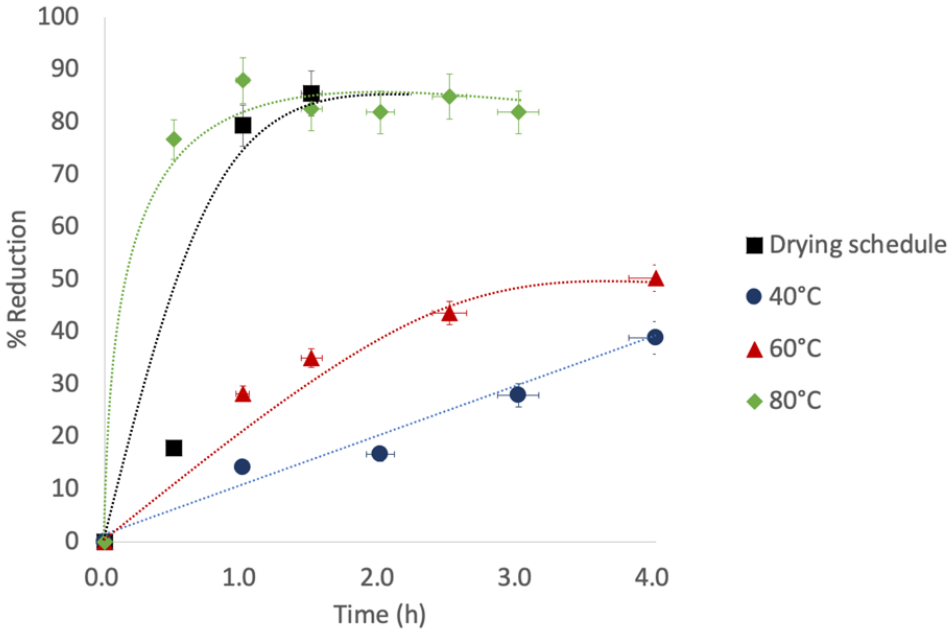

Figure 14. *Effect of fluidized drying on trypsin inhibitor activity (TIA) reduction at different inlet air temperatures.*

Figure 14 shows the results of trypsin inhibitor activity (TIA) reduction at different drying temperatures and drying times. As would be expected, the reduction of TIA was slow at a low inlet air temperature (40 ºC) and fast at a high inlet air temperature (80 ºC). The reduction rate at 60 ºC is higher than that at 40 ºC. The higher the temperature, the easier it is for the trypsin inhibitor to be removed. From the data at 80 ºC, in the initial stage, the rate of decrease of

trypsin inhibitor was very fast. The rate of decrease gradually slowed down after the reduction reached 80%. The decrease rate of trypsin inhibitor is slow at low inlet air temperature. In the study of soybean drying by Stewart et al., it was also found that the reduction of TIA was more pronounced at higher inlet air temperatures [103]. Osella et al. reported the inactivation of trypsin inhibitors as a function of fluidised bed drying time [51]. The trypsin inhibitor is rapidly inactivated in the initial stage, and then the inactivation rate of the trypsin inhibitor decreases. The change in the trend for the trypsin inhibitor inactivation from Osella et al. is consistent with the results of this experiment [51].

2.2 Drying Schedule

Based on FTIR and trypsin inhibitor results from the constant inlet air temperature experiments, this study found that, after drying at 80 ºC for 30 minutes, protein denaturation was not severe, and a large fraction of the trypsin inhibitor could be removed. This observation suggested that the rate of protein denaturation and the rate of trypsin inhibitor reduction are different, and this observation was our motivation for choosing 80 ºC as a starting temperature in developing a drying schedule.

It was observed that prolonged exposure to an inlet air temperature of 80 ºC gave significant protein degradation, so it was decided to reduce the inlet air temperature after the initial high level of 80 ºC to 60 ºC in developing a drying schedule. This subsequent lower inlet air temperature of 60 ºC gave a significantly slower rate of protein degradation while still reducing the levels of trypsin inhibitor. In this chapter, it is shown how such a drying schedule can reduce the level of trypsin inhibitor significantly while still preserving the protein structure.

2.2.1 Drying Curve and Simulation Modelling – Drying Schedule

The initial inlet air temperature was 80 ºC, and after 30 minutes the inlet air temperature was reduced to 60 ºC. As before, a sample was removed every 30 minutes, and its moisture content was measured. From Figure 15, in the first 30 minutes at 80 ºC, the drying rate is very high. When the temperature changed to 60 ºC, the drying rate drops gradually. The target moisture content was reached in two hours.

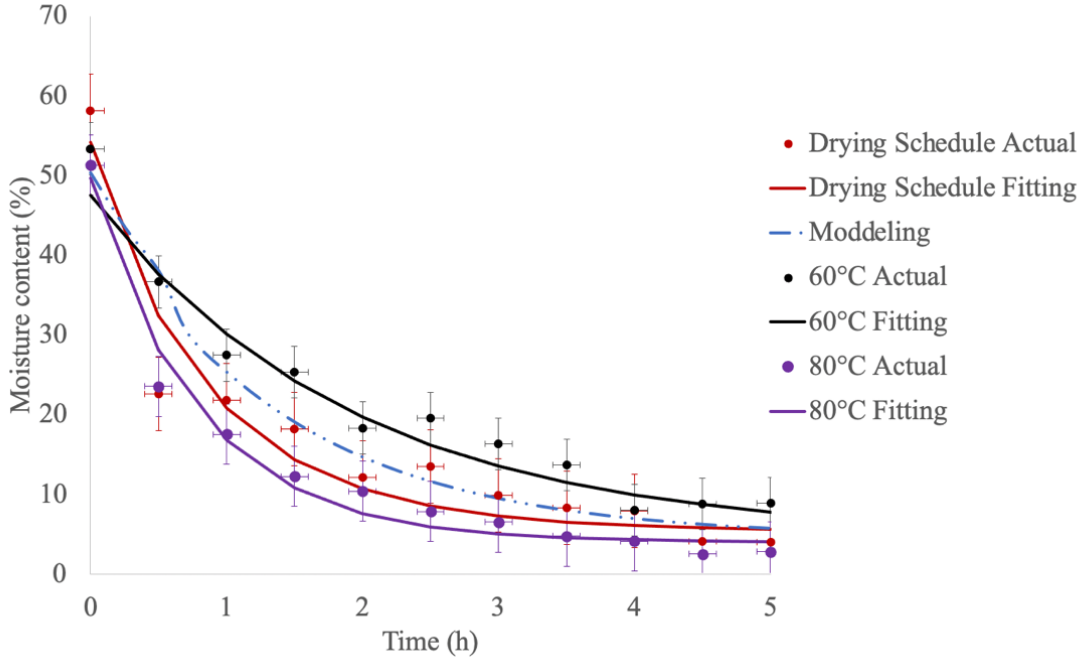

Figure 15. *Moisture content-time curves for chickpeas fluidized bed drying process for each drying condition (60, 80ºC and the drying schedule). The actual data points and fitted curves for the constant temperature experiments at 60 and 80ºC show that the model fits the experimental data for these conditions within the error bars. The actual data points and modelled curves for the drying schedule shows that the model predicts the experimental data within the error bars in the experimental data.*

At same time, the dotted line is the predicted result from the scaling model for a slow drying material. Figure 15 shows that the forecasts deviate slightly from the actual drying schedule data, but most of the points are within the error bars. These results further confirmed that the

slow-drying material model is suitable for describing the fluidized-bed drying process of chickpeas.

2.2.2 Protein Conformation Modification

This study has used Gaussian convolution spectral data processing technology to analyse changes in the protein conformation, enhancing the resolution of infrared spectra and distinguishing significantly overlapping spectral bands. Among them, the amide I region is the most sensitive to protein secondary structures, containing α-helices, β-sheets, β-turns, and random coils [110, 111]. Therefore, this project has analyzed this amide I region to estimate the secondary structural components of pulse proteins [23].

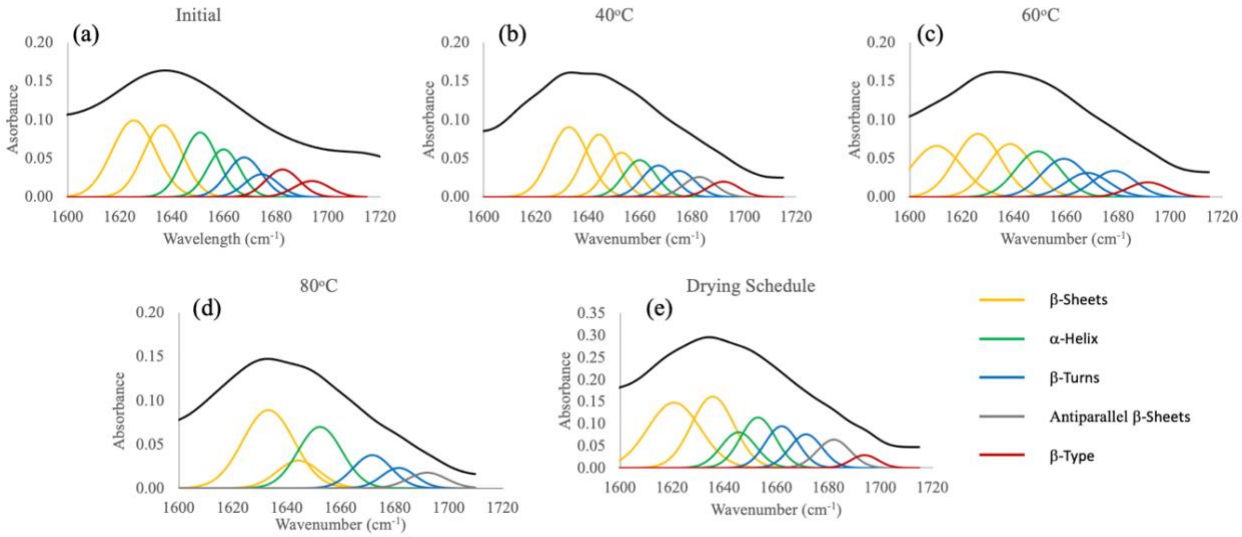

Figure 16. FTIR *spectrum showing amide I bands of chickpeas powder. The outer envelope is the original spectrum, and the individual component peaks underneath are the results of regression analysis. The peaks are associated with different secondary structures. (a) Initial chickpeas, (b) 40°C drying for 6 hours, (c) 60°C drying for 3 hours, (d) 80°C drying for 1.5hours, and (d) Drying schedule for 2 hours.*

Figure 16 shows the amide I spectrum of the initial chickpeas (after soaking) together with its Gaussian spectral convolution. As an example, eight Gaussian bands have been resolved for the initial chickpeas, centred at 1625, 1636, 1650, 1659, 1667, 1674, 1692 and 1693cm^{-1}. According to Table 1 from Shevkani et al., the FT-IR amide I (1600–1700 cm^{-1}) bands of the secondary structure components for pulse proteins can be assigned as follows [23]. For the initial chickpea samples, the peak at 1625cm^{-1} was considered to represent an antiparallel β-sheet or aggregated strand. The peak at 1636cm^{-1} was interpreted as a β-sheet. The waveband from 1650cm^{-1} to 1660cm^{-1} was assigned to α-helices, while the band from 1660 cm^{-1} to 1695 cm^{-1} was assessed as β-turns or β-type structures. In addition, the percentage of α-helices, β-sheets and β-turns can be calculated from the band area. Figure 16 shows amide I bands for the chickpeas. The black outer envelope is the original spectrum.

From the comparison with the initial protein secondary structure, the inlet air temperatures of 40°C and 60°C showed similar changes to the protein secondary structure. At an inlet temperature of 80°C, the secondary structure of the protein was significantly changed. This is also consistent with the results from Figure 16. The drying schedule appeared to have a good protective effect on β-sheets, α-helices and β-turns, and the percentages of these three secondary structures did not change greatly. Compared with the results from the constant drying temperatures, the drying schedule showed the smallest changes in the secondary structures of this pulse protein. In other words, the drying schedule appeared to reduce the denaturation of pulse protein compared with constant inlet air temperature drying.

Table 10. *Population (relative percentages) of different structural components in the secondary structure of pulse proteins in amide I regions for different inlet air temperatures.*

Secondary structure component	Frequency (cm^{-1})	Initial	40°C	60°C	80°C	Drying schedule
β-sheets	1600-1638	46%	66%	55%	67%	48%
α-helices	1650-1660	28%	9%	14%	10%	23%
β-turns	1660-1680	16%	15%	27%	17%	18%
Antiparallel β-sheets	1680-1688	0	5%	0	5%	7%
β-type	1690-1695	11%	4%	4%	0	3%
σ (standard error, compared with initial results)			0.23	0.21	0.31	0.13

The percentages of, α-helices, β-sheets and β-turns have been calculated as follows. For example, with the α-helices, the percentage has been calculated as the areas for the bands assigned to α-helices divided by the total band area (Yazdanpanah and Langrish, 2013). The ratios for different structure components in the secondary structure of pulse proteins in the amide I region for different drying temperatures (40°C, 60°C, 80°C and drying schedule) have been shown in Table 10. According to literature, β-sheets accounted for about 40.4%, α-helices accounted for 32.7%, and β-turns accounted for 18.9% of the total secondary structure for chickpeas [112]. These values are close to the initial chickpea data obtained in Table 10. From Table 10, during the drying process, the proportion of β-Sheets and β-Turns increased, while the proportions of α-helices decreased. When drying at an inlet air temperature of 60°C, the structure of β-Turns changed significantly.

2.2.3 Trypsin Inhibitor

Table 11 shows the trypsin inhibitor activity at the target moisture content for different drying temperatures. The results from this study have been compared with the literature. At an inlet air temperature of 40 ºC, six hours drying reduced the trypsin inhibitor levels by 47.7%. Three hours reduced the trypsin inhibitor levels by 46.3% at an inlet air temperature of 60 ºC. The results show that, at inlet air temperatures of 40 ºC or 60 ºC, there was little reduction in the TIA levels at the target moisture content. In other words, the TIA levels reduced slowly at low temperatures. At an inlet air temperature of 80 ºC, the TIA levels reduced rapidly, decreasing by 81.8% in 1.5h. The inlet air temperature for the first 30 minutes of the drying schedule was 80 ºC. This temperature quickly reduced the TIA within 30 minutes. Then the inlet air temperature changed to 60 ºC, and at this stage, the TIA reduction rate gradually decreased. At the target moisture content, 85.5% of TIA was removed using the drying schedule. The drying schedule balances the denaturation of the protein and the removal of the trypsin inhibitor. Table 4 shows the effect of different drying conditions on the activity of trypsin inhibitor. This inlet air temperature of 80 ºC also causes the denaturation of the protein to be severe. Stewart et al. found that TIA from soybeans loses activity irreversibly in the temperature range from 80 ºC to 110 ºC. Low temperature and microwave treatment were found to be inadequate for removing trypsin inhibitor [103].

Table 11. *Trypsin inhibitor activity at the target moisture content for different inlet air temperatures.*

Drying temperature	TIU/ml	TIA Reduction (%)
40 ºC-6h	8.6	48±2
60 ºC-3h	10	46±3
80 ºC-1.5h	4.1	82±6
Drying schedule-2h	5.64	86±9

Table 12. *The effect of different drying conditions on the trypsin inhibitor activity.*

Materials	Drying Temperature (°C)	Drying Time (min)	Drying Methods	TIA Reduction (%)	Literatures
Soybeans	121	60	Autoclaved	96	[143]
Soybeans	140	10	Fuidized Bed	95	[51]
Soybeans	60	-	Forced Convection	27.2	[103]

3.Conclusions

This chapter focuses on the fluidized bed drying process of chickpeas and their product quality. First, the process using constant temperature drying (40, 60 and 80 °C) was studied. This study found that, at an inlet air temperature of 40 °C, the process displayed the slowest drying rate, requiring six hours to reach the target moisture content (14%). The fastest drying rate was recorded at an inlet air temperature of 80 °C, reaching the target moisture content (14%) in 1.5 hours. At an inlet temperature of 60 °C, the process required three hours to achieve the target moisture content (14%). Second, this study also simulated the drying process of chickpeas using a scaling technique. It can be concluded that a slow material drying model is suitable for describing the fluidized bed drying process of chickpeas. Third, this study addressed the challenge of pulse protein denaturation and the removal of anti-nutritional factors during the drying of chickpeas through developing a drying schedule. This study not only addresses the problem of ensuring the protein quality of chickpeas during the drying process but also provides a basis for simulating the drying rate of this material.

For further study, other ANFs may be considered, if they can be reduced by the thermal treatment involved in drying. The scaling technique is fit for purpose for the range of

temperatures that were studied here (40-80 ^{o}C), but it may have limitations at higher temperatures. Higher drying temperatures can also be considered and studied in the future. The drying strategies developed here are further evaluated in Chapter 5 through a techno-economic analysis, providing insight into the cost-effectiveness and scalability of these approaches.

Chapter 5. Technico-Economic Analysis for the Costs of Drying Chickpeas: An Example Showing the Trade-off between Capital and Operating Costs for Different Inlet Air Temperatures

1. Introduction

Following the experimental work in Chapter 4, this chapter assesses the economic feasibility of fluidized bed drying for chickpeas. Cost models are developed to examine trade-offs between capital investment and operating efficiency. Chickpeas, lentils, and faba beans are the main types of pulses in Australia (AEGIC, 2017). According to Chapter 4, it has developed a drying schedule for chickpeas, with inlet air temperatures between 40 ^{o}C and 80 ^{o}C for various lengths of time, to reduce the concentrations of trypsin inhibitors during drying. It is worth considering, from both financial and carbon emission perspectives, how this drying schedule might be implemented in practice and what the processing arrangements might be for this implementation.

Technico economic assessment for food processing is an established approach, with Olabode *et al.* [113] discussing different processing and marketing modes for potatoes under American conditions in the late 1970's. Their work accounted for the energy required for one serving of potatoes using ten different processing methods. Each of these different modes have various steps and requirements during processing, affecting the supply chain from production, warehouse storage, transport and home usage. Similar energy accounting calculations have been performed for peas, snap beans and corn by Rao [114]. Limitations of the calculations by Olabode *et al.* [113] and Rao [114] include the scope of accounted energy, ending with consumption in the home. Notwithstanding the long track record for the application of technico-economic analysis to food processing, combined technical and economic analysis of

drying technology continues to be seen as a relevant approach to assessing the value of investment in this type of processing.

Chapter 4 compared the technico economic assessment of shipping orange juice from Australia to China, or the juice concentrate, involving refrigeration, with spray drying the juice to form powder, then using non-refrigerated transport for the powder. They concluded that spray drying of juice was economically desirable compared with refrigerated transport. A technico-economic assessment of a hybrid solar-electric dryer has been performed by Nwakuba et al., finding that the new dryer had a rapid payback time of 0.72 years and would save almost $1500 per year relative to a conventional electrically-heated dryer [115]. A greenhouse-type solar dryer has been studied by Philip et al. [116] using technico-economic analysis, again concluding that the greenhouse-type dryer was more economically beneficial than an electric dryer for agricultural produce, with a payback time of 1.5-2.1 years. Haque and Haque did a technico-economic analysis for biomass drying, comparing fluidized bed [117], rotary drum, stationary bed, pneumatic conveying and moving belt dryers, with hot air, humidified air, and superheated steam as drying media. The use of the dry biomass was recommended to reduce the overall carbon emissions from a typical black coal-fired power plant, because of fuel switching. With the open-loop drying configurations that they studied, the carbon emissions were significant, being around 9.2-9.3 kg CO_2 equivalent per unit mass of biomass. Moving belt and rotary drum dryers were considered to be practical choices. The economic evaluation of the production of phenolic powder, by considering its properties, has been explored by Dian and Langrish [118], but without considering the costs of manufacture and transportation of powder compared with refrigerated liquid juice.

Open literature that considers the technico-economic merits of air recycling and uses technico-economic analysis in the optimization of the recycle ratio is relatively uncommon, possibly due to potential commercial sensitivities. This chapter explores the application of technico-

economic criteria to the optimization of the recycle ratio during the drying of chickpeas, where this drying reduces the levels of trypsin inhibitors, which are anti-nutritional compounds that may be reduced during drying schedule.

2. Results and Discussion

2.1 Capacity and Basis Calculations

The basis is assumed to be a throughput of 60 kg h^{-1} total solids for (an assumed) 8000 operating hours per year, which would cover around 10% (480 t/year) of the export volume for chickpeas in Australia (450,276 t/year in 2020) [119].

Based on Chapter 4, this study assumed that the initial moisture content is 55% on a dry basis (d.b.), with a final moisture content of 14% (d.b.), or 0.5 kg water (kg dry solids)$^{-1}$, or 0.33 kg water (kg total solids)$^{-1}$ input.

Here, the evaporative load is given by the following calculation:

$$\begin{aligned}\text{Evaporative load (overall drying rate)} &= \frac{(55\% - 14\%)\ \text{kg water}}{100\%\ \text{kg dry solid}} \\ &\times \frac{60\ \text{kg h}^{-1}\ \text{total solids}}{1.55\ \text{kg (dry solid + water)(kg total solid)}^{-1}} \\ &= 15.871\ \text{kg water h}^{-1} = 0.00441\ \text{kg water s}^{-1}\end{aligned} \quad (15)$$

This evaporative load is also the overall drying rate, which is relevant to the calculation of both capital and operating costs.

The situation for a straight-through, open-loop, fluidized-bed drying system for chickpeas will be analyzed first, showing the need for the recycle of air to create a partially closed system that is more economical.

2.2 Open Loop

2.2.1 *Drying Rate, Drying Flux and Fluidized Bed Sizing Calculations*

The drying data from Chapter 4 show that 200 g of chickpeas can be dried in a 0.1 m diameter fluidized bed at various inlet air temperatures in different drying times from an initial moisture content of 55% to a final moisture content of 14%. Then, the scaling (drying) model assessed by Chapter 4 (and found to be valid) allows for the effects of different air inlet temperatures (T_G) over a range from 40ºC to 80ºC, as follows:

$$Z = \frac{\Delta\tau_2}{\Delta\tau_1} = \frac{(T_{G1} - T_{wb1})}{(T_{G2} - T_{wb2})} \tag{16}$$

Where the subscripts 1 and 2 refer to different drying conditions, and $\Delta\tau$ is the drying time. The model accounts for the effects of varying air humidities through the effect of humidity on the wet-bulb temperature (T_{wb}). The wet-bulb temperature (T_{win}) for the (T_G) 60ºC experiment in Chapter 4 was 26.5ºC, giving a drying time of 3 hours, corresponding to an inlet air humidity of 0.0077 kg kg^{-1}.

Equation 14 may be rewritten for the drying time ($\Delta\tau$) for a range of wet-bulb depressions (T_G – T_{wb}), as follows:

$$\Delta\tau = (3\text{ h})\frac{(60\ ^{o}\text{C} - 26.5\ ^{o}\text{C})}{(T_G - T_{wb})} = \frac{100.5\text{ K h}}{(T_G - T_{wb})} \tag{17}$$

In terms of the drying flux, this equation may be used as follows:

$$\text{Drying flux} = \frac{(55\% - 14\%)}{100\%} \times \frac{200\ \text{g}}{1000 \frac{\text{g}}{\text{kg}}} \times \frac{1}{\Delta\tau} \times \frac{1}{\pi/4\ (0.1\ \text{m})^2} \tag{18}$$

$$= \frac{10.44}{\Delta\tau}\ \text{kg m}^{-2}\ \text{h}^{-1} = \frac{10.44}{100.5}(T_G - T_{wb})\ \text{kg m}^{-2}\ \text{h}^{-1}$$

$$= 0.1039\ (T_G - T_{wb})\ \text{kg m}^{-2}\ \text{h}^{-1}$$

This equation then gives the required fluidized-bed cross-sectional area (A, m^2), initial and final moisture for this required drying rate of 15.9 kg h^{-1}:

$$A = \frac{15.871\ \text{kg water h}^{-1}}{0.1039\ (T_G - T_{wb})\ \text{kg m}^{-2}\ \text{h}^{-1}} = \frac{152.77}{(T_G - T_{wb})}\ \text{m}^2 \tag{19}$$

The full set of drying time, drying (evaporation) flux, and full-scale fluidized-bed sizing calculations for chickpeas, based on the drying data of Chapter 4 for 200 g of chickpeas, from an initial moisture content of 55% (dry basis) to a final moisture content 14% (d.b.), is shown in Table 13 for air temperatures between 40 °C and 80 °C.

Table 13. Drying (evaporation) flux, and full-scale fluidized-bed sizing calculations for chickpeas, based on the drying data of Chapter 4, from an initial moisture content of 55% (dry basis) to a final moisture content 14% (d.b.)

Inlet air drying temperature	**Wet-bulb temperature for an inlet air humidity of 0.0077 kg kg^{-1}**	**Drying flux (evaporative flux)**	**Full-scale fluidized bed cross-sectional area**
(°C)	(°C)	(kg m^{-2} bed area h^{-1})	(m^2)
40	21.04	1.97	8.06
60	26.50	3.48	4.56
80	31.06	5.09	3.12

These required fluidized-bed cross-sectional areas (fluidized-bed sizing) reflect the decreasing size of bed required at higher temperatures.

2.2.2 Capital Costs

Turton et al. have produced a computer program, Capcost_2017.xlsm, which contains capital cost estimates for dryers, including tray, rotary, and spray dryers [94]. In this study, the area-based cost correlation for tray dryers from Capcost_2017.xlsm was used as an approximation for estimating FBD capital costs. This assumption was made with the understanding that both tray dryers and fluidised bed dryers share similar structural elements, including vessel construction, airflow systems, and auxiliary components. Furthermore, the capital cost of both systems is largely influenced by surface area and airflow capacity, which supports the use of area-based scaling. Therefore, although tray and fluidised bed dryers differ in drying mechanisms, this approximation provides a reasonable estimate for comparative for scaling purposes in the absence of a specific FBD cost model. This program gives typical capital costs

in United States dollars for equipment built from mild steel as purchased equipment costs (PEC). The fluidized bed sizes in Table 13 have been used to predict the costs of the fluidized beds in Table 14, assuming that the costs of the fluidized beds are similar to those of tray dryers.

The basic capital cost of the equipment (PEC), as a functional of cross-sectional area (A, m^2), may be represented by the following equation:

$$\text{PEC} = \$6{,}350\ A^{0.587} \tag{20}$$

With the multipliers (Lang factor, stainless steel, dollar conversion), the equation for the Process Plant Cost (PPC, in Australian dollars) becomes:

$$\text{PPC} = \text{AU}\$49{,}529\ A^{0.587} \tag{21}$$

An adjustment, called the Lang factor, is always made between purchased equipment costs (PEC) and process plant costs (PPC), which is a multiplier of 3-4 (taken here as 4). The extra costs include allowances for site preparation, foundations and support structures, piping, instrumentation, control and monitoring equipment, electrical connections, painting, insulation, installation costs and overheads, and other purchase costs [93]. Towler and Sinnott [93] also note that plant costs exhibited only very minor changes between 2013 and 2022, indicating that there is no need to scale capital costs over this period. This conclusion is supported by the Chemical Engineering Plant Cost Index (CEPCI) data presented in their text [93] (Figure 7.3, Section 7.7: *Cost Escalation*). The CEPCI—a composite index published monthly by *Chemical Engineering* and widely used to monitor cost trends in the U.S. process plant industry—shows minimal variation across these years. Although *Chemical Engineering* previously published the Marshall and Swift (M&S) equipment cost index, this was discontinued after 2010 and

therefore does not contribute to recent cost trend analysis. The relative stability of the CEPCI between 2013 and 2022 confirms that cost escalation is negligible, thereby justifying the decision not to apply temporal cost scaling in this study. An allowance should be made for relative costs between carbon steel (material factor, 1.0) and stainless steel (material factor, 1.3, since the final equipment is for food applications) [93]. The conversion factor between the United States dollar and the Australian one has been assumed to be AS$1.5 = US$1. Table 14 therefore also allows for these extra multipliers (Lang factor, 4; stainless steel costs, 1.3; Australian dollar to US dollar conversion, 1.5).

Table 14. *Estimated costs of fluidized beds for chickpea drying, including the conversion from purchased equipment costs (PEC) to process plant costs (PPC, the Lang factor, 4), allowing for stainless steel construction (1.3) and the Australian dollar to US dollar conversion (1.5)*

Inlet air drying temperature	**Basic capital cost (based on tray dryer) (PEC)**	**Process plant cost after using Lang factor, allowing for stainless steel (PPC)**	**Process plant cost in Australian dollars (PPC)**	**Annual Capital Recovery Costs**
(°C)	(US$)	(US$)	(AU$)	(AU$/year)
40	20,800	108,160	162,240	26,445
60	17,000	88,400	132,600	21,614
80	11,700	60,840	91,260	14,875

As outlined in the previous calculations, the inlet air temperature significantly influences the drying flux, which is directly related to the wet-bulb depression and drying time. A higher wet-bulb depression leads to a higher drying flux, thereby reducing the required cross-sectional area of the fluidized bed dryer. This relationship is illustrated in Table 13, where the required dryer area decreases with increasing inlet air temperature.

Since the capital cost of a fluidized bed dryer is generally proportional to the cross-sectional area. A lower inlet air temperature, which requires a larger dryer to achieve the same throughput, results in a higher estimated capital cost. This is why, in Table 14, lower temperatures are associated with higher equipment costs. It is important to note that the capital cost estimates presented in Table 14 do not account for operating costs, including energy consumption. These are addressed separately in Table 16, where energy costs are shown to increase with higher inlet air temperatures due to greater thermal input requirements.

2.2.3 Capital Costs over Time: The Time Value of Money

The time value of money means that the initial capital costs must be recovered over time, and these costs may be added to the operating costs to give the overall cost of manufacturing the final product. These costs are capital recovery costs and are estimated by multiplying the total initial capital cost by a Capital Recovery Factor to give an annual capital recovery cost. The Capital Recovery Factor (*CRF*, 0-1, dimensionless) is defined as[120]:

$$CRF = \frac{i\,(1+i)^n}{(1+i)^n - 1} \tag{22}$$

Here *i* is the interest rate (fractional), and *n* is the number of repayments.

If *i* = 10% (0.1), and *n* = 10 (years), then the *CRF* = 0.163, and these values of the expected interest rate (10%) and capital recovery period (10 years) will be assumed here. This factor is multiplied by the Process Plant Cost (PPC, in Australian dollars) to give the annual capital recovery costs in Table 14.

2.2.4 Operating Costs

The main operating costs for the drying of chickpeas in a fluidized bed are the costs to heat and pump the air required for fluidization and drying and the costs of compensating for heat losses, which are connected with utilities costs. Other ongoing costs include labour and personnel, labour costs per person are quoted in Brennan [120] as being A$80,000 per year per person, with a typical multiplication cost of 3.8 due to supervision expenses, payroll, plant, and laboratory overheads, and the costs of operating supplies. Allowing for selling expenses and [120] the costs associated with research and development, and administration, Brennan also suggests that the overall (total) operating costs should be multiplied by a factor of 1.2 .

The following calculations and discussion focus first on the utility operating costs, since the costs of the utilities for heating are often very significant for drying applications [121]. A

fundamental assumption is that the ambient air temperature is 25°C and that the ambient humidity is 0.0077 kg kg^{-1}.

The air mass flow rate through the fluidized bed (G, kg s^{-1}) may be limited by either [120] the requirement for maintaining a sufficient driving force for drying or by the need to maintain bed fluidization. The fluidization velocity (u_f) used in chickpeas fluidized bed drying was 9.5 m s^{-1}, giving the following air flow rates to meet the need for maintaining bed fluidization:

$$G, \text{Air mass flow rate (kg s}^{-1}) = \rho\, A\, u_f = 9.5\, \rho\, A \tag{23}$$

Where the air density is ρ (kg m^{-3}), and A is the cross-sectional area of the fluidized bed (Table 13). The density of the air may be estimated from the ideal gas equation, as follows:

$$\rho = \frac{P\, M}{R\, T} \tag{24}$$

Here P is the air pressure (101325 Pa at sea level), M is the molecular weight (29×10^{-3} kg mol^{-1} for air), R is the gas constant (8.314 J mol^{-1} K^{-1}), and T is the absolute air temperature (K). With these constant parameters, the air density at the inlet to the fluidized bed is given by the following equation:

$$\rho = \frac{101325 \times 29 \times 10^{-3}}{8.314\ (T_{Gin} + 273.15)} = \frac{353.4}{(T_{Gin} + 273.15)} \tag{25}$$

From a basic mass balance, as described by Pakowski and Mujumdar [122], there is the following equation across the fluidized bed:

$$Y_{out} = Y_{in} + \Delta Y = Y_{in} + \frac{\dot{m}}{G} \tag{26}$$

Here $\dot{m}$ is the drying rate, or evaporative load, 0.00441 kg s^{-1} from equation (1), Y_{out} is the gas humidity out of the dryer (kg kg^{-1}), Y_{in} is the gas humidity into the dryer (kg kg^{-1}), ΔY is the change in gas humidity across the dryer (kg kg^{-1}), and G is the air mass flow rate (kg s^{-1}).

The following equation is given by Pakowski and Mujumdar [122], representing an energy balance for an adiabatic dryer:

$$T_{Gout} = T_{Gin} + \Delta T_G = T_{Gin} - \frac{\Delta H_{vw}}{C_{PY}} \Delta Y \tag{27}$$

In this equation, T_{Gout} is the gas temperature out of the dryer (K), T_{Gin} is the gas temperature into the dryer (K), ΔT_G is the change in gas temperature across the dryer (K), ΔH_{vw} is the latent heat of vaporization for water (around 2200 kJ kg^{-1}), C_{PY} is the specific heat capacity of the gas (around 1000 J kg^{-1} K^{-1} for air), and ΔY has been defined above.

Table 15 shows the predicted air flow rates for maintaining fluidization, the predicted changes in air humidity and temperature across the fluidized bed during drying, and the outlet air humidities and temperatures for each of the inlet air drying temperatures. It is noteworthy that the changes in gas temperature and humidity across the fluidized bed in one pass are very small compared with the inlet air drying temperature and humidity.

Table 15. *The effect of different inlet air drying temperatures on the predicted air flow rates for maintaining fluidization, the predicted changes in air humidity and temperature across the fluidized bed during drying, and the outlet air humidities and temperatures*

Inlet air drying temperature	**G, air flow rate for fluidization**	**ΔY, change in air humidity**	**ΔT_G, change in air temperature**	**Y_{out}, outlet air humidity**	**T_{Gout}, outlet air temperature**
(^oC)	(kg s^{-1})	($\times 10^{-3}$ kg kg^{-1})	(^oC)	(kg kg^{-1})	(^oC)
40	86.4	0.0510	0.112	0.010051	39.9
60	46.0	0.0959	0.211	0.010096	59.8
80	29.7	0.1490	0.327	0.010149	79.7

Given that the evaporative load (overall drying time) is constant at 0.00441 kg s^{-1} for all inlet air temperatures, the energy flow rate required for evaporation or drying is the same, at 9.7 kW. However, the thermal energy required for heating the air (Q, W) to the inlet air temperature is equal to the product of the air mass flow rate, the specific heat capacity of the air (C_{PY}), and the difference between the drying air temperature (T_{Gin}) and the ambient temperature (T_{amb}, i.e. how much the air must be heated up), as shown in the following equation:

$$Q = G\ C_{PY}\ (T_{Gin} - T_{amb}) \tag{28}$$

The pressure drop (Δp, Pa) for the air across the fluidized bed used for the laboratory scale experiments in Chapter 4 was less than 100 Pa. In this study, the superficial air velocity used exceeded the minimum fluidization velocity (u_{mf}), ensuring stable fluidization.

As supported by literature, including Law and Mujumdar [123], the relationship between pressure drop and air velocity in a fluidized bed follows a well-characterized pattern: initially, pressure drop increases with air velocity in the packed bed regime. Once the air velocity reaches u_{mf}, the pressure drop stabilizes, indicating the onset of fluidization. Beyond u_{mf}, the

pressure drop remains relatively constant, independent of further increases in velocity, until excessive velocities lead to particle elutriation and a decline in pressure drop.

In this study, the operating velocities were selected just above u_{mf}, thereby resulting in a relatively low and stable pressure drop (<100 Pa), consistent with the expected behavior for a fluidized bed operating under these conditions. This approach aligns with theoretical and empirical findings related to pressure drop behavior in fluidized systems of similar scale and material properties.

The power (P, W) required for pumping the air required for fluidization may be calculated by the following equation:

$$P = \Delta p \, \frac{G}{\rho} = 100 \, \frac{G}{\rho} \tag{29}$$

For the heat losses, the exposed surface area of the equipment is likely to be proportional to the bed surface area, since the bed surface area determines the overall size of the equipment. The exposed area consists of the top, bottom, and sides of the equipment, together with an associated pipework, so the exposed surface area for heat losses will be taken as five times the bed surface area for estimating the heat losses.

Heat losses are normally limited by natural convection, for which typical natural convection heat-transfer coefficients are around 1^{-10} W m^{-2} K^{-1} [124] and they will be taken as 10 W m^{-2} K^{-1} here as an initial estimate.

Then the heat-transfer rate for heat loss may be estimated from the equation:

$$Q_L = U \, A \, (T_{Gin} - T_{amb}) \tag{30}$$

Here Q_L (W) is the heat loss rate, U is the natural convection heat-transfer coefficient (10 W m^{-2} K^{-1}), and A is the exposed surface area (m^2, five times the bed area). The temperature driving force has been estimated to be the difference between the inlet air drying temperature (T_{Gin}) and the ambient temperature (T_{amb}).

Table 16 shows these predicted thermal and pumping energy requirements, and predicted heat losses, for the different air inlet temperatures.

Table 16. *The effect of different inlet air drying temperatures on the predicted thermal energies required to heat the air at the required flow rates, predicted air pumping power required for fluidization, and predicted heat losses.*

Inlet air drying temperature	***Q*, thermal energy required to heat the air**	***P*, pumping power required to fluidize the bed**	***Q_L*, heat losses**
(ºC)	(kW)	(kW)	(kW)
40	1296	7.7	6.0
60	1632	4.3	8.0
80	1192	3.0	8.6

Given that the drying rate is constant at 0.00441 kg s^{-1} for all inlet air temperatures, the energy flow rate required for evaporation or drying is the same, at about 10 kW. The pumping costs will be electrically driven, while the energy requirements for air heating, evaporation of moisture, and compensating for heat losses will be assumed to be supplied by natural gas. The pressure drop (Δp, Pa) for the air across the fluidized bed used for the laboratory scale experiments in this Chapter was less than 100 Pa. G represents the air mass flow rate and is directly proportional to the cross-sectional area of the fluidized bed dryer. The main reason P varies significantly across different temperatures is due to the variation in G, the air mass flow rate. As described earlier, G is directly proportional to the cross-sectional area of the fluidized bed dryer, which in turn depends on the drying flux. Lower inlet air temperatures result in reduced drying flux and thus require a larger bed area to maintain the same drying capacity. This leads to a higher G and therefore a higher pumping power requirement.

Conversely, at higher temperatures, the drying flux increases, requiring a smaller bed area and reducing the air mass flow rate and pumping power. This temperature dependency of G explains the substantial differences observed in P across drying temperatures.

The costs of electricity in the third quarter of 2023 (Australian Energy Regulator, 2023) were \$31 to \$114 / MWh or \$8.61 to \$31.67 / GJ, compared with gas, at \$10.23 to \$10.80 / GJ, so gas prices were generally lower per unit of energy than electricity ones. The cost for thermal energy (Q) here will be taken as \$10.80 / GJ, while the cost for the electricity used for blowing the air (P) will be taken as \$20 / GJ. Assuming that the process is operated for 8000 hours/year, the gas and electricity costs are given in Table 16 for this situation (60 kg h^{-1} of chickpeas).

For example, consider the figures for an inlet air temperature of 40°C, where Q = 1295.6 kW, Q_L = 6.0 kW, Q_{EV} = 9.7 kW, and the calculations of the gas heating costs follow:

$$\text{Gas cost} = \$10.80 / \text{GJ} \times (1295.6 + 6.0 + 9.7)\,\text{kW} \times 8000\,\text{h/year} / (1000\,\text{kWh} / \text{MWh}) \times 3.6\,\text{GJ} / \text{MWh} = \$407{,}900/\text{year} \quad (31)$$

The following calculation present electricity cost:

$$\text{Electricity cost} = \$20 / \text{GJ} \times 7.7\,\text{kW} \times 8000\,\text{h/year} / \left(1000 \frac{\text{kWh}}{\text{MWh}}\right) \times 3.6\,\text{GJ} / \text{MWh} = \$4{,}410/\text{year} \quad (32)$$

The utilities cost per unit mass of chickpeas can then be calculated, as follows:

$$\text{Utilities cost per unit mass of chickpeas} = (\$407{,}900 + \$4{,}410)\,/\text{year} / \left(60 \frac{\text{kg}}{\text{h}} \times 8000\ \frac{\text{h}}{\text{year}}\right) = \$0.86/\text{kg} \quad (33)$$

For this drying condition and the other conditions, Table 17 summarizes the utilities costs. Labour costs have not been considered here, since the dryer will be assumed to be operated, together with other operating and packaging equipment, using automated process control systems. The utilities cost has, however, been multiplied by 1.2 as suggested by Brennan (2020) to give the total operating costs, allowing for selling expenses and the costs associated with research and development, and administration, as also shown in Table 17. The annual cost of capital has been addressed in Table 16 by multiplying the Process Plant Cost in Australian dollars (PPC, as predicted by using lang factors) by the Capital Recovery Factor (CRF) as shown in equation (7). Combining the annual cost of capital with the total operating costs and dividing by the throughput (60 kg h^{-1} × 8000 h/year) gives the total capital and operating costs per unit mass in Table 17.

Table 17. *Gas and electricity costs, utilities costs, total operating and capital costs, for the once-through drying system when processing 60 kg h^{-1} of chickpeas*

Inlet air drying temperature	**Annual gas heating costs**	**Annual electricity (fan) costs**	**Utilities cost per unit mass of chickpeas**	**Total operating costs per unit mass of chickpeas**	**Total capital and operating costs per unit mass**
(ºC)	($/year)	($/year)	($/kg)	($/kg)	($/kg)
40	407,900	4,410	0.86	1.03	1.09
60	505,700	2,500	1.06	1.27	1.32
80	513,300	1,710	1.07	1.29	1.32

2.2 Raw Material Considerations

The cost of processing (shown in Table 17) adds to raw material costs, so it is appropriate to consider the relative size of the processing costs relative to the raw material ones so assess the

cost addition from processing. The current retail prices in Australia for chickpeas range from AU$ 1.45 to AUS 4.36 / kg [125], but export prices have declined from AU$ 46 / kg in 2012 to AU$ 8.30 / kg in 2022 as chickpea supplies increase. Increased use of chickpeas is likely to increase prices, while increases in the availability of chickpeas may decrease the prices [126]. The processing costs in Table 16 are in the same order of magnitude as the raw material costs, which effectively double the underlying costs of the processed chickpeas compared with the costs of the raw material.

2.4 Closed Loop, Air Recycling

As expected, the operating costs of open-loop, straight-through, air flow are very high due to the high natural gas costs to heat the fluidizing air, so some recycling of the air appears to be indicated as a possibility for reducing the energy consumption.

From a fundamental overall mass balance, at steady state, the flow rate of purged air is equal to the flow rate of make-up air (b in Figure 7). When considering a mass balance for water, the drying rate (or evaporative load), N, must be equal to the net rate at which water leaves the system, being equal to the difference between the make-up and purged air water flow rates, b ($Y_{out} - Y_{amb}$).

A make-up ratio (r) may be defined as follows:

$$r = \frac{b}{G} \tag{34}$$

With this make-up and purge system, the purge flow rate (b) cannot be greater than the gas flow rate through the dryer, G, due to the physical need for a finite gas flow rate between the purge and make-up air points, so the ratio r may vary from 0 to 1. A make-up ratio (r) of unity ($b = G$) corresponds to the open loop system that has just been analyzed. Also, if there was

complete recycle ($b = 0$, $r = 0$), there would be no way for water to leave the system, and the air humidity would increase until drying stopped completely. Smaller values of b correspond to more air being recycled.

In terms of the make-up ratio, the make -up and purged air flow rate is then given as follows:

$$b = r\,G \tag{35}$$

In terms of mixing between the make-up air and the recycle air, as denoted in Figure 7, the mixed air humidity (also the inlet humidity to the dryer, Y_{in}) is given (in terms of the ambient and dryer outlet air humidities) by the following equation:

$$Y_{in} = \frac{b\,Y_{amb} + (G - b)\,Y_{out}}{G} \tag{36}$$

From any humidity, the wet-bulb temperature (T_{wb}) may be obtained, using the procedure outlined in Hecht et al. [126], and this wet-bulb temperature may be used in equation (2) to predict the drying time and drying rate.

Likewise, the mixed air temperature (also the inlet temperature to the heater, T_{mix}) is given (in terms of the ambient and dryer outlet air temperatures) by the following equation:

$$T_{mix} = \frac{b\,T_{amb} + (G - b)\,T_{Gout}}{G} \tag{37}$$

Procedure

1. Specify the inlet air temperature to the fluidized bed dryer (T_{Gin}) and the make-up ratio (r).
2. Guess the dryer cross-sectional area (A), outlet gas humidity (Y_{out}), and outlet air temperature (T_{Gout}).

3. Start the iteration.
4. Calculate the gas flow rate (G) from equation (23).
5. Calculate the purge flow rate (b) from equation (35).
6. Calculate the inlet air humidity (Y_{in}) from equation (36).
7. Calculate the mixed air temperature (T_{mix}) from equation (37).
8. Calculate the outlet air humidity (Y_{out}) from equation (26).
9. Calculate the outlet air temperature (T_{Gout}) from equation (27).
10. Calculate the wet-bulb temperature (T_{wb}) using the procedure outlined in Hecht et al. [126].
11. Recalculate the dryer cross-sectional area (A) from equation (19).
12. Repeat the calculations from step 3.

When this iteration has converged (area values constant within 0.1%), the air flow rates, temperatures and humidities will all satisfy mass and energy balances. The capital cost (PPC) comes from equation (21), translated into annual costs through the CRF, equation (8). The gas cost comes from equation (31), the electricity cost comes from equation (32), with the utilities cost per unit mass coming from equation (33).

Figure 17 shows a very clear and significant decrease in the processing cost per unit mass as the make-up ratio decreases (and the recycle ratio increases) from over A$1.32/kg of chickpeas down to A$0.0885/kg of chickpeas as the make-up ratio changes from 1.0 to 0.01, and the recycle ratio increases (correspondingly) from 0.0 to 0.99 (0%, open loop, to 99%). Figure 17 also shows that, at low recycle ratios (high make-up ratios), the lowest processing cost per unit mass occurs at the lowest inlet air temperature of 40^{o}C (A$1.09/kg chickpeas, compared with

A$1.32/kg at 80ºC). However, a close-up of the surface plot in Figure 18 with high recycle ratios (low make-up ratios) show that the lowest processing cost per unit mass occurs at the highest inlet air temperature of 80ºC and at a make-up ratio close to 0.01 (a recycle ratio of 99%) at this temperature. Use of the fminbnd and fminsearch functions in Matlab leads to a minimum cost at a make-up ratio at 0.0092, which is very close to 0.01. The cost function is very flat in this region, so the difference between make-up ratios of 0.0092 and 0.01 is only a cost difference between A$0.0885/kg of chickpeas and A$0.0886/kg. Recycling the gas leads to an increase in the inlet air humidity from 0.01 kg kg^{-1} (ambient, and open-loop inlet conditions) to 0.0495 kg kg^{-1}.

It is noteworthy that, with open loop processing, the lowest overall processing cost per unit mass ($1.09/kg) occurs with the lowest inlet air temperature (40ºC), due mainly to the lower gas heating costs even with the higher gas flow rate, in this case with a relatively small temperature rise. However, with the exhaust air recycling (closed loop) at the optimum recycle rate (99%), the optimum inlet air temperature is 80ºC. The dramatic decrease in annual processing cost (from $1.09/kg to $0.09/kg) due to the use of recycle and the closed-loop drying operation may also be seen in Table 17.

The key reason for this difference in inlet air temperature at the point of minimum processing cost (but including the annualized capital cost), can be seen from Table 16, which compares the distribution of processing costs between the open-loop and closed-loop cases. The largest difference is the large decrease in air heating costs by using recycle and closed-loop drying, since less air needs to be heated, while the existing air is reused. The key reason is therefore this decrease in natural gas heating costs.

Table 18. *Distribution of costs for optimum open loop and optimized closed loop processing conditions.*

	Open loop, no recycle	Closed loop, recycle ratio 99%
Inlet air temperature (°C)	40	80
Area of fluidized bed (m^2)	8.06	4.41
Annualized capital costs ($ $year^{-1}$)	26,500	19,300
Annual gas heating costs ($ $year^{-1}$)	407,900	17,000
Gas flow rate (kg s^{-1})	86.4	42.0
Annual electricity (fan) costs ($ $year^{-1}$)	4,410	2,240
Total processing cost per unit mass ($ kg^{-1})	1.09	0.09

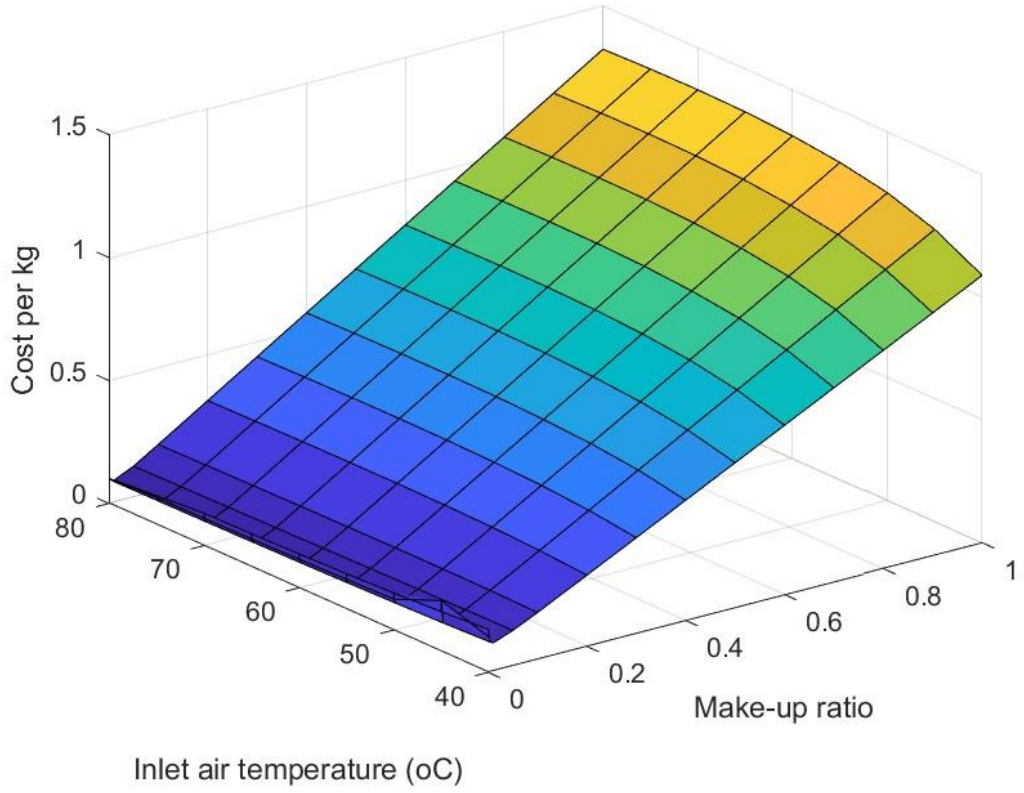

Figure 17*. Surface plot for the cost of processing per unit mass of chickpeas processed as a function of the make-up ratio and the inlet air temperature, for a range of make-up ratios from 0.001 to 1.0 and a range of inlet air temperatures to the fluidized bed of 40-80°C*

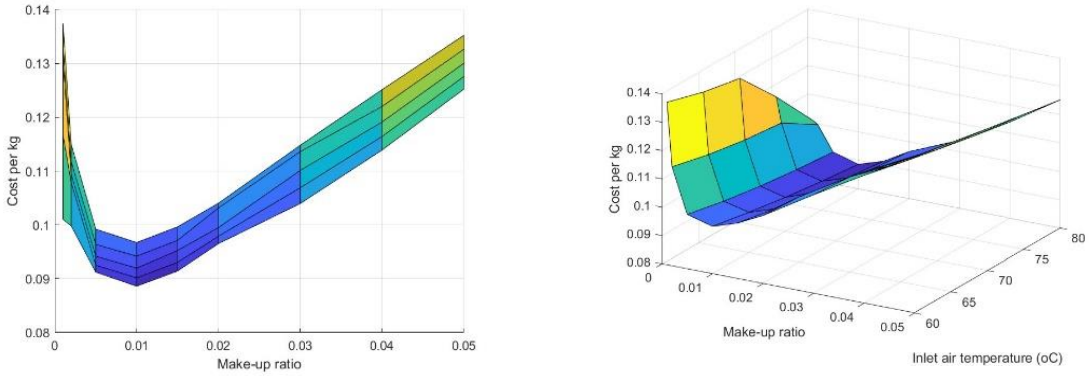

(a) View from the make-up ratio axis

(b) Isometric view

Figure 18. *Surface plot (close-up of Figure 4) for the cost of processing per unit mass of chickpeas processed as a function of the make-up ratio and the inlet air temperature, for a range of make-up ratios from 0.001 to 0.05 and a range of inlet air temperatures to the fluidized bed of 60-80°C.*

2.5 Carbon Emissions

These outcomes may be reviewed in the light of carbon emissions, since both the combustion of natural gas and the generation of electricity contribute to carbon emissions. The carbon emission factors in Australia for electricity and natural gas combustion have been taken from the document Australian National Greenhouse Accounts Factors from Department of Climate Change, Energy, the Environment, and Water, DCCEEW [127]. For electricity, these are 217 kg CO_2-e/GJ, and for natural gas, 65.5 kg CO_2-e/GJ. The resulting plots are very similar in shape to those for financial costs.

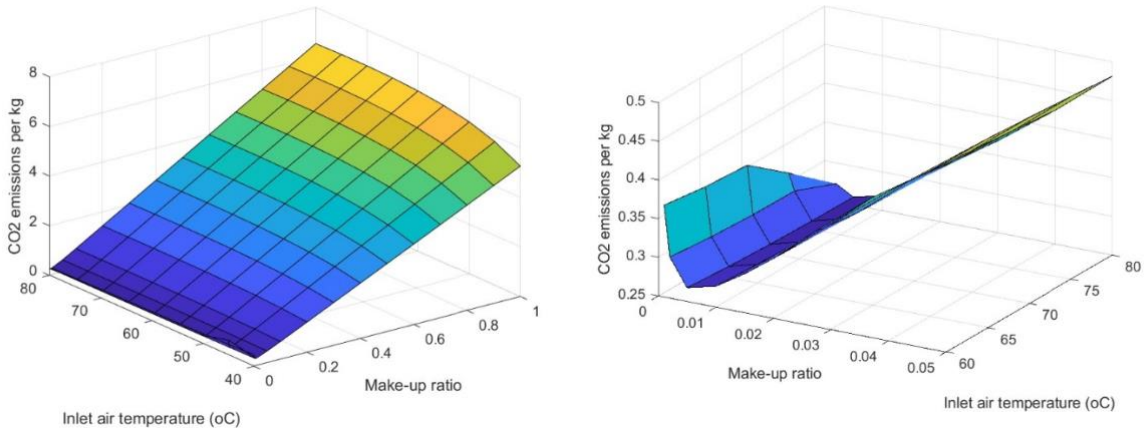

(a) Make-up ratios from 0.001 to 1.0 and a range of inlet air temperatures to the fluidized bed of 40-80 ºC

(b) Make-up ratios from 0.001 to 0.05 and a range of inlet air temperatures to the fluidized bed of 60-80 ºC

Figure 19. S*urface plot for the operating carbon emissions per unit mass of chickpeas processed as a function of the make-up ratio and the inlet air temperature.*

The minimum operating carbon emissions occur at a slightly different make-up ratio (0.0055) to that for the minimum cost (r = 0.0092), with a flat minimum in the operating carbon emissions of around 0.259 kg CO_2 equivalent from the processing per kg of chickpeas. Again, as with the costs, recycling the air more (and reducing the make-up ratio) decreases the carbon emissions from over 6 to 0.259 kg CO_2 equivalent from the processing per kg of chickpeas.

The carbon dioxide emissions (kg CO_2 equivalent) embodied in the stainless steel used for the fluidized bed dryer have been recently quoted as 6.15 kg CO_2 equivalent / kg stainless steel [128]. If the mass of the fluidized bed dryer is assumed to be 500 kg of stainless steel, then the total (capital) embodied CO_2 content for the equipment is 3075 kg CO_2 equivalent. Using the approach described in Hasan and Langrish [129], whereby the Capital Recovery Factor (CRF) from financial analysis is used to annualize the embodied energy and embodied carbon in capital structures, such as this fluidized bed dryer, the same CRF as used in the financial

analysis (0.163) may be used to annualize the total (capital) embodied CO_2 content for the equipment. This approach gives an equivalent annual carbon dioxide emission for the fluidized bed dryer of 501 kg CO_2 equivalent per year. Given the processing of 60 kg h^{-1} and 8000 h $year^{-1}$, the inclusion of the embodied carbon into this analysis adds 501/(60 × 8000) = 0.001 kg CO_2 equivalent emissions per kg of chickpeas that are processed. This addition (0.001 kg CO_2 (kg chickpeas)$^{-1}$) is small compared with the carbon emissions associated with the operating and processing costs (over 0.259 kg CO_2 (kg chickpeas)$^{-1}$).

2.6 Product Quality Considerations

Given that the drying schedule for chickpeas uses inlet air temperatures from 40°C to 80°C, the techno-economic implications of this range of temperatures is worth considering. Reviewing the techno economic results in Figures 2-4, the cost of processing per unit mass and the equivalent carbon dioxide emissions per unit mass show only a very modest variation with the inlet air (drying) temperature, so using a recycle ratio of 99% for the range of temperatures used in the drying schedule (ibid.) will be both financially advantageous and beneficial in terms of minimizing carbon emissions. Implementing this drying schedule in the recycle scheme shown in Figure 17 should also not require any special changes to the schedule.

3. Conclusions

There is a significant decrease in the processing cost per unit mass as the make-up ratio decreases (and the recycle ratio increases) from over A$1.32/kg of chickpeas down to A$0.0885/kg of chickpeas as the process configuration changes from open loop (one through, no recycle) to 99% recycle. At low recycle ratios, the lowest processing cost per unit mass occurs at the lowest inlet air temperature of 40 °C (A$1.09/kg chickpeas, compared with

A$1.32/kg at 80ºC). However, with high recycle ratios (low make-up ratios) show that the lowest processing cost per unit mass occurs at the highest inlet air temperature of 80 ºC. For carbon dioxide emissions, the pattern is the same, in terms of having the lowest emissions at high recycle ratios and high inlet air temperatures. Adding the embodied carbon in the construction of the fluidized bed dryer raises the equivalent carbon emissions by 0.001 kg CO_2 (kg chickpeas)$^{-1}$, which is small compared with the carbon emissions associated with the operating and processing costs (over 0.259 kg CO_2 (kg chickpeas)$^{-1}$). In terms of product quality considerations, no special changes to the previously-produced drying schedule should be necessary to achieve minimum financial cost for processing and minimum carbon emissions from this processing.

Chapter 6. The Effects of Fluidized Bed Drying, Soaking and Microwaving on Phytic Acid Content, Protein Structure and Digestibility in Dehulled Faba Beans

1. Introduction

Expanding on the approach used for chickpeas, this chapter examines how different processing techniques affect phytic acid content and protein structure in dehulled faba beans. Faba beans are an important crop that is grown and consumed around the world [130]. In Australia, the average annual faba bean production from 2016-2021 was 391,000 t [2]. The objective of this study was to remove antinutritional factors, particularly phytic acid, from faba beans with different treatments. In faba beans, alpha-amylase inhibitor, haemagglutinin activity and phytic acid are the three most abundant anti-nutritional factors. Phytic acid, also known as nositol hexaphosphate, serves as the main form of storage of phophorus in the seed. Phytic acid creates complexes with minerals, especially essential minerals such as iron, zinc, magnesium, and calcium, exhibiting "chelation" [131,132,133]. It limits the bioavailability of these minerals in the human diet. This situation can lead to significant mineral deficiencies in humans and animals [134]. This is also an important reason for this study to remove phytic acid from faba beans.

Thermal treatments, such as cooking, have previously been reported to deactivate heat-sensitive factors such as trypsin inhibitors and volatile compounds [135]. Thermal treatments have no significant effect on the removal of phytic acid. Therefore, other potential treatments have been investigated. Table 2, from Sarkhel et al. [136], summarizes the experimental results of different pretreatments for different pulse types regarding the removal of phytic acid. For lentils, soaking under acidic conditions also removed 37% of the phytic acid [67]. Soaking

Indian tribal pulses in alkaline conditions removed 11% of the phytic acid [136], so this study has also investigated the effect of different soaking conditions on the removal of phytic acid from faba beans.

Microwaving is another industrial practice. It is often used in timber drying to change product properties, and in food drying it has been used to reduce anti-nutritional factors. In the review by Sarkhel et al. [136], Table 2 shows that microwave drying after soaking can remove around 50% of the phytic acid [137] in lentils. Suhag et al. [137] used microwave oven processing to reduce anti-nutritional factors, such as phytic acid, trypsin inhibitor, tannin, saponin and oxalate in pulses. This approach also improves the safety and quality of edible grains. The advantage of microwave treatment technology lies in the rapid, safe and green reduction of anti-nutritional factors. According to Rafiq et al. [138], the power and duration of microwave treatment had a significant effect on the inactivation of phytic acid. Most of these papers are aimed at the reduction of phytic acid in chickpeas [139], soybeans [140] and some other grains [140, 141]. Few studies have investigated the effect of the microwaving process on phytic acid levels in faba beans, in conjunction with drying.

As drivers for sustainability increase, the importance of plant proteins is growing for food security [142]. According to the study from Kumar et al. [60], phytic acid can also form complexes with proteins, thereby reducing protein solubility. Therefore, phytic acid reduces the activity of key digestive enzymes such as lipase, a-amylase, pepsin, trypsin, and chymotrypsin [60], which is the basis of this study, in which in-vitro protein digestibility was investigated after different treatment conditions has been studied here. This study has not only aimed to examine the influence of microwaving on phytic acid levels in faba beans but has also

studied the changes in the protein structure of faba beans and the change in the cell structure of faba beans during microwaving.

2. Results and Discussion

2.1 Fluidized Bed Drying

This study has analyzed the fluidized bed drying curve and simulation modelling of dehulled faba beans. This section describes the drying curve, simulation modelling, phytic acid and protein conformation modifications at high constant-drying temperature conditions of 120 ^{o}C and 140 ^{o}C.

2.1.1Drying Curve and Simulation Modelling

The drying curve is an intuitive technique for calculating drying rates and times. The moisture content-time curves in Figure 4 were obtained by sampling dehulled faba beans every two minutes to measure the moisture content of faba beans. Figure 4 shows the moisture content-time curves at 120 ^{o}C and 140^{o}C. The marker is the measured moisture content, and the curve was obtained from the fitting equation (Equation from the section 2.2). To reach the target moisture content (12%), the process at inlet air temperature of 120 ^{o}C required a duration of 15 minutes. For the inlet air temperature of 140 ^{o}C, 10 minutes was required to reach the target moisture content. At an inlet air temperature of 120 ^{o}C, the drying rate was slower than at the inlet air temperature of 140 ^{o}C. As expected, the drying rate increased with the increasing temperature. Changing the inlet air temperature only changed the drying rate and had no effect on the shape of the drying curve. The result is consistent with the findings for chickpeas.

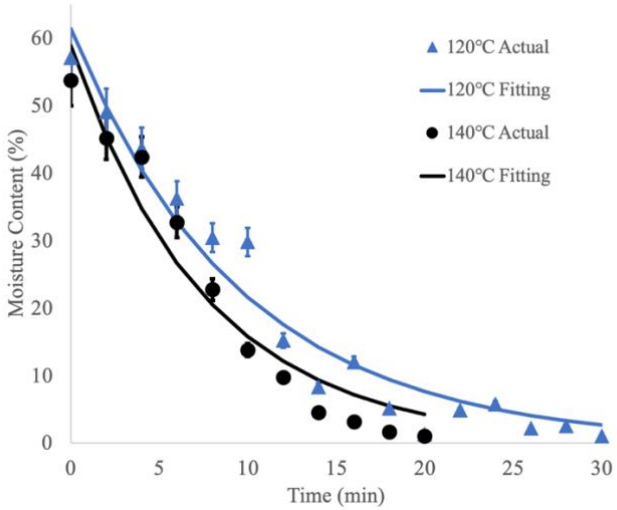

Figure 20. *Moisture content-time curves for the fluidized drying process of dehulled faba beans at 120 °C and 140 °C.*

The relative humidities for the inlet air temperatures of 120 °C and 140 °C are shown in Table 19. These values were calculated from the dry-bulb and wet-bulb temperatures. According to Equation 4, the Kemp and Oakley slow-material model appears to be valid for predicting the drying curves of the fluidized bed drying process at different inlet air temperatures [87]. As shown in Figure 20, the dotted line is the prediction from the slow-material model. Figure 21(a) shows the transformation from the curve at an inlet air temperature of 140 °C to the curve at an inlet temperature of 120 °C, and Figure 21(b) shows the transformation from the curve at an inlet air temperature of 120 °C to the curve at an inlet temperature of 140 °C. Figure 21 shows that the predicted results are consistent with the actual data, and most points fall within the range of error bars. It can be concluded that the Kemp and Oakley model is suitable for describing the fluidized bed drying process of dehulled faba beans in the temperature range from 120 °C to 140 °C.

Table 19. *Relative humidity for the inlet air drying of 120 °C and 140 °C calculated by dry-bulb and wet-bulb temperature.*

Average Humidity		
Dry-bulb (°C)	120.0	140.0
Wet-bulb (°C)	41.1	43.9
Relative Humidity (%)	1.2	0.6

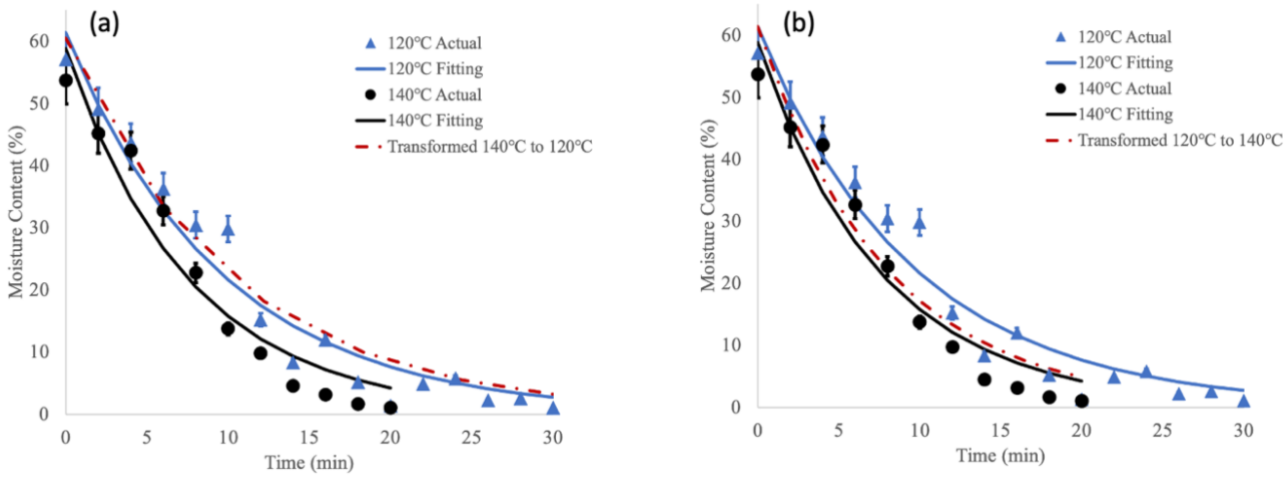

Figure 21. *Predicted drying curve for dehulled faba bean at high temperature, (a) transformed from 120 °C to 140 °C, (b) transformed from 140 °C to 120 °C*

2.1.2 Phytic Acid

The phytic acid content in broad beans can negatively affect the bioavailability of minerals and have an inhibitory effect on protein absorption [35]. The content of phytic acid in raw dehulled faba beans is around 710 mg/100g on dry basis. This range of concentrations for phytic acid is reasonable. The values reported by Dhull et al. also supports this range of values [143]. For instance, the level of phytic acid in untreated faba beans here was 8.36 mg/g, which is in the same range. Further, in this experiment dehulled faba beans were used. Dehulling is a common form of processing for pulses, in which the seed hull is separated from the cotyledon. Nutrient

compositions and the level of anti-nutritional factors are also affected by the dehulling process [5].

Tables 19 and 20 show the changes in phytic acid concentrations over 5 min intervals from 120 °C and 140 °C fluidized bed drying. At the target moisture content (12%), 120 °C fluidized bed drying for around 15 minutes reduced the phytic acid content by about 15%. In addition, 8% of the phytic acid content was reduced by drying in the fluidized bed at 140 °C for 10 min. Comparing the concentrations at the target moisture content from drying temperatures of 140 °C and 120 °C, the phytic acid content did not decrease with an increase in the drying temperature. As shown in Table 20, with the extension of drying time, the content of phytic acid showed a downward trend, and the content of phytic acid decreased to a limited extent. However, this trend is not significant at the inlet air temperature of 140 °C. This means that fluidized bed drying did not play a significant role in reducing the phytic acid content. The results are consistent with the literature where it has been found that phytic acid is more stable than trypsin inhibitor during the drying process [144].

Table 20. *The effect of different drying times on phytic acid reduction for fluidized bed drying at 120 °C*

Drying Time (min)	Moisture Content (%)	Phytic acid (mg/100g)	Reduction (%)
5	40	770	<=0
10	22	656	8
15	10	603	15
20	8	562	21

Table 21. *The effect of different drying times on phytic acid reduction for fluidized bed drying at 140 °C*

Drying Time (min)	Moisture Content (%)	Phytic acid (mg/100g)	Reduction (%)
5	31	572	19
10	14	655	8
15	8	548	22
20	4	814	<=0

2.2 Soaking

This study has analysed the effect of different soaking conditions on phytic acid concentrations. This section compares the change in the phytic acid levels after soaking in acidic, alkaline and neutral solutions for 12 hours, and the change in the phytic acid levels at different temperatures (room temperature and 37 °C).

Soaking is the most popular processing method to remove phytic acid, or reduce the phytate content, of pulses [67]. According to Table 22, soaking can help to reduce the phytic acid content to a certain extent. After soaking for 12 hours, 10%-50% phytic acid was removed under different conditions. In particular, soaking for 12 hours under acidic conditions at 37°C removed 50% of phytic acid in this study. According to the research of Osman et al. [144], soaking goat pea in water for 6 hours at RT reduced phytic acid concentrations by 3.94%. Vidal-Valverde et al. [67] found that soaking lentils in 0.1% citric acid at room temperature reduced phytic acid concentrations by 37%. The results obtained in this experiment are slightly higher than those in the literature, possibly because dehulled faba beans were used in this experiment. The seed coat of pulses is likely to resist water penetration during soaking.

***Table 22**. The effect of different soaking conditions on phytic acid.*

Pre-treatment	Moisture content (%)	Phytic acid (mg/100g)	Reduction (%)
Water 12h	55	435.7	39%
Water 12h 37^{o}C	57	605.3	15%
Acid 12h*	56	538.1	24%
Acid 12h 37^{o}C	55	174.4	51%
Alkali 12h**	54	552.6	22%
Alkali 12h 37^{o}C	55	640.4	10%

* Acid Soaking (0.1% citric acid, pH 3)

**Alkali soaking (1% $NaHCO_3$, pH 8)

Soaking can remove part of the phytic acid, but the reduction may not be significant on its own. The soaking process may play a small role in removing phytic acid due to the following reasons. Soaking pulse in water results in the release of water-soluble phytic acid or phytate (sodium or potassium salt) [67, 68]. During the soaking process, diffusion of water occurs into the pulse matrix, the phytic acid dissolves in the water, and the phytase is activated. The pulse matrix is inherently porous, and this type of structure allows for faster water diffusion and dissolution of phytic acid in water [67]. Studies have shown that soaking for a certain period of time can effectively reduce phytic acid concentrations [145-147]. The effect of soaking on phytic acid reduction depends largely on the soaking conditions, namely the pH and temperature of the soaking solution. However, longer soaking periods can also lead to loss of soluble proteins [148].

2.3 Microwaving

Applications of microwaves in food processing have been reported and studied, such as in thawing, blanching, baking, drying, pasteurization, sterilization and extraction of biologically active compounds [138, 149]. Table 23 shows the effect of different microwaving conditions on phytic acid concentrations. In this study, dehulled faba beans were soaked in neutral, acid and alkali solutions before subject to microwaving, then they were microwaved for 30 s, 1 min and 2 min. As the microwave time increases, the phytic acid content decreased. This trend was most pronounced for acidic soaking conditions. After two minutes of microwaving, most of the phytic acid was removed. In other words, microwaving removed phytic acid from dehulled faba beans. According to the study of Suhag et al. [137], microwaves can help reduce anti-nutritional compounds present in foods, thereby improving in-vitro protein digestibility, safety and quality of food grains. This conclusion is also consistent with these results.

Microwaving is not an uncommon method for (partial) processing of natural bioproducts [150] and it is used in timber drying processes. For example, Terziev el al. [149] reported that in timber drying, the advantage of microwaving is that it can dry timber faster than conventional drying methods and preserve quality. The microwaving process changes wood structures, such as pit openings, by rupturing the pit membranes or weakening the middle lamella in timber cell walls. This change is due to microwave heating being concentrated in the wet regions of moist wood, evaporating water and creating pressure gradients between cells [151, 152]. This process also happens in the faba bean microwave process, which assists in the reduction of phytic acid levels. The next section on Scanning Electron Microscopy (SEM) also illustrates the structural changes in faba beans during the microwaving process.

Table 23. *The effect of different microwaving conditions on phytic acid.*

Pre-treatment	Moisture content (%)	Phytic acid (mg/100g)	Reduction (%)
Water Soaking 12h+30s Microwaving	48	339.9	62%
Water Soaking 12h+1min Microwaving	37	393.4	56%
Water Soaking 12h + 2min Microwaving	13	<=0	100%
Acid Soaking 12h* +30s Microwaving	52	632.6	29%
Acid Soaking12h* + 1min Microwaving	31	317.0	64%
Acid Soaking 12h* + 2min Microwaving	6	35.3	96%
Alkali Soaking 12h* * + 2min Microwaving	12	254.2	71%
Alkali Soaking 12h (37^{o}C) * * + 2min Microwaving	16	<=0	100%

* Acid Soaking (0.1% citric acid, pH 3)

**Alkali soaking (1% $NaHCO_3$, pH 8)

2.4 Scanning Electron Microscopy

Figures 22(a) and 22(b) show the SEM images of raw faba beans at different magnifications. Figures 22(c) and 22(d) show the structure of faba beans after soaking. These images are all characteristic of the internal structure of faba bean slices. Under high magnification, Figure 7(a) shows the starches, proteins, and cell walls in faba beans. In the dry condition (raw faba bean), the intercellular spaces are large, as shown in Figure 22(b). After soaking, the cells tended to expand significantly and the intercellular space decreased.

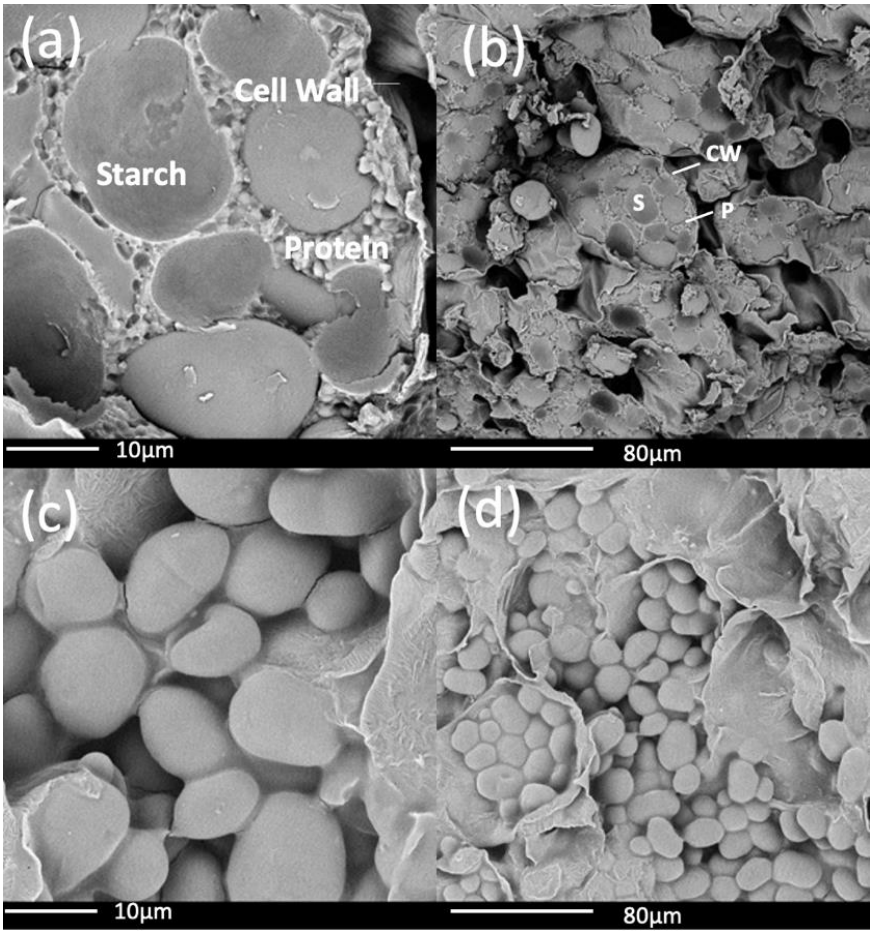

Figure 22. *SEM images, slices of faba beans at different magnifications (1000x-5000x) (a) raw faba beans (dehulled), 5000x; (b)raw faba beans (dehulled), 1000x; (c) Soaking in water for 12h,3000x; (d) Soaking in water for 12h,1000x; The structure shows starch (S), protein (P) and cell wall (CW).*

Figures 23(a) and 23(b) show the SEM images after microwaving at different magnifications. The cell wall of faba beans is damaged after microwaving. Starch and protein have been lost in some cells. These losses are consistent with the significant changes in the protein secondary structure after microwaving. Compared with raw faba beans, the structure inside the cells is not so restricted. This change may be a significant reason for the reduction in phytic acid levels.

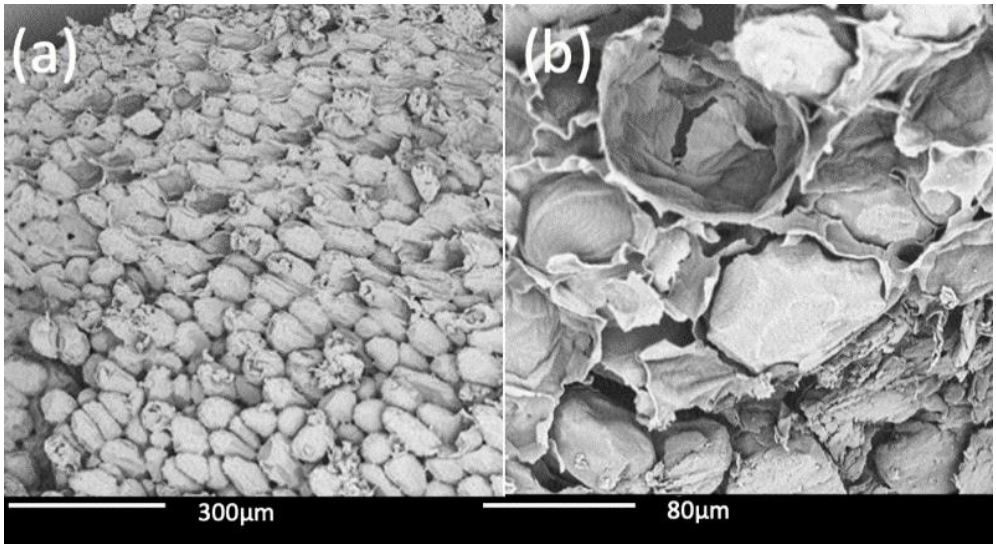

Figure 23. *SEM images, slices of faba beans after microwaving at different magnifications (255x - 5000x) (a) duhulled faba beans after 12 h soaking in water and 30 s microwaving, 255x and (b) dehulled faba beans after 12 h soaking in water and 2 min microwaving, 1000x*

2.5 In-vitro Protein Digestibility

This study has analysed the changes in protein digestibility under different treatment conditions. All the treatments in this experiment were based on dehulled faba beans. For the fresh faba bean seeds with hulls, the in-vitro protein digestibility was 75.5%. For fresh faba beans, regardless of whether they were dehulled, treated in a microwave and dehulled, soaked and dehulled or fluidized bed dried and dehulled, the in-vitro protein digestibility has been significantly improved. Among them, the in-vitro digestibility of protein is the highest after 12 hours of water soaking and 2 min of microwave processing, at a value of 88.2%.

Table 24. *The effect of different pre-treatment conditions on in-vitro protein digestibility.*

	Treatment	pH	Digestibility (%)	Increase (%)
1	Fresh faba bean (Hulled)	7.5	75.5 ± 0.5	
2	Raw faba beans (Dehulled)	6.8	87.4 ± 1.6	15.7
3	FBD 140oC for 10min (Dehulled)	6.8	88.0 ± 1.5	16.5
4	FBD 120oC for 15min (Dehulled)	6.8	88.0 ± 0.5	16.4
5	Water Soaking 12h + Microwaving 30s (Dehulled)	6.9	86.4 ± 0.7	14.4
6	Water Soaking 12h + Microwaving 2min (Dehulled)	6.8	88.3 ± 0.6	16.8
7	Soaking for 12h (Dehulled)	7.0	84.9 ± 0.2	12.4

These results are consistent with those of Luo et al [152]. According to that study [152], the in-vitro protein digestibility of raw seed was 72.7%. The dehulling process increased the digestibility by 3.8%. Soaking increased the digestibility by 1.2%-2.6%. This result means that the dehulling process had a positive effect on protein digestibility. The soaking process had little effect on protein digestibility. The digestibility of combining microwave, soaking and dehulling reached 82.3%. There are many factors that affect pulse protein in-vitro digestibility, such as anti-nutritional factors (phytic acid, tannins), and thermal treatment [138, 153]. For the fresh faba beans (hulled), the content of phytic acid was around 980mg/100g [154]. This result was much higher than the content of phytic acid in raw faba beans (dehulled) (710mg/100g).

Compared with fresh faba beans (hulled), the in-vitro protein digestibility of the raw faba beans increased by 11.9%. This result means that the decrease in the phytic acid content appears to improve in-vitro protein digestibility.

2.6 Protein Conformation Modification

In the Fourier transform infrared (FTIR) spectrum, there are typical protein bands: Amide I (1600–1700 cm^{-1}), Amide II (1500–1580 cm^{-1}) and Amide III (1200–1400 cm^{-1}). Amide I delineates the strongest vibrational mode and is important for revealing and analysing protein secondary structures [153]. In this study, Gaussian deconvolution analysis was carried out for the Amide I region. This analysis helps to quantify changes in protein secondary structure. In the amide I region, protein secondary structures include β-sheets (1600-1638cm^{-1}), unordered structures (1638-1650cm^{-1}), α-helices (1650-1600cm^{-1}), β-turns (1660-1680cm^{-1}), antiparallel β-sheets (1680-1688cm^{-1}) and β-type structures (1690-1695 cm^{-1}) [154].

Figure 24(a) shows the amide I spectrum of the raw faba bean with its Gaussian spectral deconvolution. As shown in Figure 24, raw faba beans have the most peaks, which were neatly arranged. After different treatments, the secondary structure of the protein was changed. Especially after soaking (Figure 24(d)) and microwave treatment (Figure 24(e)), the number and shape of the peaks showed significant changes.

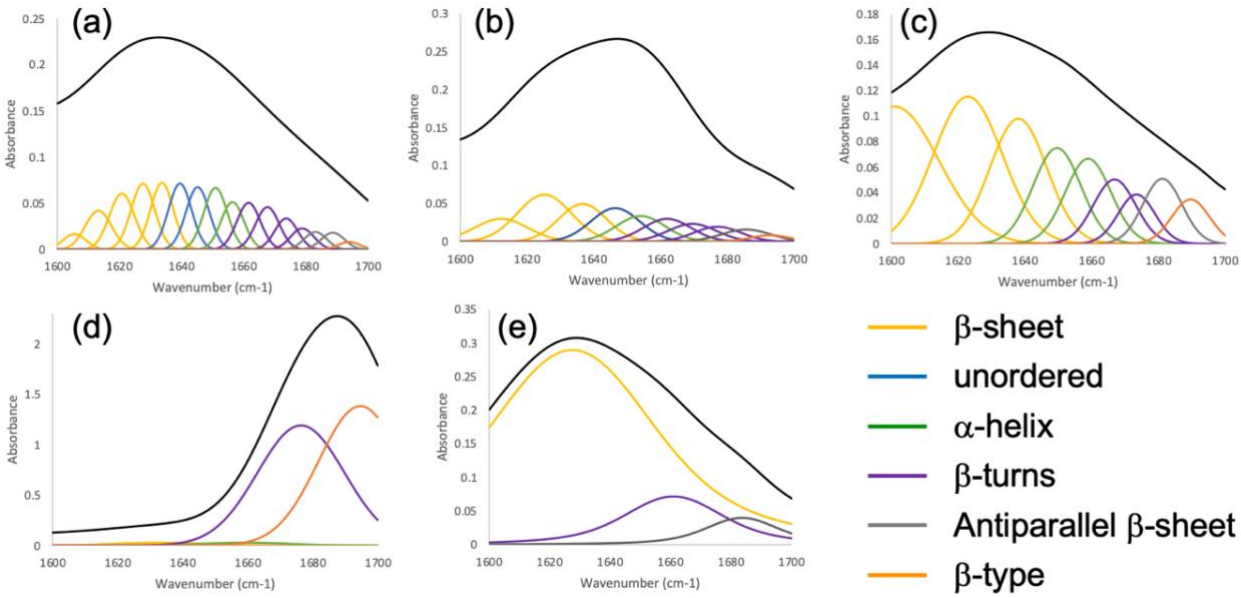

***Figure 24**. FTIR spectrum showing amide I bands of faba bean powder. The outer envelope is the original spectrum, and the individual component peaks underneath are the results of regression analysis. The peaks are associated with different secondary structures. (a) raw faba bean, (b) 120°C fluidized bed drying for 15 min after soaking, (c) 140 °C drying for 10 min after soaking, (d) soaking for 12 h (undried), and (d) microwaving for 2 min (soaked, not dried in the fluidized bed, but having a moisture content of 5-7%).*

As an example, sixteen Gaussian bands have been resolved for raw faba bean (Figure 7(a)), centered at 1606, 1613, 1621, 1628, 1634, 1639, 1645, 1651, 1656, 1662, 1667, 1674, 1679, 1683, 1689 and 1694 cm^{-1}. Among them, the peaks at 1606-1634 cm^{-1} were considered to represent the secondary structure of β-sheets. The peaks at 1639 and 1645 cm^{-1} were assigned to unordered structures. The peaks at 1651 and 1656 cm^{-1} were interpreted as α-helices. The wavebands from 1662-1679 cm^{-1} were considered to be β-turns. The peaks at 1683 and 1689 cm^{-1} were considered to be antiparallel β-sheets. The peak at 1694 cm^{-1} was interpreted as a β-type structure. In Figure 7, peaks of the same color represent the same protein secondary structure. By calculating the peak area, the proportion of different protein secondary structures can be obtained. The relative percentages of different structural components in the secondary structure of raw faba bean are shown in Table 25.

By comparing with the protein secondary structure in raw faba bean, it can be observed the effect of different treatments on the protein secondary structures. For raw faba beans, the β-sheet content is 42%, and after fluidized bed drying and microwaving, the content of β-sheets increased. In comparison, the content of b-sheets decreased to 1% after another 12 hours of soaking. By comparing the standard error with that for the raw faba beans, it was observed that in the fluidized bed drying process, when the target moisture content is present, the higher the drying temperature, the greater is the change in the secondary structure of the protein. This conclusion is also consistent with the results of chickpeas. On the other hand, soaking had the greatest impact on the secondary structure of proteins among the three different treatments; this may be due to the high moisture content (%) of the faba bean samples after soaking. Also applying two minutes of microwaving had an impact on the protein secondary structure.

Table 25. *The relative percentages of different structural components in the secondary structure of raw faba bean, fluidized bed dried at 120 °C and 140 °C after soaking, soaked faba beans (undried) and microwaved faba beans (soaked, not dried in the fluidized bed, but having a moisture content of 5-7%).*

Secondary structure component	**Frequency (cm^{-1})**	**Raw faba bean (%)**	**FBD 120°C_15 min (%)**	**FBD 140°C_10 min (%)**	**Soaking 12 h (%)**	**Microwaving 2 min (%)**
β-sheets	1600-1638	42	46	58	1	79
Unordered	1638-1650	18	14	0	0	0
α-helices	1650-1660	15	11	21	1	0
β-turns	1660-1680	20	22	11	55	15
Antiparallel β-sheets	1680-1688	5	5	6	0	6
β-type structures	1690-1695	1	2	4	42	0
σ (standard error, compared with raw faba bean)			0.08	0.27	0.71	0.45

3. Conclusions

This paper has studied the effect of different treatments for dehulled faba beans on the reduction of phytic acid concentrations in these beans. Treatments applied in faba beans were fluidized bed drying, soaking and microwaving. Fluidized bed drying did not reduce the concentration of phytic acid from faba beans significantly, suggesting that thermal treatment had little effect on phytic acid levels. Soaking reduced phytic acid levels to a certain extent, and microwaving had a higher effect in reducing phytic acid levels in the faba beans.

This study used SEM and FTIR to analyse the physical structure of faba beans under different treatment conditions and the secondary structures of proteins in faba beans. Results showed that the physical structure of the faba bean and the secondary structure of the protein changed after microwaving, which may connect with the reduction in phytic acid levels. The in-vitro

protein digestibility with different treatments showed that dehulling faba bean improved the digestibility of the proteins. On the other hand, after microwaving the digestibility of protein also showed some improvement. In general results showed that microwaving is a potential pulse protein processing technology because it not only reduces the content of anti-nutritional factors, but it also improves the digestibility of the proteins. The results from this Chapter presented here are used in Chapter 7 to conduct a techno-economic analysis and evaluate the practicality of applying these processes at scale.

Chapter 7. Technico Economic Analysis: Microwave Processing to Remove Phytic Acid from Dehulled Faba Beans

1.Introduction

Using data from Chapter 6, this chapter evaluates the economic implications of applying microwave and boiling treatments to faba beans. The analysis emphasizes the trade-offs between performance and cost. According to Chapter 6, microwaving is an effective way to reduce phytic acid. In this study, the phytic acid reductions for different masses of faba beans (10 g, 20 g, 50 g, 100 g, 200 g and 500 g) and different microwaving times (30 s, 60 s, 120 s, 300 s and 600 s) have been studied. From Table 26, the reduction of phytic acid increased with microwaving time. At the same time, the temperature of the dehulled faba beans increases with microwaving time as well. However, as the mass of faba beans increased, the reduction of phytic acid decreased at the same microwaving time.

Table 26. *Microwave processing to reduce phytic acid concentrations.*

Scholars	Microwaving	Reduction of Phytic Acid	Reasons
[62]	900 W, 2450 MHz, 2-12 min	34.7%-35.6%	Low levels of inositol and inositol phosphate due to the effects of free radicals produced during irradiation
[156]	2450 MHz, 15 min	17.6%-54.4%	Decreased water extractability of phytate caused by heating processes which included pressure cooking, microwave cooking and roasting.
[139]	2450 MHz, 30 min	62.69%-64.88%	Phytic acid is relatively heat-labile hence, it was decreased very easily after thermal processing, especially autoclaving

[157]	2450 MHz, 30 min	24.6%	Hydrolysis during soaking, and sensitivity to thermal treatment, and insoluble complexes formed between phytic acid and other components

The results in Table 26 suggest that the reduction of phytic acid during microwave processing is due to hydrolysis. Soaking before microwave treatment further enhanced the potential for phytic acid hydrolysis. Phytic acid in dried grains is entirely in the form of a water-soluble salt. During processing, phytate is converted into pentaphosphate and tetraphosphate [93]. At the same time, high temperatures during microwaving may promote the hydrolysis reaction to a certain degree. Since phytic acid removal is caused by hydrolysis, boiling should remove phytic acid.

The whole process is shown in Figure 25. Both microwaving and boiling may remove phytic acid from faba beans. After the reduction of phytic acid, reaching the desired moisture content in faba beans is critical to ensure their stability during storage and suitability for subsequent processing. These two different processes for phytic acid removal have been studied in this work.

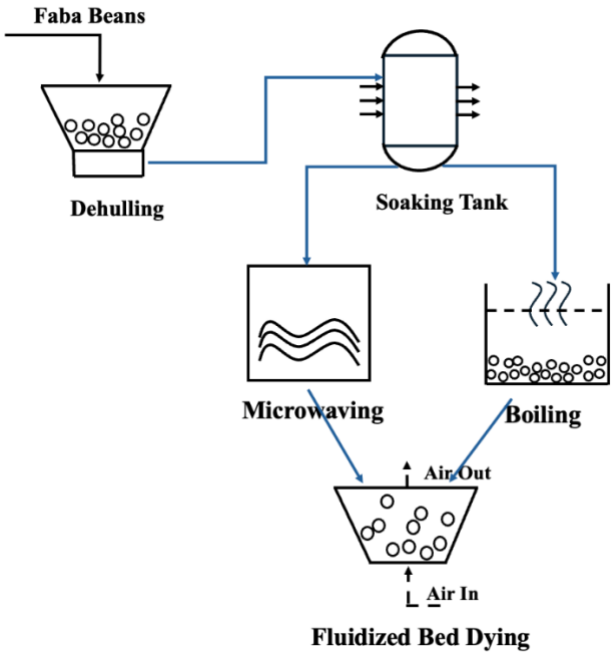

Figure 25. *The flow chart of dehulled faba beans drying and phytic acid removing process.*

This work presents a technico-economic analysis of the faba bean processing chain, focusing on the integration of dehulling, boiling, microwaving, and fluidized bed drying techniques. In particular, the study includes the use of air recycle with fluidized bed drying, which is intended to achieve low energy consumption and cost efficiency. By examining the economic and technical performance of these processes, this study aims to assess their feasibility and optimization potential for large-scale implementation in faba bean processing.

2. Results and Discussion

2.1 The Content of Phytic Acid

By using different concentration of phytate salt, a calibration curve was obtained (shown in Figure 26), which is given by the following equation:

$$y = -0.0046x+1.00 \qquad (37)$$

Here y is the content of phytic acid (μg/ml), and x is the absorbance of a solution containing phytate salt at 519 nm measured by a UV-Vis spectrophotometer.

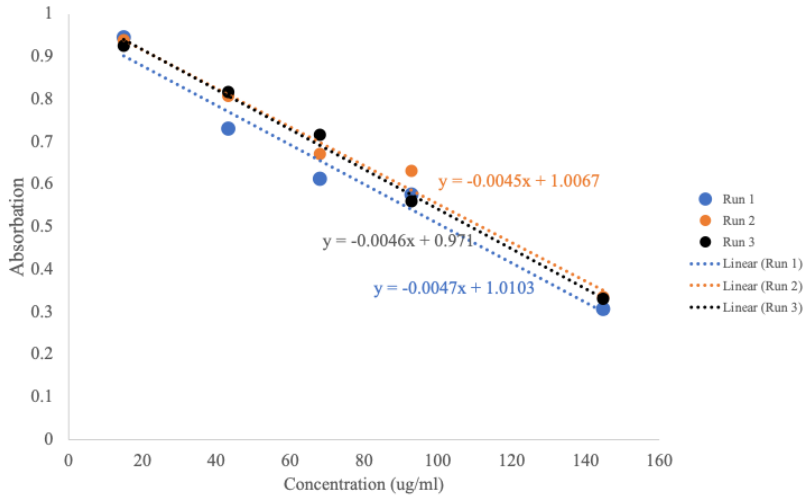

Figure 26. *Calibration curve for the phytic acid concentration.*

For example, 10 g of drained faba beans were microwaved for 30 seconds. The absorbance at 519 nm was 0.7623. The moisture content of the faba beans after drying was 50.67%. For raw faba beans, the content of phytic acid was around 712.07 mg/100g.

- The content of phytic acid is 42.25 μg/ml.
- After correcting for the moisture content, phytic acid content is 91.72 μg/ml (which is 458.61 mg/100g) .
- Reduction of the phytic acid is 35.59%

2.1.1 Technical Measurements of Phytic Acid Reduction During Bench-Scale Microwaving Treatment

By using the domestic bench top microwave oven, data for the amounts of phytic acid reduction at different microwaving times for various masses of pulses are given in Table 27.

Table 27 presents the final moisture content of faba beans subjected to microwave treatment across different sample masses and exposure times. The data indicate that for smaller sample masses (≤100 g), the moisture content decreases noticeably with increasing microwave exposure time, reflecting higher rates of moisture removal. In contrast, for larger sample masses (200 g and 500 g), the final moisture content remains relatively stable—around 10%—regardless of exposure time. This trend suggests that moisture loss during microwaving becomes limited as the sample size increases, likely due to reduced heating uniformity and slower internal heat transfer at larger scales.

Table 27. *The reductions of phytic acid in different masses of dehulled faba beans at different microwaving times.*

Mass of pulses (g)	Microwaving time (s)	Microwave intensity (kJ/g)	Temperature _ faba beans (K)	Actual Reduction	Fitting Reduction	Final Moisture Content (%)
10	30	1.6	326	33%	40%	47%
10	60	3.3	327	64%	54%	36%
10	120	6.5	334	75%	84%	17%
20	30	0.82	332	30%	36 %	45%
20	60	1.6	337	38 %	45%	39%
20	120	3.3	340	68%	60 %	21 %
50	30	0.33	336	33 %	34 %	51%
50	60	0.65	349	62%	43%	48%
50	120	1.3	351	70 %	50%	33%
100	30	0.16	341	46%	35%	52%
100	60	0.33	355	46%	44%	53%
100	120	0.65	355	52%	46 %	37%
200	30	0.08	321	12%	25 %	57%
200	60	0.16	341	22%	35%	54%
200	120	0.33	360	26%	46 %	54%
200	300	0.82	356	44%	48%	52%
500	30	0.03	305	28%	16%	49%
500	60	0.07	320	40%	24%	44%
500	120	0.13	348	39%	38%	45%
500	300	0.33	364	40%	48%	45%
500	600	0.65	366	56%	52%	43%

Based on Table 27, the microwave intensity may be calculated using equation 38. The actual reduction of phytic acid comes from the experiment. For the fitting reduction of phytic acid,

the Solver in MS Excel has been used to minimize the sum of squares of the difference between the actual reduction of phytic acid and the fitted reduction by adjusting the fitting parameters *a* and *b*, as shown in the following equation 38. The standard error from the fitting equation is 1.1%, and the average of phytic acid reduction is 43.9%, which means this equation is reliable to predict the reduction of phytic acid during microwaving process".

$$\text{Reduction of phytic acid (\%)} = 0.075 \times I + 0.001 \times T \quad (38)$$

Where I is the microwave intensity (kJ/g) and T is the temperature (K) here. Equation 36 allows the reduction of phytic acid to be predicted as a function of the microwave intensity. By comparing the coefficients of temperature and microwave intensity (0.075 and 0.001), the microwave intensity has a greater impact on the reduction of phytic acid, while temperature has a modest impact on the reduction of phytic acid. This result is consistent with the results from Chapter 6 that phytic acid is more stable than other anti-nutritional factors, such as trypsin inhibitors, during thermal treatment.

2.1.2 The Capacity of Microwave Processing (Scaling up Microwave Processing)

This study assumes that the maximum temperature during the microwaving process is 373 K (100^{o}C), which is the temperature at boiling point of water. The basic procedure for estimating the microwave intensity was described earlier and has been used here. The required reduction of phytic acid (96.5%) then gives the throughput. For the mictrowave intensity, which is related to the microwaving time and mass, as show in equation (39):

$$\text{Microwave intensity (I)} = 20\ \text{kW} \times \text{time/mass} \quad (39)$$

The time here means the batch time, which corresponds to the residence time in a continuous system. Solving this equation gives the mass/time that the 20kW unit can process.

By using the 20kW industrial microwave oven, 5.4 tonnes of dehulled faba beans per day can be processed. The processing capacity in this study is set to be 5.4 tonnes per day.

2.1.3 Technical Measurements of Phytic Acid Reduction During Boiling Treatment

According to Table 28, the reduction of phytic acid increased with longer boiling times. Boiling for 10 minutes removed 81 ± 3% of the phytic acid. Extending the boiling time to 20 minutes resulted in the removal of most of the phytic acid in the dehulled faba beans. Boiling for 15 minutes achieving the target reduction levels. A boiling time of 15 minutes has been used in this study. It took 20 minutes of fluidized bed drying to reach the target moisture content after 15 minutes of boiling.

Table 28. *The reductions of phytic acid in different masses of dehulled faba beans at different boiling times.*

Mass of dehulled faba beans (g)	FDB Drying Time (min)	FDB Drying Temp (°C)	Boiling Time (min)	Average Reduction (%)
200	50	120	10	81 ± 3
200	20	120	15	89 ±14
200	20	120	20	97±9

2.2 The Capital and Energy Costs of the Dehulling and Soaking Process

2.2.1 Dehuller

In this study a ball mill was considered for the dehulling process during the removal of phytic acid from faba beans [158]. Two different methods were used in this study to analysis the capital costs and energy costs of the dehuller (detailed calculation attached in appendix). One calculation is based on the literature from Schultz and Mehta [158], while another calculation is based on the price of industrial dehullers directly.

A comparison of the two dehulling methods revealed similar total processing costs per unit mass throughput, with values of 0.03 AU$/kg and 0.04 AU$/kg from methods 1 and 2, respectively. The method from the literature, originally reported in 1991, represents a 33-year-old approach. Method 1 (literature-based) predicts lower purchased equipment costs (PEC, AU$3,448) and process plant costs (PPC, AU$13,797); however, it predicts higher utility costs (AU$63,151). In contrast, Method 2 (the quote from industrial) predicts higher PEC (AU$,45,000) and PPC (AU180,000, which is 12 times higher than method (1) but predicts lower utility costs (AU$11,353, which is 82% lower than method (1).

2.2.2 Soaking Tank

Based on Chapter 6, the ratio between water and faba beans is 5:1. For 5.4 tonnes dehulled faba beans, 27 tonnes of water would be required in this situation. A 1100L large automatic soak tank from Soak Tank Australia costs US$1,430 (quoted cost), which is AU$2,145. Peters et al [160] report the "*six-tenth-factor rule*". The relationship between the cost of equipment and capacity shown in *section 2.1.2*. To meet the needs of 27 tonnes of water / day, equation 38 can be used to predict the price of a larger soaking tank. The capital cost of required soaking tank is AU$16,372 .The detailed calculation of PEC, PPC and Annual Capital Recovery Cost as shown in Appendix.

$$Cost\ of\ equip\ a = \ Cost\ of\ equip\ b\ (\frac{capac.equip.a}{capac.equip.b})^{0.6} \quad (40)$$

From Peters et al [160], when the capacity is around 32L, the cost of the 304 stainless steel tank is around $16,000. The cost is consistent with the calculation using the quote and the six-tenth-factor rule.

In this study, 27 tonnes of water per day will be used. According to a report from Sydney Water (2020), the average water cost is between $2.15 and $3.18 per kilolitre. The water cost of 2.6 AU$/ kL will be taken here. The water cost in this situation is 72 AU$ /day. The total cost of soaking process, including the cost of the soaking tank and the water (as shown in Appendix). The total cost from the soaking process is 0.02AU$/kg.

2.3 The Capital and Energy Costs of the Microwaving Process

For the industrial microwave, a 20kW microwave (Ferrite Microwave Technologies, MIP3) was quoted to cost US$ 200,000, which is AU$300,000. By using the Lang factor, the PPC of the microwave is AU$ 1,200,000.

$$\begin{aligned} &Annual\ Capital\ Recovery\ Costs \\ &= (300{,}000 + 1{,}200{,}000)\frac{AU\$}{year} \times CRF(0.163) \\ &= 244{,}500 AU\$/year \end{aligned} \tag{41}$$

For scaling up the microwave process, the electricity cost for the microwave unit may be calculated as follows,

$$Electricity\ cost\ from\ microwave \tag{42}$$

$$= \frac{\$20}{GJ} \times 20\ kW \times \frac{\frac{8000h}{year}}{1000\frac{kWh}{MWh}} \times 3.6\frac{GJ}{MWh} = \$11{,}520/year$$

The total cost of the microwaving process has included the capital costs of the microwave unit and the electricity costs (as shown in following equation). The total costs from the soaking process are 0.13AU$/kg.

$$\begin{aligned} Total\ Cost\ of\ soaking\ process &= \frac{\frac{(244{,}5000 + 11{,}520)AU\$}{year}}{5400\frac{kg}{day} \times 365 days/year} \\ &= 0.13 AU\$/kg \end{aligned} \tag{43}$$

2.4 The Capital and Energy Costs of the Boiling Process

Boilers play a crucial role in food processes, providing the necessary heat and steam for different operations. According to Figure B-3 from Peters et al., [160], the total purchased equipment cost of a packaged boiler may be obtained. The total cost including the PEC and PPC of the boiler. The temperature of boiling water in this study is taken as 100ºC, and the mass of boiling water is 27 tonnes every day. The required steam capacity is 14,881 lb/h. The purchase cost in the Figure B-3 [160] is around US$300,000, which is equal to A$450,000. According to Peters et al., [160], when the target temperature is 100ºC, the price should be multiplied by factors (1.10 here), so, the cost for the boiler is A$495,000. The price includes a complete boiler, feed-water deaerator, boiler feed pumps, chemical injection system, stack and shop assembly labor. Based on the CRF used here of 0.163, the Annual Capital Recovery Cost for the boiler is AU$80,685/year.

Natural gas cost - boiler

The steam capacity used in this study for the boiler is 14,881lb/h from above, which is 6750 kg/h. 27 tonnes of water per day (1125 kg/h) are required in this study. The capacity of the boiler is enough to support the capacity of the whole processing. The water temperature change from 20ºC to 100ºC without boiling, so the temperature difference (ΔT) is 80℃. That means the required energy is 900GJ. The total cost of the boiling process includes the cost of the boiler and the natural gas (as shown in Appendix). The total costs of the boiling process is 0.06AU$/kg.

2.5 The Capital and Energy Costs of Fluidized Bed Drying (After Microwaving)

The drying data from Chapter 6 show that 200 g dehulled faba beans were dried in a 0.1m diameter fluidized bed at inlet air temperatures of 120ºC and 140ºC. The initial moisture content is 60%, and the target moisture content is 12%. The following Table 29 shows the different drying times required to reach the target moisture content after microwaving and boiling. After boiling, a longer drying time is needed to reach the final 12% moisture content. This means the drying rate after boiling is slower than that after microwaving. The reason is that microwaving may change the physical structure of the faba beans and increase the drying rates. The costs of the two methods for fluidized bed drying have been analysed separately (microwaving first, boiling second).

Table 29. The drying time required to reach the target moisture content after microwaving and boiling.

Drying Temperature (ºC)	Drying Time _ microwaving(min)	Drying Time _ boiling (min)
120	15±2	25±3
140	10±1	20±3

According to Table 27, when microwaving a significant amount of pulses (200 g, 500 g), the moisture content during microwaving does not change significantly, as shown in Table 27. The initial moisture content is 60% and the final moisture content is 12%. According to Chapter 5, the evaporative load of overall drying rate can be calculated by the following equation.

The basis will be assumed to be a throughput of 60 kg h^{-1} total solids for (an assumed) 8000 operating hours per year, which would cover around 5.4 t/day of faba beans.

This study assumed that the initial moisture content is 60% on a dry basis (d.b.), with a final moisture content of 12% (d.b.), or 0.5 kg water (kg dry solids)$^{-1}$, or 0.33 kg water (kg total solids)$^{-1}$ input.

Here, the evaporative load is given by the following calculation:

$$\begin{aligned}&\text{Evaporative load (overall drying rate)} \qquad (44)\\&= \frac{(60\% - 12\%)\text{kg water}}{100\%\text{ kg dry solid}}\\&\times \frac{228\text{ kg h}^{-1}\text{ total solids}}{1.6\text{ kg (dry solid + water)(kg total solid)}^{-1}}\\&= 68.4\text{ kg water h}^{-1} = 0.019\text{ kg water s}^{-1}\end{aligned}$$

This evaporative load is also the overall drying rate, which is relevant to the calculation of both capital and operating costs.

The Kemp and Oakley slow-material model was assessed and accepted in Chapter 3 to scale the fluidized bed drying of dehulled faba beans for inlet air temperatures between 100ºC and 140ºC. The Kemp and Oakley slow-material model is shown in equation (4).

Where $\Delta\tau$ is the drying time, T_G is the dry-bulb temperature and T_{wb} is the wet-bulb temperature. These data, as shown in Table 30, come from Chapter 6.

Table 30. Dry-bulb, wet-bulb temperature, relative humidity, and the drying time at the inlet air drying temperatures of 120 °C and 140 °C in fluidized bed drying of microwave-treated faba beans

Dry-bulb temperature (ºC)	Wet-bulb temperature (ºC)	Relative humidity (%)	Drying time (min)
120	41	1.2	15
140	44	0.6	10

By using these data for the inlet air drying temperature of 120 ºC in Table 29, the model can be rewritten as follows:

$$\Delta\tau = (\frac{15}{60}\text{h})\frac{(120\ ^{o}\text{C} - 41\ ^{o}\text{C})}{(T_G - T_{wb})} = \frac{19.8\ \text{K h}}{(T_G - T_{wb})} \quad (45)$$

Equation 44 shows the calculation of the drying flux,

$$\text{Drying flux} = \frac{(60\% - 12\%)}{100\%} \times \frac{200\ \text{g}}{1000\frac{\text{g}}{kg}} \times \frac{1}{\Delta\tau} \times \frac{1}{\frac{\pi}{4}(0.1\ m)^2} \quad (46)$$

$$= \frac{12.23}{\Delta\tau}\ \text{kg m}^{-2}\ \text{h}^{-1} = \frac{12.23}{19.8}\ (T_G - T_{wb})\ \text{kg m}^{-2}\ \text{h}^{-1}$$

$$= 0.62\ (T_G - T_{wb})\ \text{kg m}^{-2}\ \text{h}^{-1}$$

Then the following equation gives the required fluidized-bed cross-sectional area (A, m^2). The required drying rate has been obtained, which is 68.4 kg h^{-1}.

$$A = \frac{68.4\ \text{kg water h}^{-1}}{0.62(T_G - T_{wb})\ \text{kg water m}^{-2}\ \text{h}^{-1}} = \frac{110.32}{(T_G - T_{wb})}\ \text{m}^2 \quad (47)$$

The cross-sectional area for the fluidized bed can be calculated in Table 31. According to Chapter 6, the basic capital cost of a fluidized bed dryer is related to the cross-sectional area.

$$\text{PEC} = \$6{,}350\ A^{0.587} \quad (48)$$

Table 31. *Drying flux, cross-sectional area and PEC of full-scale fluidized bed drying in the microwaving process with faba beans.*

Inlet air drying temperature	**Drying flux (evaporative flux)**	**Full-scale fluidized bed cross-sectionalarea**	**Capital cost of fluidized bed dryer**	
(°C)	(kg m^{-2} bed area h^{-1})	(m^2)	US$	A$
120	48.9	1.40	7,736	10,338
140	59.5	1.15	6,892	11,640

2.6 Energy Analysis (FBD after microwaving)

2.6.1 *Natural Gas and Electricity Cost for a Fluidized Bed Dryer*

According to Chapter 6, the fluidization velocity (u_f) by drying the dehulled faba beans was 8.5 m s^{-1}. The cross-sectional area of the fluidized bed dryer is shown in Table 32, and the calculation of the air mass flow rate is shown in Equation 49. A sufficient air mass flow rate through the fluidized bed is needed to fluidize the dehulled faba beans.

$$Air\ mass\ flow\ rate\ (kg\ s^{-1}) = \rho\ A\ u_f = 8.5\ \rho\ A \quad (49)$$

The same calculation methods have been used as in Chapter 6. The results are shown in Table 32.

Table 32. *The effect of different inlet air drying temperatures on the predicted air flow rates for maintaining fluidization, the predicted changes in air humidity and temperature across the fluidized bed during drying, and the outlet air humidities and temperatures for the fluidized bed drying in the microwaving process with faba beans.*

Inlet air drying temperature	**G, air flow rate for fluidization**	**ΔY, change in air humidity**	**ΔT_G, change in air temperature**	**Y_{out}, outlet air humidity**	**T_{Gout}, outlet air temperature**
(^oC)	(kg s^{-1})	($\times 10^{-3}$ kg kg^{-1})	(^oC)	(kg kg^{-1})	(^oC)
120	10.7	1.27	2.79	0.727	117.2
140	8.4	1.98	4.36	0.014	135.6

Table 33 shows the effect of different inlet air drying temperatures after the microwaving process on predicted thermal energies required to heat the air at the required flow rates, the predicted air pumping power required for fluidization, and the predicted heat losses for the microwaving process.

Table 33. *The effect of different inlet air drying temperatures on the predicted thermal energies required to heat the air at the required flow rates, predicted air pumping power required for fluidization, and predicted heat losses fluidized bed drying in the microwaving process with faba beans..*

Inlet air drying temperature	**Q, thermal energy required to heat the air**	**P, pumping power required to fluidize the bed**	**Q_L, heat losses**
(^oC)	(kW)	(kW)	(kW)
120	1070	1.19	7
140	1003	0.98	6.9

For the cost of electricity, $20/GJ was used here (Australian Energy Regulator, 2023). For the cost of gas, according to the report from Australian Energy Regulator (2023), $10.80 / GJ was used.

The gas cost during fluidized bed drying at inlet air temperature of 120 ºC is shown in equation 48:

$$\text{Gas cost} = \$10.80 / \text{GJ} \times (1070 + 7)\,\text{kW} \times 8000\,\text{h/year} / \left(1000\frac{\text{kWh}}{\text{MWh}}\right) \times 3.6\,\text{GJ / MWh} = \$334{,}990/\text{year} \quad (50)$$

The electrical energy required by the fan at inlet air temperature of 120ºC is shown in following equation 49.

$$\text{Electricity cost} = \$20 / \text{GJ} \times 1.19\,\text{kW} \times \left(\frac{15}{60} \times 365\right)\text{h/year} / \left(1000\frac{\text{kWh}}{\text{MWh}}\right) \times 3.6\,\text{GJ / MWh} = \$685/\text{year} \quad (51)$$

The total cost of the fluidized bed drying process has included the capital cost of the fluidized bed dryer, and the operating costs of the electricity and the natural gas (as shown in following equation). The total costs from the fluidized bed drying process after microwaving at an inlet air temperature of 120 ºC is 0.17AU$/kg.

$$Total\ Cost\ of\ drying\ process = \frac{(8425 + 334{,}900 + 685)AU\$}{5400\frac{kg}{day} \times 365 days/year} = 0.17 AU\$/kg \quad (52)$$

2.7 The Capital and Energy Costs of Fluidized Bed Drying (After Boiling)

2.7.1 Capital Costs of Fluidized Bed Drying after Boiling

The same calculation method was used for the boiling process as for the microwaving one. To reach the target moisture content, the fluidized bed drying time at 120 ^{o}C is 25 minutes. It takes 20 minutes at inlet air temperature of 140 ^{o}C to reach the target moisture content. The capital cost of fluidized bed dryer is shown in Table 34. Due to the longer drying time than that for the microwaving process, the capital cost of the fluidized bed dryer is greater than that for microwaving.

Table 34. Drying flux, cross-sectional area and PEC of full-scale fluidized bed (boiling, open loop process), boiling process, faba beans.

Inlet air drying temperature	**Drying flux (evaporative flux)**	**Full-scale fluidized bed cross-sectional area**	**Capital cost of fluidized bed dryer**	
(^{o}C)	(kg m^{-2} bed area h^{-1})	(m^{2})	US$	AU$
120	33	1.5	8,164	12,245
140	26	2.3	10,434	15,561

2.7.2 Energy Costs of Fluidized Bed Drying after Boiling

The same methods have been used as those for the fluidized-bed drying process after microwaving. Tables 34 and 35 show the energy consumption from this process.

Table 35. The effect of different inlet air drying temperatures on the predicted air flow rates for maintaining fluidization, the predicted changes in air humidity and temperature across the fluidized bed during drying, and the outlet air humidities and temperatures for the fluidized bed drying in the boiling process.

Inlet air drying temperature	G, air flow rate for fluidization	ΔY, change in air humidity	ΔT_G, change in air temperature	Y_{out}, outlet air humidity	T_{Gout}, outlet air temperature
(^oC)	(kg s^{-1})	($\times 10^{-3}$ kg kg^{-1})	(^oC)	($\times 10^{-2}$ kg kg^{-1})	(^oC)
120	17.57	0.8	1.32	0.68	118.7
140	10.9	1.5	2.2	1.4	137.8

Table 36. The effect of different inlet air drying temperatures on the predicted thermal energies required to heat the air at the required flow rates, predicted air pumping power required for fluidization, and predicted heat losses for the fluidized bed drying in the boiling process.

Inlet air drying temperature	Q, thermal energy required to heat the air	P, pumping power required to fluidize the bed	Q_L, heat losses
(^oC)	(kW)	(kW)	(kW)
120	1757	2.0	11.5
140	1309	1.3	9

The same costs of electricity ($20/GJ) and the cost of gas ($10.80 / GJ) was used here, from the microwaving process.

The natural gas cost of fluidized bed drying is shown in Equation 53.

$$\text{Gas cost} = \$10.80 / \text{GJ} \times (1757 + 11.5)\,\text{kW} \times 8000\text{h/year} / \left(1000\frac{\text{kWh}}{\text{MWh}}\right) \times 3.6\,\text{GJ / MWh} = \$550{,}074\text{/year} \quad (53)$$

The electrical energy for the fan is shown in Equation 54,

$$\text{Electricity cost} \tag{54}$$

$$= \$20 \,/\, \text{GJ} \times 2\,\text{kW} \times 8000\,\text{h/year} \,/\, \left(1000\frac{\text{kWh}}{\text{MWh}}\right)$$

$$\times\ 3.6\,\text{GJ} \,/\, \text{MWh} = \$1{,}129/\text{year}$$

The total cost of the fluidized bed drying process, including the capital cost of the fluidized bed dryer, and the operating costs for the electricity and the natural gas are shown in the following equation. The total costs from the fluidized bed drying process after boiling at an inlet air temperature of 120 ^{o}C is 0.28AU$/kg.

$$Total\ Cost\ of\ drying\ process = \frac{(9980 + 550{,}074 + 1{,}129)AU\$}{5400\frac{kg}{day} \times 365 days/year} \tag{55}$$

$$= 0.29 AU\$/kg$$

2.9 Total Capital and Operating Costs of Processing Using Microwaving

According to Figure 27, this process includes four main sections: the dehuller, the soaking tank, an industrial microwave oven and the fluidized-bed dryer. The capital cost includes calculating the Purchase Equipment Cost (PEC) and the Process Plant Cost (PPC). The analysis follows the different steps of this process.

The summaries of the capital cost and process plant cost of all equipment used in this study are shown in Table 37.

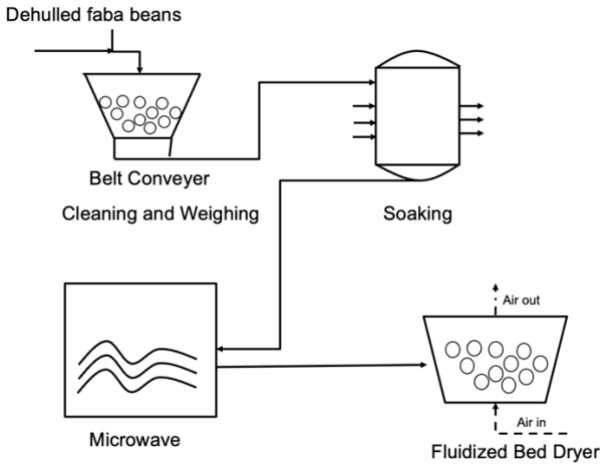

Figure 27. *Simplified flow diagram of the dehulled faba beans microwaving process.*

Table 37. Summary of the capital cost (PEC) and process plant cost (PPC) of the equipment for the microwaving process for dehulled faba beans.

Equipment	**Type**	**Capital Cost (PEC)**	**Process Plant Cost, using Lang factor (PPC)**	**Annual Capital Recovery Costs**
		AU$	**AU$**	**AU$/year**
Dehuller		3,449 /year	13,797 /year	28,110
Soaking tank	*304 stainless steel tank, 32L capacity*	16,327	65,308± 6,500	13,307 ± 1,330
Microwave	5.4 tonnes capacity	300,000	1,200,000 ± 120,000	244,500 ± 24,450
Fluidized bed dryer	1.15 – 1.4 m^2	10,338-11,640	41,325 ± 4,000	8,965 ± 530
Total		330,765 ±33,000	1,320,430± 132,043	269,591±26,959

The main part of the capital cost for the process is the microwave system, and the other costs are relatively minor aspects. The total utilities cost in this study include the electricity cost of the fluidized bed dryer, the electricity cost for the microwave equipment, the gas heating cost and the water cost of the soaking tank. The utilities cost per unit mass of dehulled faba beans and the total capital and operating cost per unit mass is shown in Table 38.

Table 38. *Gas and electricity costs, utilities costs, total operating and capital costs, for the once-through drying system when processing 5.4-ton day^{-1} of dehulled faba beans, microwaving process.*

Annual gas heating costs (FBD)	**Annual electricity (dehuller) costs**	**Annual electricity (microwave) costs**	**Annual electricity (fan) costs**	**Water cost (soaking tank)**	**Utilities cost per unit mass of faba beans**	**Total capital and operating costs per unit mass**	**Total costs per unit mass**
($/year)	($/year)	($/year)	($/year)	($/year)	($/kg)	($/kg)	($/kg)
334,990	63,151	11,520	685	26,280	0.12	0.23	0.35

The annual gas heating costs in the fluidized bed drying process is the main utilities cost. The utilities cost per unit mass of faba beans is 0.12 AU$/kg. The capital and operating costs per unit mass of dehulled faba beans is 0.23 AU$/kg. Overall, the total costs per unit mass of dehulled faba beans during microwaving processing is 0.4 AU$/kg.

2.10 Total Capital and Operating Costs of Processing Using Boiling

According to Figure 28, this process includes three main sections: the dehuller, the boiler and the fluidized-bed dryer. The capital cost includes calculating the Purchase Equipment Cost (PEC) and the Process Plant Cost (PPC). The analysis follows the different steps of this process.

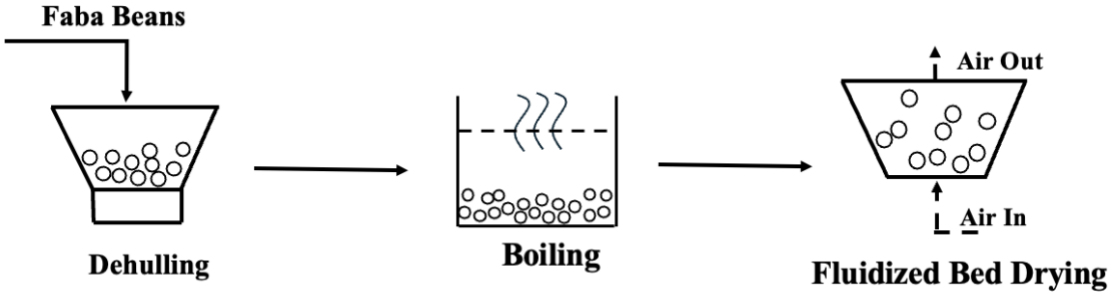

Figure 28. *Simplified flow diagram of the dehulled faba beans boiling process.*

The summaries of the capital cost and process plant cost of all equipment used in this study are shown in Table 39.

Table 39. *Summary of the capital cost (PEC) and process plant cost (PPC) of equipment (boiling process).*

Equipment	**Type**	**Capital Cost (PEC)**	**Process Plant Cost, using Lang factor (PPC)**	**Annual Capital Recovery Costs**
		AU$	**AU$**	**AU$/year**
Dehuller		3,449/year	13,797/year	28,110
Boiler	14,881 lb/h Steam capacity	495,000 ± 49,500		80,685±8,069
Fluidized bed dryer	2.3 – 2.8 m^2	12,245- 15,561	55,612 ± 6,630	11,331 ± 103
Total		581,761 ±50,000		$707,922 ± $70,792

The capital cost and the processing costs for the process are lower than those for the microwaving process. The total utilities cost in this study include the electricity cost of the fluidized bed dryer, and the natural gas cost of the boiler. The utilities cost per unit mass of dehulled faba beans and the total capital and operating cost per unit mass is shown in Table 40.

Table 40. *Gas and electricity costs, utilities costs, total operating and capital costs, for the once-through drying system when processing 5.4-ton day^{-1} of dehulled faba beans.*

Annual gas heating costs	Annual electricity (dehuller) costs	Annual electricity (boiler) costs	Annual electricity (fan) costs	Water cost (boiler)	Utilities cost per unit mass of faba beans	Capital and operating costs per unit mass	Total costs per unit mass
($/year)	($/year)	($/year)	($/year)	($/year)	($/kg)	($/kg)	($/kg)
550,074	65,131	65,308	1,129	26,280	0.33	0.05	0.38

The same situation as microwaving processing occurs in that the annual gas heating costs in the fluidized bed drying process are the main utilities costs. The utilities cost per unit mass of faba beans here is 0.33 AU$/kg. The capital and operating costs per unit mass of dehulled faba beans is 0.05AU$/kg. Overall, the total costs per unit mass of dehulled faba beans during microwaving processing is 0.4 AU$/kg. Compared with microwaving processing, the capital and operating costs are much lower by using boiling process. However, due to the high drying time, the utilities cost is higher than that for the microwaving process. To reduce the utilities cost and keep low energy consumption processing, an air recycle system has been used in the fluidized bed dryer in following parts of this work.

2.11 Comparison of Processing and Raw Material Consideration

To fully understand the financial impact, it is essential to compare the processing costs with the raw material costs. This study shows that the cost of processing significantly adds to the raw material costs. In Australia, the retail price for faba beans currently ranges from AU$ 2.99 to AU$ 6.50 per kilogram. According to Transparency Market Research (2020), the global market for faba beans is expected to grow from US$ 52 million in 2020 to US$ 79 million by 2030, driven by the increasing demand for natural protein ingredients.

2.12 Cost of Operational Labor (COL)

Turton et al. [94] proposed a method to calculate the number of operators required per shift (N_{OL}), which is shown in following equation:

$$N_{OL} = (6.29 + 31.7P^2 + 0.23N_{np})^{0.5} \quad (56)$$

Where P is the number of processing steps involving the handling of solids (transport, particle size control, particulate removal), and N_{np} is the number of nonparticulate processing steps (including compression, heating, cooling, mixing, separation and reaction, but not including pumps and vessels).

For the microwaving process, the steps in this study include: Soaking – dehulling – microwaving - fluidized bed drying.

$P = 4$, $N_{np} = 0$

$$N_{OL} = (6.29 + 31.7 \times 1^2 + 0.23 \times 4)^{0.5} = 7 \quad (57)$$

An operator has been considered to work 49 weeks per year (3 weeks off for sick leave and vacation deducted from 52 total weeks in a year). 5 shifts per week, and 8 h per shift.

$$Cost\ of\ operating\ labour\ (C_{OL}) = N_{OL} \times \frac{total\ shifts\ in\ a\ year}{shifts\ per\ operator} \times salary \quad (58)$$

$$Shifts\ per\ operator = 5\frac{shifts}{week} \times 49\frac{weeks}{year} = 245\ shifts \quad (59)$$

A plant generally requires operators 365 days a year including maintenance and shutdowns. One day is split into three eight-hour shifts.

$$Total\ shifts\ in\ a\ year = 365days \times 3\frac{shifts}{day} = 1{,}095\ operating\ shifts \quad (60)$$

The salary of operator in Australia ranges from $58,059 to $87,150. The average salary $64,254/annual has been used in this study.

$$cost\ of\ operating\ labour\ (C_{OL}) = 7 \times \frac{1{,}095}{245} \times \frac{AU\$64{,}254}{year} \quad (61)$$

$$= AU\$2{,}009{,}951$$

$$Labor\ cost\ \frac{AU\$}{kg\ faba\ beans} = \frac{2{,}009{,}951\ AU\$/year}{1{,}971{,}000\ kg/year} = 1.01 AU/kg \quad (62)$$

For the boiling process, the steps in this study include: Dehulling - boiling - fluidized bed drying.

$$N_{OL} = (6.29 + 31.7 \times 1^2 + 0.23 \times 3)^{0.5} = 6 \quad (61)$$

$$cost\ of\ operating\ labour\ (C_{OL}) = 6 \times \frac{1{,}095}{245} \times \frac{AU\$64{,}254}{year} \quad (62)$$

$$= AU\$1{,}723{,}056$$

$$Labor\ cost\ \frac{AU\$}{kg\ faba\ beans} = \frac{1{,}723{,}056\ AU\$/year}{1{,}971{,}000\ kg/year} = 0.87 AU/kg \quad (65)$$

Overall, the labour costs of microwaving process are 1.01 AU$/kg dehulled faba beans and of the boiling process if 0.87 AU$/kg dehulled faba beans. The COL of the boiling process is cheaper, since the number of steps in the boiling process is less than that for the microwaving process.

2.13 Cost of Manufacturing (COM)

The manufacturing cost of orange peel extract powder was calculated using the equation proposed by Turton et al. [94], as shown in Eq. (66). The cost of manufacturing (COM) is a function of the fixed capital cost of investment (FCI), the cost of operational labor (COL), the cost of utilities (CUT), the cost of water treatment (CWT), and the cost of raw material (CRW).

$$COM\left(\frac{AU}{year}\right) = 0.280 \times FCI + 2.37 \times COL + 1.23 \times (CUT + CWT + CRM) \quad (66)$$

The range of the price of faba beans in the Australian market [Farmtender,2024] is from 0.004 to 0.015 AU$/kg. The average price 0.01 AU$/kg has been used here. In this study, 5.4 tonnes faba beans have been processed per day (1,971,000 kg faba beans / year).

$$CRM = \frac{0.01 AU\$}{kg} \times 1{,}971{,}000 \frac{kg}{year} = 19{,}075\ AU\$/year \quad (67)$$

In this study, no chemical use has been assumed to be used during the water treatment process. The secondary wastewater treatment process, which includes filtration and activated sludge, is considered sufficient. According to Turton et al. [94], the cost of secondary wastewater treatment is estimated at $41 per 1,000 m³. Given that 27 tonnes of water are used daily in this process, this cost provides a reasonable basis for estimating the overall water treatment expenses, so the cost of wastewater treatment is shown below,

$$CWT = \frac{41\ US\$}{1000\ m^3} \times 27{,}000\ \frac{kg}{day} \times \frac{m^3}{1000\ kg} \times\ 1.5 \frac{AU\$}{US\$} \times 365\ \frac{days}{year} = 606\ AU\$/year \quad (68)$$

For the microwaving process, the COM has been shown in equations 68 and 69.

$$COM\left(\frac{AU}{year}\right) = 0.28 \times 330{,}765 + 2.37 \times 2{,}009{,}951 + 1.23 \times (606 + 236{,}520 + 19{,}075) = 5{,}171{,}325\ AU\$/year \quad (69)$$

$$COM\left(\frac{AU\$}{kg}\right) = \frac{5{,}171{,}325\ AU\$/year}{\frac{5400kg}{day} \times 365days/year} = 2.6\ AU\$/kg \quad (70)$$

The COM of the microwaving process is estimated to be 2.6 AU$/kg of dehulled faba beans. The same calculation method has been used in the boiling process. The COM of boiling process is estimated to be 2.5 AU$/kg. The microwaving process is likely to require higher capital costs for the microwave unit, compared with the boiler. The boiling process is likely to require a longer drying time. The utilities cost of fluidized bed drying process is higher for the boiling

process. There are four processing steps in the microwaving process and three steps in the boiling process. That means the COL cost of the microwaving process is likely to be higher. Overall, the COM of the boiling process is likely to be cheaper than that of the microwaving process.

2.14 Air recycling, Sample calculation

For open loop drying, the natural gas heating cost is very high, and the energy loss during this process is very large. By using air recycle instead of open loop drying, some of the hot air may be recycled to reduce the overall energy consumption and cost. The same methods (in Chapter 5) have been used here. The following Table 41 shows the costs differences between using air recycle and the open loop system at inlet conditions to the fluidized bed dryer of both 120^{o}C and 140 ^{o}C.

***Table 41**. PEC and PPC of microwaving and boiling processing during closed-loop fluidized bed drying, at the make-up ratio (r) is 0.1.*

Processing	**120 ºC**		**140 ºC**	
`	Open-loop	Air recycle	Open-loop	Air recycle
Make-up ratio	0	0.1	0	0.1
Cross section area (A, m^2)	1.4	1.0	2.3	1.2
PEC (AU$)	10,338	6,381	12,245	8,869
PPC (AU$)	41,352	25,522	48,980	35,476
Annualized capital costs ($ $year^{-1}$)	8,425	5,137	9,979	7,228
Annualized utilities costs ($ $year^{-1}$)	334,990	153,490	551,203	190,857
Total cost per unit mass ($ kg^{-1})	0.2	0.05	0.3	0.1

The air recycle system with the fluidized bed dryer significantly enhances economic efficiency. At a make-up air ratio of 0.1, the total cost per unit mass of dried faba beans is

reduced by 0.1 – 0.15 AU$/kg compared with the open-loop system, which incurs a cost of 0.1–0.2 AU$/kg at the same operating temperature. Additionally, the annualized utilities costs are reduced by more than 50%, primarily due to the recycle of the hot air during the drying process. The air recycle process minimizes the demand for heating gas, thereby lowering overall energy consumption and operational expenses. The adoption of such a system not only improves cost-effectiveness but also aligns with sustainable processing by reducing energy wastage and emissions.

Figure 29 presents a surface plot illustrating the processing cost per unit mass of dehulled faba beans as a function of the make-up ratio and inlet air temperature. The analysis considers make-up ratios ranging from 0.1 to 1.0 and inlet air temperatures between 120°C and 140°C in the fluidized bed drying system. The results indicate that the lowest processing costs in the air recycle system occur at make-up ratios between 0 and 0.1, which aligns with the findings reported in Chapter 5.

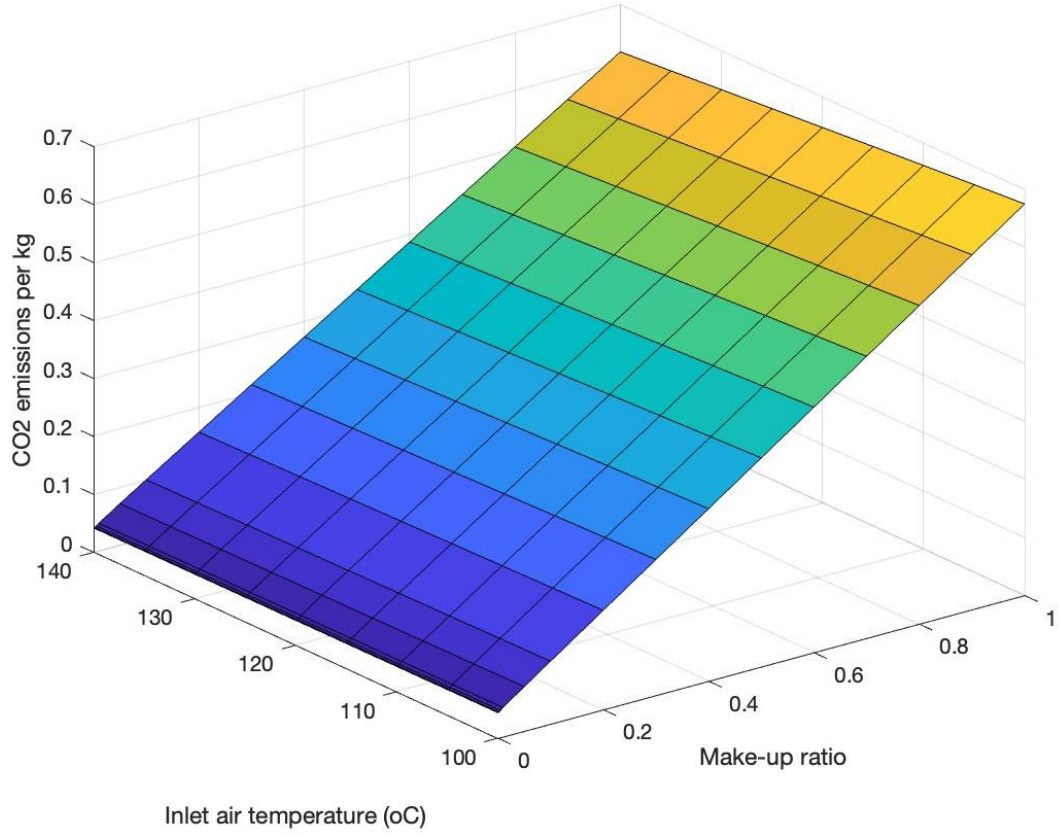

Figure 29. Surface plot for the cost of processing per unit mass of dehulled faba beans processed as a function of the make-up ratio and the inlet air temperature, for a range of make-up ratios from 0.1 to 1.0 and a range of inlet air temperatures to the fluidized bed of 120-140^{o}C

Tables 41 and 42 contain the capital costs, the processing plant costs and the utilities costs for the whole processing operation (microwaving first, boiling second). The costs of the remaining processing steps (include soaking, boiling, dehulling and microwaving) are same costs as the open loop one. The only variable cost component in this analysis pertains to the fluidized bed drying stage, which differs from the open-loop case due to the air recycle system.

Table 42. *Summary of the capital costs (PEC) and process plant costs (PPC) of equipment (microwaving process, air recycle system).*

Equipment	**Type**	**Capital Cost (PEC)**	**Process Plant Cost, using Lang factor (PPC)**	**Annual Capital Recovery Costs**	**Annualized utilities costs**
		AU$	**AU$**	**AU$/year**	**AU$/year**
Soaking tank		16,327	65,308	13,307	26,280
Dehuller	*304 stainless steel tank, 32L capacity*	3,449/year	13,797/year	28,110	63,151
Microwave	5.4 tonnes capacity	300,000	1,200,000	244,500	11,520
Fluidized bed dryer	1.0 m^2	6,381	25,522	5,137	153,490
Total		1,704,363		277,747	228,161

Table 43. *Summary of the capital cost (PEC) and process plant cost (PPC) of equipment (boiling process, air recycle system).*

Equipment	**Type**	**Capital Cost (PEC)**	**Process Plant Cost, Using Lang factor (PPC)**	**Annual Capital Recovery Costs**	**Annualized Utilities Costs**
		AU$	**AU$**	**AU$/year**	**AU$/year**
Dehuller		3,449/year	13,797/year	28,110	63,151
Boiler	14,881 lb/h Steam capacity	495,000 ± 49,500		80,685±8,069	35,730
Fluidized bed dryer	1.2 m^2	8,869	35,476	7,228	190,857
Total		556,591 ±50,000		116,023 ± 12,000	289,738

Based on the cost analysis presented in Tables 41 and 42, the PEC, PPC, and utilities cost associated with each processing method using an air recycle system are summarized. In boiling-based processing, utilities costs are notably higher due to the extended drying duration required to achieve the target moisture content. However, the implementation of an air recycle system significantly reduces utility costs, decreasing from AU$551,203 in the open-loop system to AU$190,807 in the air recycle system (a reduction of approximately 65.4%).

The same cost estimation methodology used for the calculation of the *Cost of Manufacturing (COM)* has been applied here. The COM for each processing method is detailed in Tables 44 and 44, providing a comprehensive comparison of the economic feasibility of open-loop versus air-recycle drying systems.

Table 44. *The total costs associated with four different processing methods: microwaving with an open loop, microwaving with an air recycle system, boiling with an open loop, and boiling with an air recycle system. The cost components include FCI, CUT, CWT, and COM both in AU$/year and per unit mass (AU$/kg).*

Processing	**FCI(AU$/year)**	**CUT(AU$/year)**	**CWT (AU$/year)**	**COM(AU$/year)**	**COM(AU$/kg)**
Microwaving, open loop	1751440	411097	606	5825879	2.96
Microwaving, air recycle	1727190	249411	606	5619633	2.85
Boiling, open loop	429108	639968	1212	5706146	2.90
Boiling, air recycle	437920	353650.35	1212	5356654	2.72

According to Table 44, the results shows that the air recycle system reduces the overall cost of manufacturing for both microwaving and boiling processes. Specifically, microwaving with air recycling has a lower COM (AU$/kg) at 2.85 compared with 2.96 for the open-loop system.

Similarly, boiling with air recycling results in a lower COM (AU$/kg) of 2.72 compared with 2.90 for the open-loop system. The reduction in costs is primarily due to a decrease in annualized utility costs, as the air recycle system improves energy efficiency by reusing heated air. The findings suggest that implementing an air recycle system in fluidized bed drying can lead to significant cost savings in pulse protein processing while maintaining process efficiency.

In additional, microwave ovens operate by causing water molecules within food to vibrate. This molecular vibration generates friction, which in turn produces heat, facilitating the cooking or drying process. However, a damaged microwave oven poses the risk of microwave energy leakage, which can be a safety concern. One of the potential costs associated with microwave technology is risk control. To minimize the risk of leakage, stringent safety measures must be implemented, leading to potentially high maintenance costs. Regular inspection, component replacement, and compliance with safety regulations contribute to these additional operational expenses.

Overall, boiling combined with an air recycle drying system emerges as the optimal processing method. This approach demonstrates economic efficiency by reducing overall costs while maintaining high processing performance. Additionally, it enhances safety by minimizing potential risks associated with microwave processing and ensuring controlled drying conditions.

Chapter 8. Overall Discussion and Conclusions

This chapter starts with an overall discussion of exergy analysis (energy quality) and pressure drops across the fluidized bed dryer used in this study, compared with another commercial fluidized bed dryer, before reviewing this Thesis as a whole as an overview and giving the overall conclusions and recommendations for future work.

1. Overall Discussion: Exergy Analysis and Pressure Drop

A distinctive feature of a fluidized bed dryer from energy and exergy perspectives, apart from the use of thermal energy for drying, is the pressure drop across the distributor and the pressure drop involved in supplying the drying air to the equipment. This section compares the exergy consumption between a commercial small-scale fluidized bed dryer that uses compressed air for the main air flow, and the fluidized bed dryer used in this study. The commercial dryer is a widely-used small-scale fluidized bed dryer and granulator, particularly in the pharmaceutical and catalysis industries. For instance, Chen et al. employed this type of equipment in the development of a pharmaceutical powder [99], while Leung et al. used this type of equipment to enhance the drying of catalysts [161]. The principal feature of the commercial fluidized-bed dryer, for the purpose of this analysis, is the use of compressed air at 6 bar to create the main air flow through the fluidized bed equipment. By comparison, the fluidized bed dryer used in this study is shown in Chapter 3.

A definition for exergy that includes both temperature and pressure components (of exergy) may be given as follows [71]:

$$Ex = \dot{m}C_p\left\{\left[(T_{in} - T_{out}) - T_{out}\ \ln\left(\frac{T_{in}}{T_{out}}\right)\right]\right. \tag{71}$$

$$\left. + T_{out} \ln\left(\frac{p_{in}}{p_{out}}\right)\right\}$$

where $\dot{m}$ is the mass flow rate for the stream (kg/s), Tin and Tout are the inlet and outlet stream temperatures (K), respectively, pin and pout are the inlet and outlet stream pressures (Pa), respectively, and Cp is the specific heat capacity for the stream (around 1000 J /(kg K) for air).

To specify a case study, suppose that the inlet temperature and pressure to the fluidized bed are 353 K and 101,500 Pa (just above standard atmospheric pressure, accounting for the pressure drop across the fluidized bed), respectively. Table 45 shows the inlet and outlet stream temperatures in the commercial dryer and the fluidized bed dryer used in this study. The temperatures in the commercial dryer were obtained from Chen et al's study [99].

Table 45. Inlet and outlet stream temperatures in two different fluidized bed dryers system.

Type	T_{in} (K)	T_{out} (K)	Δ T (K)
Commercial dryer	353	303	50
Fluidized bed used in this thesis	353	307	46

The pressure drop across fluidized bed dryer in this study was measured to be less than 50 Pa, and the exergy drop across the fluidized bed due to the pressure change is given by the following calculation:

$$\frac{Ex}{\dot{m}} = 1000\ \mathrm{J\ kg^{-1}K^{-1}}\ 300\ \mathrm{K} \ln\left[\frac{(50 + 101325\ )\ \mathrm{Pa}}{101325\ \mathrm{Pa}}\right] = 151 \mathrm{J\ kg^{-1}} \quad (72)$$

This exergy drop across the bed may be compared with the corresponding exergy drop for typical temperature drops across the fluidized bed dryer using the same equipment as reported by Chapter 4. When the inlet air temperature of the fluidized dryer is 353 K, the outlet air of temperature is 303 K. The temperature drops across the fluidized bed dryer is 50 K, and the exergy change across the bed is given by the following calculation:

$$\frac{Ex}{\dot{m}} = 1000\ \mathrm{J\ kg^{-1}\ K^{-1}}\ \left[(353\ \mathrm{K} - 303\ \mathrm{K}) - 303\ \mathrm{K} \ln\left(\frac{353\ \mathrm{K}}{303\mathrm{K}}\right)\right] \quad (73)$$

$$= 3{,}721\ \mathrm{J\ kg^{-1}}$$

The pressure drop of 50 Pa across the fluidized bed has a lower exergy drop (151 J kg^{-1}) than a temperature drop of 50 K, so the loss in exergy due to pressure drops in this fluidized-bed system is negligible compared with the loss in exergy due to thermal energy changes (3,721 J kg^{-1}).

However, this negligible exergy drop due to the bed pressure drop is not always the case for fluidized bed dryers. For example, a typical commercial fluidized bed dryer in the pharmaceutical industry [99] involves reducing the pressure of compressed air from at least 6 bar to atmospheric pressure in order to supply the drying air to the equipment. The corresponding exergy drop for this pressure drop is given by the following calculation:

$$\frac{Ex}{\dot{m}} = 1000\ \mathrm{J\ kg^{-1}\ K^{-1}}\ 300\ \mathrm{K} \ln\left(\frac{600000\ \mathrm{Pa}}{101325\ \mathrm{Pa}}\right) \quad (74)$$

$$= 533{,}579\ \mathrm{J\ kg^{-1}}$$

This exergy drop would correspond to a temperature drop of 56 K, as shown by the following calculation:

$$\frac{Ex}{\dot{m}} = 1000\ \mathrm{J\ kg^{-1}\ K^{-1}} \left[(353\ \mathrm{K} - 307\mathrm{K}) - 307\ \mathrm{K} \ln\left(\frac{353\ \mathrm{K}}{307\ \mathrm{K}}\right)\right] \tag{75}$$

$$= 3{,}137\ \mathrm{J\ kg^{-1}}$$

To achieve an exergydrop of 533,579 J kg^{-1} due to a pressure drop of 6 bar, the corresponding temperature drop must exceed 540 K. Consequently, when compressed air at 6 bar is utilized as the fluidizing gas in a commercial fluidized bed dryer, the exergy drop attributed to the pressure drop is significantly larger than that caused by temperature changes. As shown in Table 46, the commercial equipment is therefore not as exergy efficient as the fluidized bed dryer used in this study.

Table 46. Summary of the exergy drop and temperature drop between fluidized bed dryer used in this study *and commercial dryer*.

	Fluidized Bed Dryer Used in this Study (Figure 5)	Commercial dryer
Pressure drop (Pa)	50	600,000
Exergy drop due to pressure drop (J kg^{-1})	148	482,831
Difference between inlet and outlet temperatures (K)	50	55.8
Exergy drop due to temperature drop (J kg^{-1})	3721	3137

Overall, both temperature difference and pressure drop are important in fluidized bed drying. Temperature difference is an inevitable consequence of drying, and it is always present, being proportional to the drying rate. However, the extent of pressure drop depends on the design of the dryer. The calculations here show that the design of the air distributor for the fluidized bed, which is critical to the exergy loss due to pressure drop, is a controllable parameter in the design process for a fluidized bed dryer. The exergy loss due to the pressure drop over the air distributor may be the dominant parameter in a fluidized bed where the design is sub optimal, but in a well-designed fluidized bed, it should be a smaller term and comparable to the exergy drop due to drying and the accompanying temperature difference.

Future research could expand on this work by exploring combined drying methods, such as microwave-assisted fluidized bed drying, to further enhance drying efficiency and ANF reduction. Additionally, scaling these processes for industrial applications and assessing their impact on a broader range of pulse varieties would contribute to the development of more sustainable and efficient pulse processing technologies.

2. Overview and Conclusions

This thesis has successfully addressed key research gaps in pulse processing by exploring the application of fluidized bed drying (FBD) to reduce anti-nutritional factors in chickpeas and dehulled faba beans. The experimental studies demonstrated that the optimization of FBD parameters, such as inlet air temperature, is critical to achieving effective reductions in trypsin inhibitors content while preserving the nutritional and functional quality of the pulses by using a drying schedule. Combined with soaking, boiling and microwaving may reduce the content of phytic acid.

The techno-economic analyses further highlighted the economic viability of FBD, emphasizing the benefits of incorporating air recycle systems to enhance energy efficiency and reduce carbon dioxide emissions. These findings not only establish FBD as a sustainable and cost-effective drying method for pulse processing but also provide a roadmap for integrating advanced technologies into industrial applications.

Overall, this thesis highlights the significant potential of fluidized bed drying in enhancing the quality and sustainability of pulse processing. The integration of air recycling technology further improves economic feasibility while reducing environmental impact. These insights contribute to the broader effort of developing sustainable food processing methods that align with global trends in energy efficiency and food security. Future research should focus on scaling up these findings for industrial applications, investigating the potential of combined drying techniques such as microwave-assisted FBD, and exploring the impact of these processing methods on a wider variety of pulses to further advance sustainable food processing technologies.

3. Recommendations for Future Work

While this study has provided valuable insights into the application of fluidized bed drying (FBD) for pulse processing, several areas require further investigation. One important area for consideration is related to the modeling of drying kinetics. Another key area for future work is the uncertainty associated with TEA.

3.1 Drying Kitntics and Simulation Modelling

In Chapter 4, it has been found that the Kemp and Oakley slow-material model is useful to predict fluidized bed drying of whole chickpeas at the low inlet air drying temperature (the range between 40 to 80 ºC). As shown in Figure 30, it has limitations for predicting the drying process of high temperature for whole chickpeas. For the dehulled faba beans, it has been found that the Kemp and Oakley slow-material models is useful to predict fluidized bed drying at the high inlet air drying temperature (the range between 100 to 140 ºC), as shown in Figure 31.

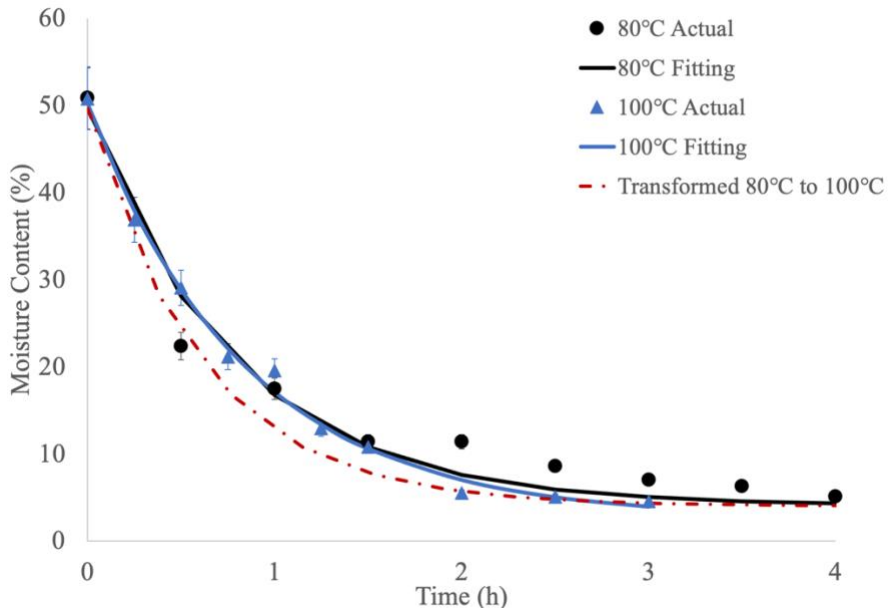

Figure 30. Predicted drying curve for whole chickpeas at high temprature, transformed from 80ºC to 100ºC.

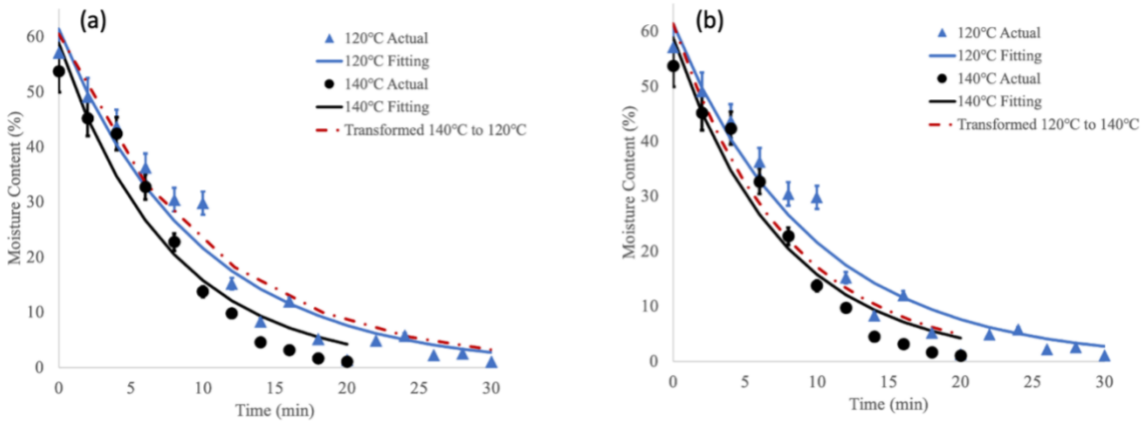

Figure 31. Predicted drying curve for dehulled faba bean at high temprature, (a) transformed from 120°C to 140°C, (b) transformed from 140°C to 120°C.

Future research could focus on refining drying models to incorporate material-specific properties, such as porosity, structural integrity, and moisture diffusion characteristics. Additionally, exploring alternative modeling approaches that integrate real-time moisture kinetics data could enhance the predictive accuracy of drying processes. Investigating the combined effects of drying conditions and pulse composition on drying efficiency and product quality would further contribute to the development of optimized drying strategies for pulse processing. By addressing these research gaps, future studies can improve the accuracy of drying models, leading to more efficient and sustainable processing techniques for pulses.

3.2 Uncertainties in Technico-economic Analysis

Another key area for future work is the uncertainty associated with the techno-economic analysis (TEA). While this study provides an initial assessment of the economic feasibility of FBD processing for chickpeas and faba beans, multiple factors contribute to uncertainty in cost estimations. Variability in energy (gas and electricity) prices, capital investment costs, labor expenses, and market demand for pulse products can significantly impact the accuracy of TEA outcomes. Future studies should incorporate sensitivity analysis and probabilistic modeling approaches, such as Monte Carlo simulations, to quantify the impact of these uncertainties. A

more detailed evaluation of real-world operational conditions, including large-scale industry data and case studies, would further enhance the reliability of economic projections for pulse drying technologies.

By addressing these research gaps, future studies can improve the accuracy of drying models and techno-economic assessments, leading to more efficient and economically viable processing techniques for pulses.

References

[1] C. Hall, C. Hillen, J. Garden Robinson, Composition, nutritional value, and health benefits of pulses, Cereal Chemistry 94(1) (2017) 11-31.

[2] AEGIC, Australian pulses: Quality, versatility, nutrition, (2017).

[3] Y. Kumar, S. Basu, D. Goswami, M. Devi, U.S. Shivhare, R.K. Vishwakarma, Anti-nutritional compounds in pulses: Implications and alleviation methods, Legume Science 4(2) (2022) e111.

[4] L. Oatway, T. Vasanthan, J.H. Helm, Phytic acid, Food Reviews International 17(4) (2001) 419-431.

[5] C.A. Patterson, J. Curran, T. Der, Effect of processing on antinutrient compounds in pulses, Cereal Chemistry 94(1) (2017) 2-10.

[6] B. Kozanoglu, J. Martinez, S. Alvarez, J. Guerrero-Beltrán, J. Welti-Chanes, Influence of particle size on vacuum–fluidized bed drying, Drying technology 30(2) (2012) 138-145.

[7] J. Grace, G. Sun, Influence of particle size distribution on the performance of fluidized bed reactors, The Canadian Journal of Chemical Engineering 69(5) (1991) 1126-1134.

[8] H. Darvishi, M.H. Khoshtaghaza, S. Minaei, Effects of fluidized bed drying on the quality of soybean kernels, Journal of the Saudi Society of Agricultural Sciences 14(2) (2015) 134-139.

[9] S. Dondee, N. Meeso, S. Soponronnarit, S. Siriamornpun, Reducing cracking and breakage of soybean grains under combined near-infrared radiation and fluidized-bed drying, Journal of Food Engineering 104(1) (2011) 6-13.

[10] S. Prachayawarakorn, P. Prachayawasin, S. Soponronnarit, Heating process of soybean using hot-air and superheated-steam fluidized-bed dryers, LWT-Food science and Technology 39(7) (2006) 770-778.

[11] C. Niamnuy, M. Nachaisin, J. Laohavanich, S. Devahastin, Evaluation of bioactive compounds and bioactivities of soybean dried by different methods and conditions, Food Chemistry 129(3) (2011) 899-906.

[12] S. Tirawanichakul, S. Prachayawarakorn, W. Varanyanond, P. Tungtrakul, S. Soponronnarit, Effect of fluidized bed drying temperature on various quality attributes of paddy, Drying Technology 22(7) (2004) 1731-1754.

[13] S. Pang, C. Ma, N. Zhang, L. He, Investigation of the solubility enhancement mechanism of rebaudioside D using a solid dispersion technique with potassium sorbate as a carrier, Food Chemistry 174 (2015) 564-570.

[14] Y. Lan, M. Xu, J.-B. Ohm, B. Chen, J. Rao, Solid dispersion-based spray-drying improves solubility and mitigates beany flavour of pea protein isolate, Food chemistry 278 (2019) 665-673.

[15] C. Nindo, J. Tang, Refractance window dehydration technology: a novel contact drying method, Drying technology 25(1) (2007) 37-48.

[16] J.M. Renkema, C.M. Lakemond, H.H. de Jongh, H. Gruppen, T. van Vliet, The effect of pH on heat denaturation and gel forming properties of soy proteins, Journal of Biotechnology 79(3) (2000) 223-230.

[17] K. Yoha, J. Moses, C. Anandharamakrishnan, Conductive hydro drying through refractance window drying–An alternative technique for drying of Lactobacillus plantarum (NCIM 2083), Drying Technology 38(5-6) (2020) 610-620.

[18] M.C. Onwezen, E.P. Bouwman, M.J. Reinders, H. Dagevos, A systematic review on consumer acceptance of alternative proteins: Pulses, algae, insects, plant-based meat alternatives, and cultured meat, Appetite 159 (2021) 105058.

[19] D. Enneking, M. Wink, Towards the elimination of anti-nutritional factors in grain legumes, Linking research and marketing opportunities for pulses in the 21st century, Springer2000, pp. 671-683.

[20] N. Haron, J. Zakaria, M.M. Batcha, Recent advances in fluidized bed drying, IOP Conference Series: Materials Science and Engineering, IOP Publishing, 2017, p. 012038.

[21] R. Sivakumar, R. Saravanan, A.E. Perumal, S. Iniyan, Fluidized bed drying of some agro products–A review, Renewable and Sustainable Energy Reviews 61 (2016) 280-301.

[22] A.N. Mudryj, N. Yu, H.M. Aukema, Nutritional and health benefits of pulses, Applied Physiology, Nutrition, and Metabolism 39(11) (2014) 1197-1204.

[23] K. Shevkani, N. Singh, Y. Chen, A. Kaur, L. Yu, Pulse proteins: Secondary structure, functionality and applications, Journal of food science and technology 56(6) (2019) 2787-2798.

[24] Z. Lei, T. Langrish, Energy and exergy analysis for a laboratory-scale closed-loop spray drying system: Experiments and simulations, Drying Technology (2024) 1-20.

[25] S. Moejes, Q. Visser, J. Bitter, A. Van Boxtel, Closed-loop spray drying solutions for energy efficient powder production, Innovative Food Science & Emerging Technologies 47 (2018) 24-37.

[26] L. Shi, A quantitative assessment of the anti-nutritional properties of Canadian pulses, 2015.

[27] L. Shi, K. Mu, S.D. Arntfield, M.T. Nickerson, Changes in levels of enzyme inhibitors during soaking and cooking for pulses available in Canada, Journal of food science and technology 54 (2017) 1014-1022.

[28] P. Kumar, P.K. Joshi, S. Parappurathu, Changing consumption patterns and roles of pulses in nutrition, and future demand projections, Pulses for nutrition in India: changing patterns from farm to fork (2017) 21-61.

[29] F. Boukid, Chickpea (Cicer arietinum L.) protein as a prospective plant-based ingredient: a review, International Journal of Food Science & Technology 56(11) (2021) 5435-5444.

[30] C. Vidal-Valverde, J. Frias, C. Sotomayor, C. Diaz-Pollan, M. Fernandez, G. Urbano, Nutrients and antinutritional factors in faba beans as affected by processing, Zeitschrift für Lebensmitteluntersuchung und-Forschung A 207 (1998) 140-145.

[31] R.P. Rathod, U.S. Annapure, Effect of extrusion process on antinutritional factors and protein and starch digestibility of lentil splits, LWT-Food Science and Technology 66 (2016) 114-123.

[32] T.A. El-Adawy, Nutritional composition and antinutritional factors of chickpeas (Cicer arietinum L.) undergoing different cooking methods and germination, Plant foods for human nutrition 57 (2002) 83-97.

[33] A. Sharma, S. Sehgal, Effect of processing and cooking on the antinutritional factors of faba bean (Vicia faba), Food chemistry 43(5) (1992) 383-385.

[34] B. Singh, J.P. Singh, N. Singh, A. Kaur, Saponins in pulses and their health promoting activities: A review, Food chemistry 233 (2017) 540-549.

[35] R. Alonso, A. Aguirre, F. Marzo, Effects of extrusion and traditional processing methods on antinutrients and in vitro digestibility of protein and starch in faba and kidney beans, Food chemistry 68(2) (2000) 159-165.

[36] T. Hefnawy, Effect of processing methods on nutritional composition and anti-nutritional factors in lentils (Lens culinaris), Annals of Agricultural Sciences 56(2) (2011) 57-61.

[37] U. Chitra, V. Vimala, U. Singh, P. Geervani, Variability in phytic acid content and protein digestibility of grain legumes, Plant Foods for Human Nutrition 47 (1995) 163-172.

[38] E. Hove, S. King, Trypsin inhibitor contents of lupin seeds and other grain legumes, New Zealand Journal of Agricultural Research 22(1) (1979) 41-42.

[39] A. Mubarak, Nutritional composition and antinutritional factors of mung bean seeds (Phaseolus aureus) as affected by some home traditional processes, Food chemistry 89(4) (2005) 489-495.

[40] N. Singh, Pulses: an overview, Journal of Food Science and Technology 54 (2017) 853-857.

[41] M. Banti, W. Bajo, Review on nutritional importance and anti-nutritional factors of legumes, Int. J. Food Sci. Nutr 9 (2020) 138-149.

[42] J.B. Sumner, G.F. Somers, Chemistry and methods of enzymes, Academic press2014.

[43] L. Shi, S.D. Arntfield, M. Nickerson, Changes in levels of phytic acid, lectins and oxalates during soaking and cooking of Canadian pulses, Food Research International 107 (2018) 660-668.

[44] S. Avilés-Gaxiola, C. Chuck-Hernández, S.O. Serna Saldívar, Inactivation methods of trypsin inhibitor in legumes: A review, Journal of food science 83(1) (2018) 17-29.

[45] K.A. Walsh, D.L. Kauffman, K.S. Kumar, H. Neurath, On the structure and function of bovine trypsinogen and trypsin, Proceedings of the National Academy of Sciences 51(2) (1964) 301-308.

[46] A. Cabrera-Orozco, C. Jiménez-Martínez, G. Dávila-Ortiz, Soybean: Non-nutritional factors and their biological functionality, Soybean-bio-active compounds (2013) 387-410.

[47] G. Subbulakshmi, K. Ganesh Kumar, L. Venkataraman, Effect of germination on the carbohydrates, proteins, trypsin inhibitor, amylase inhibitor and hemagglutinin in horsegram and mothbean, Nutrition Reports International 13(1) (1976) 19-31.

[48] M. Marquez, R. Alonso, Inactivation of trypsin inhibitor in chickpea, Journal of Food Composition and Analysis 12(3) (1999) 211-217.

[49] S. Nielsen, I. Liener, Effect of germination on trypsin inhibitor and hemagglutinating activities in Phaseolus vulgaris, Journal of Food Science 53(1) (1988) 298-299.

[50] B.H. Vagadia, S.K. Vanga, V. Raghavan, Inactivation methods of soybean trypsin inhibitor–A review, Trends in Food Science & Technology 64 (2017) 115-125.

[51] C. Osella, N. Gordo, R. González, E. Tosi, E. Ré, Soybean heat-treated using a fluidized bed, LWT-Food Science and Technology 30(7) (1997) 676-680.

[52] K. Baintner, Trypsin-inhibitor and chymotrypsin-inhibitor studies with soybean extracts, Journal of Agricultural and Food Chemistry 29(1) (1981) 201-203.

[53] B. Svensson, K. Fukuda, P.K. Nielsen, B.C. Bønsager, Proteinaceous α-amylase inhibitors, Biochimica et Biophysica Acta (BBA)-Proteins and Proteomics 1696(2) (2004) 145-156.

[54] H. Wang, C. Chen, T. Jeng, J. Sung, Comparisons of α-amylase inhibitors from seeds of common bean mutants extracted through three phase partitioning, Food Chemistry 128(4) (2011) 1066-1071.

[55] G. Grant, J.E. Edwards, A. Pusztai, α-Amylase inhibitor levels in seeds generally available in Europe, Journal of the Science of Food and Agriculture 67(2) (1995) 235-238.

[56] M. Rekha, G. Padmaja, Alpha-amylase inhibitor changes during processing of sweet potato and taro tubers, Plant Foods for Human Nutrition 57 (2002) 285-294.

[57] A. Oshodi, V. Aletor, Functional properties of haemagglutinins (lectins) extracted from some edible varieties of lima beans (Phaseolus lunatus Linn), International journal of food sciences and nutrition 44(2) (1993) 133-136.

[58] A. Bender, Haemagglutinins (lectins) in beans, Food Chemistry 11(4) (1983) 309-320.

[59] S.A. Alajaji, T.A. El-Adawy, Nutritional composition of chickpea (Cicer arietinum L.) as affected by microwave cooking and other traditional cooking methods, Journal of Food Composition and Analysis 19(8) (2006) 806-812.

[60] A. Kumar, C. Sahu, P.A. Panda, M. Biswal, R.P. Sah, M.K. Lal, M.J. Baig, P. Swain, L. Behera, K. Chattopadhyay, Phytic acid content may affect starch digestibility and glycemic index value of rice (Oryza sativa L.), Journal of the Science of Food and Agriculture 100(4) (2020) 1598-1607.

[61] E. Feizollahi, R.S. Mirmahdi, A. Zoghi, R.T. Zijlstra, M. Roopesh, T. Vasanthan, Review of the beneficial and anti-nutritional qualities of phytic acid, and procedures for removing it from food products, Food Research International 143 (2021) 110284.

[62] B. Kala, V. Mohan, Effect of microwave treatment on the antinutritional factors of two accessions of velvet bean, Mucuna pruriens (L.) DC. var. utilis (Wall. ex Wight) Bak. ex Burck, (2012).

[63] H.R. Sharif, F. Zhong, F.M. Anjum, M.I. Khan, M.K. Sharif, M. Khan, J. Haider, F. Shah, Effect of soaking and microwave pretreatments on nutritional profile and cooking quality of different lentil cultivars, Pakistan J. Food Sci 24 (2014) 186-194.

[64] G. Manez, A. Alegria, R. Farré, A. Frigola, Effect of traditional, microwave and industrial cooking on inositol phosphate content in beans, chickpeas and lentils, International journal of food sciences and nutrition 53(6) (2002) 503-508.

[65] A.L.M. Daneluti, J.d.R. Matos, Study of thermal behavior of phytic acid, Brazilian Journal of Pharmaceutical Sciences 49 (2013) 275-283.

[66] E.-S. Mariam, M.A. Ahmed, M.A. Osman, Study of germination, soaking and cooking effects on the nutritional quality of goat pea (Securigera securidaca L.), Journal of King Saud University-Science 32(3) (2020) 2029-2033.

[67] C. Vidal-Valverde, J. Frias, I. Estrella, M.J. Gorospe, R. Ruiz, J. Bacon, Effect of processing on some antinutritional factors of lentils, Journal of Agricultural and Food Chemistry 42(10) (1994) 2291-2295.

[68] P. Siddhuraju, K. Becker, Effect of various domestic processing methods on antinutrients and in vitro protein and starch digestibility of two indigenous varieties of Indian tribal pulse, Mucuna pruriens var. utilis, Journal of Agricultural and Food Chemistry 49(6) (2001) 3058-3067.

[69] T. Bhat, A. Kannan, B. Singh, O. Sharma, Value addition of feed and fodder by alleviating the antinutritional effects of tannins, Agricultural Research 2 (2013) 189-206.

[70] E. Haslam, Plant polyphenols: vegetable tannins revisited, CUP Archive1989.

[71] S. Khandelwal, S.A. Udipi, P. Ghugre, Polyphenols and tannins in Indian pulses: Effect of soaking, germination and pressure cooking, Food Research International 43(2) (2010) 526-530.

[72] Z. Dehghanian, K. Habibi, M. Dehghanian, S. Aliyar, B.A. Lajayer, T. Astatkie, T. Minkina, C. Keswani, Reinforcing the bulwark: unravelling the efficient applications of plant phenolics and tannins against environmental stresses, Heliyon (2022).

[73] A.M. Mannino, C. Micheli, Ecological function of phenolic compounds from mediterranean fucoid algae and seagrasses: An overview on the genus Cystoseira sensu lato and Posidonia oceanica (L.) Delile, Journal of Marine Science and Engineering 8(1) (2020) 19.

[74] A.L. Girard, S.R. Bean, M. Tilley, S.L. Adrianos, J.M. Awika, Interaction mechanisms of condensed tannins (proanthocyanidins) with wheat gluten proteins, Food Chemistry 245 (2018) 1154-1162.

[75] R. Kumar, S. Vaithiyanathan, Occurrence, nutritional significance and effect on animal productivity of tannins in tree leaves, Animal feed science and technology 30(1-2) (1990) 21-38.

[76] R. Pande, H.N. Mishra, Effect of fluidized bed heat treatment on insect mortality, proximate composition and antinutritional content of stored green gram (Vigna radiata) seeds, Journal of Food Chemistry and Nutrition 1(2) (2013) 94-99.

[77] S. Muetzel, K. Becker, Extractability and biological activity of tannins from various tree leaves determined by chemical and biological assays as affected by drying procedure, Animal Feed Science and Technology 125(1-2) (2006) 139-149.

[78] S. Cheng, D.J. Skylas, C. Whiteway, V. Messina, T.A. Langrish, The Effects of Fluidized Bed Drying, Soaking, and Microwaving on the Phytic Acid Content, Protein Structure, and Digestibility of Dehulled Faba Beans, Processes 11(12) (2023) 3401.

[79] R. Sharma, S. Sharma, M. Bhandari, H. Bobade, R. Sohu, B. Singh, Characterization of bioprocessed white and red sorghum flours: Anti-nutritional and bioactive compounds,

functional properties, molecular, and morphological features, Journal of Food Science 88(8) (2023) 3287-3301.

[80] W. Kaensup, S. Wongwises, Combined microwave/fluidized bed drying of fresh peppercorns, Drying Technology 22(4) (2004) 779-794.

[81] J. Stanisławski, Drying of diced carrot in a combined microwave–fluidized bed dryer, Drying Technology 23(8) (2005) 1711-1721.

[82] M.H. Khoshtaghaza, H. Darvishi, S. Minaei, Effects of microwave-fluidized bed drying on quality, energy consumption and drying kinetics of soybean kernels, Journal of food science and technology 52 (2015) 4749-4760.

[83] P. Chupawa, S. Inchuen, D. Jaisut, F. Ronsse, W. Duangkhamchan, Effects of stepwise microwave heating and expanded bed height control on the performance of combined fluidized bed/microwave drying for preparing instant brown rice, Food and Bioprocess Technology 16(1) (2023) 199-215.

[84] D. Zare, M. Ranjbaran, Simulation and validation of microwave-assisted fluidized bed drying of soybeans, Drying Technology 30(3) (2012) 236-247.

[85] T.L.S. Cheng, Technico-Economic Analysis for the Costs of Drying Chickpeas: An Example Showing the Trade-off between Capital and Operating Costs for Different Inlet Air Temperatures, IDS 2024 – 23rd International Drying Symposium (2024).

[86] H.Z. Hosseinabadi, M. Layeghi, D. Berthold, K. Doosthosseini, S. Shahhosseini, Mathematical modeling the drying of poplar wood particles in a closed-loop triple pass rotary dryer, Drying technology 32(1) (2014) 55-67.

[87] I.C. Kemp, D.E. Oakley, Modelling of particulate drying in theory and practice, Drying Technology 20(9) (2002) 1699-1750.

[88] V.I. Goldanskii, Quantum chemical reactions in the deep cold, Scientific American 254(2) (1986) 46-53.

[89] K. Liu, Soybean trypsin inhibitor assay: further improvement of the standard method approved and reapproved by American Oil Chemists' Society and American Association of Cereal Chemists International, Journal of the American Oil Chemists' Society 96(6) (2019) 635-645.

[90] W. Haug, H.J. Lantzsch, Sensitive method for the rapid determination of phytate in cereals and cereal products, Journal of the Science of Food and Agriculture 34(12) (1983) 1423-1426.

[91] S. Bhinder, S. Kumari, B. Singh, A. Kaur, N. Singh, Impact of germination on phenolic composition, antioxidant properties, antinutritional factors, mineral content and Maillard reaction products of malted quinoa flour, Food Chemistry 346 (2021) 128915.

[92] H. Hsu, D. Vavak, L. Satterlee, G. Miller, A multienzyme technique for estimating protein digestibility, Journal of food science 42(5) (1977) 1269-1273.

[93] G. Towler, R. Sinnott, Chemical engineering design: principles, practice and economics of plant and process design, Butterworth-Heinemann2021.

[94] R. Turton, R.C. Bailie, W.B. Whiting, J.A. Shaeiwitz, Analysis, synthesis and design of chemical processes, Pearson Education2008.

[95] S. Vatansever, M.C. Tulbek, M.N. Riaz, Low-and high-moisture extrusion of pulse proteins as plant-based meat ingredients: a review, Cereal Foods World 65(4) (2020) 12-14.

[96] M. Asgar, A. Fazilah, N. Huda, R. Bhat, A. Karim, Nonmeat protein alternatives as meat extenders and meat analogs, Comprehensive reviews in food science and food safety 9(5) (2010) 513-529.

[97] J. Jang, H. Arastoopour, CFD simulation of a pharmaceutical bubbling bed drying process at three different scales, Powder technology 263 (2014) 14-25.

[98] T. Nazghelichi, M.H. Kianmehr, M. Aghbashlo, Thermodynamic analysis of fluidized bed drying of carrot cubes, Energy 35(12) (2010) 4679-4684.

[99] H. Chen, S. Rustagi, E. Diep, T.A. Langrish, B.J. Glasser, Scale-up of fluidized bed drying: Impact of process and design parameters, Powder technology 339 (2018) 8-16.

[100] Y. Liu, J. Peng, Y. Kansha, M. Ishizuka, A. Tsutsumi, D. Jia, X.T. Bi, C. Lim, S. Sokhansanj, Novel fluidized bed dryer for biomass drying, Fuel Processing Technology 122 (2014) 170-175.

[101] M. Taghavivand, K. Choi, L. Zhang, Investigation on drying kinetics and tribocharging behaviour of pharmaceutical granules in a fluidized bed dryer, Powder Technology 316 (2017) 171-180.

[102] L. Briens, M. Bojarra, Monitoring fluidized bed drying of pharmaceutical granules, Aaps Pharmscitech 11(4) (2010) 1612-1618.

[103] O. Stewart, G. Raghavan, V. Orsat, K. Golden, The effect of drying on unsaturated fatty acids and trypsin inhibitor activity in soybean, Process Biochemistry 39(4) (2003) 483-489.

[104] K. Cronin, K. Abodayeh, J. Caro-Corrales, Probabilistic analysis and design of the industrial timber drying process, Drying Technology 20(2) (2002) 307-324.

[105] T. Langrish, A. Brooke, C. Davis, H. Musch, G. Barton, An Improved Drying Achedole for Australian Ironbark Timber: Optimisation and Experimental Validation, Drying Technology 15(1) (1997) 47-70.

[106] B. Cil, A. Topuz, Fluidized bed drying of corn, bean and chickpea, Journal of food process engineering 33(6) (2010) 1079-1096.

[107] S. Gupta, C. Liu, S.K. Sathe, Quality of a chickpea-based high protein snack, Journal of food science 84(6) (2019) 1621-1630.

[108] C. Nitride, G.E. Vegarud, I. Comi, T.G. Devold, A. Røseth, A. Marti, S. Iametti, G. Mamone, G. Picariello, F. Alfieri, Effect of sprouting on the proteome of chickpea flour and on its digestibility by ex vivo gastro-duodenal digestion complemented with jejunal brush border membrane enzymes, Food Research International 154 (2022) 111012.

[109] C.-H. Tang, M.-L. Xiao, Z. Chen, X.-Q. Yang, S.-W. Yin, Properties of cast films of vicilin-rich protein isolates from Phaseolus legumes: Influence of heat curing, LWT-Food Science and Technology 42(10) (2009) 1659-1666.

[110] C.E. Chávez-Murillo, J.I. Veyna-Torres, L.M. Cavazos-Tamez, J. de la Rosa-Millán, S.O. Serna-Saldívar, Physicochemical characteristics, ATR-FTIR molecular interactions and in vitro starch and protein digestion of thermally-treated whole pulse flours, Food Research International 105 (2018) 371-383.

[111] N. Yazdanpanah, T.A. Langrish, Fast crystallization of lactose and milk powder in fluidized bed dryer/crystallizer, Dairy science & technology 91(3) (2011) 323-340.

[112] T.S. Withana-Gamage, J.P. Wanasundara, Z. Pietrasik, P.J. Shand, Physicochemical, thermal and functional characterisation of protein isolates from Kabuli and Desi chickpea (Cicer arietinum L.): A comparative study with soy (Glycine max) and pea (Pisum sativum L.), Journal of the Science of Food and Agriculture 91(6) (2011) 1022-1031.

[113] H.A. OLABODE, C.N. STANDING, P.A. CHAPMAN, Total energy to produce food servings as a function of processing and marketing modes, Journal of Food Science 42(3) (1977) 768-774.

[114] M.A. RAO, ENERGY CONSUMPTION FOR REFRIGERATED, CANNED, AND FROZEN SNAP BEANS AND CORN, Journal of Food Process Engineering 3(2) (1980) 61-76.

[115] N. Nwakuba, V.C. Okafor, O.O. Okorafor, Techno-economic analysis of a hybrid solar-electric dryer, Energy Sources, Part A: Recovery, Utilization, and Environmental Effects 46(1) (2024) 10289-10313.

[116] N. Philip, S. Duraipandi, A. Sreekumar, Techno-economic analysis of greenhouse solar dryer for drying agricultural produce, Renewable Energy 199 (2022) 613-627.

[117] N. Haque, M. Somerville, Techno-economic and environmental evaluation of biomass dryer, Procedia Engineering 56 (2013) 650-655.

[118] D. Shofinita, T. Langrish, Spray drying of orange peel extracts: Yield, total phenolic content, and economic evaluation, Journal of Food Engineering 139 (2014) 31-42.

[119] Selina Wamucii (2024), Australia Chickpeas Prices, https://www.selinawamucii.com/insights/prices/australia/chickpeas/, (accessed January 3, 2024).

[120] D. Brennan, Process industry economics: principles, concepts and applications, Elsevier 2020.

[121] A.S. Mujumdar, Handbook of Industrial Drying (4th ed.). CRC Press. 2014. https://doi.org/10.1201/b17208 .

[122] Z. Pakowski, A.S. Mujumdar, Basic Process Calculations, Handbook of Industrial Drying 51.

[123] Law, C.L. and Mujumdar, A.S., 2006. Fluidized bed dryers. Handbook of industrial drying, 3. pp162-166.

[124] S. Venkateshan, Heat transfer, Springer Nature, Introduction to the Study of Heat Transfer. (2021).

[125] S. Wamucii, Australia Chickpeas Prices, (2025). Date Accessed: 18,Nov,2025. Website: https://www.selinawamucii.com/insights/prices/australia/chickpeas/#:~:text=What%20is%20the%20price%20of,kilogram%2Fpound%20in%20Australia%20today%3F&text=The%20retail%20price%20range%20in,lb)%20in%20Canberra%20and%20Melbourne.

[126] W.V. Davis, C. Weber, G. Lucier, S.R. Skorbiansky, Vegetables and Pulses Outlook: December 2022, Outlook (2022).

[127] DCCEEW, Department of Clmate Change, Energy, the Environment, and Water,Australian National Greenhouse Accounts Factors, Australian Government, (2023).

[128] P. Maharaj, E. Friedrich, Environmental life cycle, carbon footprint and comparative economic assessment of rainwater harvesting systems in schools–a South African case study, Water SA 50(1) (2024) 80-91.

[129] M. Hasan, T.A.G. Langrish, Development of a sustainable methodology for life-cycle performance evaluation of solar dryers, Solar Energy 135 (2016) 1-13.

[130] Z.-q. Jiang, M. Pulkkinen, Y.-j. Wang, A.-M. Lampi, F.L. Stoddard, H. Salovaara, V. Piironen, T. Sontag-Strohm, Faba bean flavour and technological property improvement by thermal pre-treatments, LWT-Food Science and Technology 68 (2016) 295-305.

[131] D.J. Skylas, J.B. Johnson, J. Kalitsis, S. Richard, C. Whiteway, I. Wesley, M. Naiker, K.J. Quail, Optimised dry processing of protein concentrates from Australian pulses: A comparative study of faba bean, yellow pea and red lentil seed material, Legume Science 5(1) (2023) e161.

[132] M.G. Nosworthy, J.D. House, Factors influencing the quality of dietary proteins: Implications for pulses, Cereal Chemistry 94(1) (2017) 49-57.

[133] R. Akkad, E. Kharraz, J. Han, J.D. House, J.M. Curtis, The effect of short-term storage temperature on the key headspace volatile compounds observed in Canadian faba bean flour, Food Science and Technology International 28(2) (2022) 135-143.

[134] L.U. Thompson, Potential health benefits and problems associated with antinutrients in foods, Food Research International 26(2) (1993) 131-149.

[135] J. Frias, C. Vidal-Valverde, C. Sotomayor, C. Diaz-Pollan, G. Urbano, Influence of processing on available carbohydrate content and antinutritional factors of chickpeas, European Food Research and Technology 210 (2000) 340-345.

[136] S. Sarkhel, A. Roy, Phytic acid and its reduction in pulse matrix: Structure–function relationship owing to bioavailability enhancement of micronutrients, Journal of Food Process Engineering 45(5) (2022) e14030.

[137] R. Suhag, A. Dhiman, G. Deswal, D. Thakur, V.S. Sharanagat, K. Kumar, V. Kumar, Microwave processing: A way to reduce the anti-nutritional factors (ANFs) in food grains, LWT 150 (2021) 111960.

[138] S.I. Rafiq, S. Singh, D.C. Saxena, Physical, physicochemical and anti-nutritional properties of Horse Chestnut (Aesculus indica) seed, Journal of Food Measurement and Characterization 10 (2016) 302-310.

[139] S. Sharma, A. Singh, U. Sharma, R. Kumar, N. Yadav, Effect of thermal processing on anti nutritional factors and in vitro bioavailability of minerals in desi and kabuli cultivars of chick pea grown in North India, Legume Research-An International Journal 41(2) (2018) 267-274.

[140] H.W. Yang, C.K. Hsu, Y.F. Yang, Effect of thermal treatments on anti-nutritional factors and antioxidant capabilities in yellow soybeans and green-cotyledon small black soybeans, Journal of the Science of Food and Agriculture 94(9) (2014) 1794-1801.

[141] Y. Deng, O. Padilla-Zakour, Y. Zhao, S. Tao, Influences of high hydrostatic pressure, microwave heating, and boiling on chemical compositions, antinutritional factors, fatty acids, in vitro protein digestibility, and microstructure of buckwheat, Food and Bioprocess Technology 8 (2015) 2235-2245.

[142] M. Vogelsang-O'Dwyer, I.L. Petersen, M.S. Joehnke, J.C. Sørensen, J. Bez, A. Detzel, M. Busch, M. Krueger, J.A. O'Mahony, E.K. Arendt, Comparison of faba bean protein ingredients produced using dry fractionation and isoelectric precipitation: Techno-functional, nutritional and environmental performance, Foods 9(3) (2020) 322.

[143] S.B. Dhull, M.K. Kidwai, R. Noor, P. Chawla, P.K. Rose, A review of nutritional profile and processing of faba bean (Vicia faba L.), Legume Science 4(3) (2022) e129.

[144] A.M.A. Osman, A.B. Hassan, G.A. Osman, N. Mohammed, M.A. Rushdi, E.E. Diab, E.E. Babiker, Effects of gamma irradiation and/or cooking on nutritional quality of faba bean (Vicia faba L.) cultivars seeds, Journal of food science and technology 51 (2014) 1554-1560.

[145] E. Abd El-Hady, R. Habiba, Effect of soaking and extrusion conditions on antinutrients and protein digestibility of legume seeds, LWT-Food Science and Technology 36(3) (2003) 285-293.

[146] S. Chandrasekaran, S. Ramanathan, T. Basak, Microwave food processing—A review, Food research international 52(1) (2013) 243-261.

[147] L. Zhang, Y. Hu, X. Wang, O.A. Fakayode, H. Ma, C. Zhou, A. Xia, Q. Li, Improving soaking efficiency of soybeans through sweeping frequency ultrasound assisted by parameters optimization, Ultrasonics Sonochemistry 79 (2021) 105794.

[148] H. Feng, Y. Yin, J. Tang, Microwave drying of food and agricultural materials: basics and heat and mass transfer modeling, Food Engineering Reviews 4 (2012) 89-106.

[149] N. Terziev, G. Daniel, G. Torgovnikov, P. Vinden, Effect of microwave treatment on the wood structure of Norway spruce and radiata pine, Bioresources 15(3) (2020) 5616-5626.

[150] L. Hansson, Microwave treatment of wood, Luleå tekniska universitet, 2007.

[151] E. Kaspchak, L.I. Mafra, M.R. Mafra, Effect of heating and ionic strength on the interaction of bovine serum albumin and the antinutrients tannic and phytic acids, and its influence on in vitro protein digestibility, Food Chemistry 252 (2018) 1-8.

[152] Y.-W. Luo, W.-H. Xie, Effect of different processing methods on certain antinutritional factors and protein digestibility in green and white faba bean (Vicia faba L.), CyTA-Journal of Food 11(1) (2013) 43-49.

[153] F.H. Brishti, S.Y. Chay, K. Muhammad, M.R. Ismail-Fitry, M. Zarei, S. Karthikeyan, N. Saari, Effects of drying techniques on the physicochemical, functional, thermal, structural and rheological properties of mung bean (Vigna radiata) protein isolate powder, Food Research International 138 (2020) 109783.

[154] N. Yazdanpanah, T.A. Langrish, Comparative study of deteriorative changes in the ageing of milk powder, Journal of food engineering 114(1) (2013) 14-21.

[155] B. Fraser, S. Verma, W. Muir, Some physical properties of fababeans, Journal of Agricultural Engineering Research 23(1) (1978) 53-57.

[156] Xu, Y., Cartier, A., Obielodan, M., Jordan, K., Hairston, T., Shannon, A., & Sismour, E. (2016). Nutritional and anti-nutritional composition, and in vitro protein digestibility of Kabuli

chickpea (Cicer arietinum L.) as affected by differential processing methods. Journal of Food Measurement and Characterization, 10, 625-633.

[157] Zhong, Y., Wang, Z., & Zhao, Y. (2015). Impact of radio frequency, microwaving, and high hydrostatic pressure at elevated temperature on the nutritional and antinutritional components in black soybeans. Journal of food science, 80(12), C2732-C2739.

[158] Schultz, C.W. and Mehta, R.K., 1991. Cost optimization of stirred ball mill grinding (No. DOE/MC/11089-92/C0005; CONF-911182-6). Institute of Gas Technology, Chicago, IL (United States); Alabama Univ., University, AL (United States). Mineral Resources Inst.

[160] Peter, M.S. and Timmerhaus, K.D., 2003. Plant design and economics for chemical engineers. McGraw-Hill International Edition, Chemical And Petroleum Engineering Series, Fourth Edition.

[161] Leung, C., Adler, J., Shapley, N., Langrish, T.A. and Glasser, B.J., 2023. Fluidized bed drying of supported Catalysts: Effect of process parameters. Chemical Engineering Science, 282, p.119280.

Appendix

1. Capital and energy cost of the dehuller

Method 1 – Literature Based

The processing capacity was set as 5.4 tonnes per day, which corresponds to 3.75 kg/min. The density of faba beans is in the range of 730 to 850 kg/m^3 [154]. The feed rate of faba beans is 3.75kg/min / 790 kg/m^3 = 4750 cc/min. According to the data in Figure 2 from Schultz and Mehta [158], the capital cost at a feed rate reach to 4750 cc/min, was approximately 0.5 US$/MT in 1991. Based on the data from reserve bank of Australia, over 33 years, at an average annual inflation rate of 2.6 per cent, and adjusting for capital recovery and inflation. the estimated capital cost in 2024 is approximately 1.75 AU$/MT, which represents the Purchased Equipment Cost (PEC) per unit throughput.

$$\begin{aligned} PEC\ per\ year &= \ Capital\ cost\ per\ year \\ &= 1.75\ \frac{AU\$}{MT} \times \frac{MT}{1000kg} \times \frac{5400kg}{day} \times 365 days/year \\ &= 3{,}449\ AU\$/year \end{aligned} \tag{76}$$

The Process Plant Cost (PPC) is obtained from the PEC and the Lang factors, as follows:

$$PPC\ per\ year = 4 \times PEC = 13{,}797\ AU\$/year \tag{77}$$

Assuming an interest rate of 10%, with the number of repayments being 10 years, the value of the CRF is 0.163. The Annual Capital Recovery Costs may then be estimated as follows:

$$\begin{aligned} Annual\ Capital\ Recovery\ Costs &= (3499 + 13797)\frac{AU\$}{year} \times CRF(= 0.163) \\ &= 2{,}819 AU\$/year \end{aligned} \tag{78}$$

Based on Schultz and Mehta [158], the energy consumption of a ball mill ranges from 317 kWh/t to 445 kWh/t. For this study, assuming the use of a high rotor speed (a conservative estimate), the energy consumption is estimated at 445 kWh/t. The cost for energy (Q) here is calculated at AU$20/GJ which is consistent with the electricity cost in Chapter 5, since the rotor is likely to be driven by an electrical motor.

$$\begin{aligned} &Energy\ consumption\ per\ year \\ &= 445\frac{kWh}{ton} \times 5.4\frac{ton}{year} \times \frac{365day}{year} \times \frac{0.0036GJ}{kWh} \times \frac{20AU\$}{GJ} \\ &= 63{,}151\ AU\$/year \end{aligned} \tag{79}$$

$$\begin{aligned} Total\ Cost\ from\ dehuller = Energy\ consumption\ cost + Annual\ capital\ recovery \\ cost = 65{,}970\ AU\$/year \end{aligned} \tag{80}$$

$$Cost\ of\ dehulling\ process = \frac{65{,}970\ AU\$/year}{5{,}400\frac{kg}{day} \times \frac{365\ day}{year}} = 0.033\ AU\$/kg \tag{81}$$

- **Method 2 - A Ball Mill from Industry**

The second method utilized a ball mill sourced directly from industry and quoted. The capital cost of a ball mill (Armstrong Industries, BBM5000), with a capacity of 5,000 L, was quoted at AU$45,000 (which is purchased equipment costs, PEC). This equipment is sufficient to process 5.4 kg of faba beans per day (as shown in section 2.1.2), meeting the production requirements of this study. The Process Plant Cost (PPC) is obtained from the PEC and the Lang factors, as follows:

$$PPC\ = Process\ Plant\ Cost\ = 4 \times PEC = 180{,}000\ AU\$ \tag{82}$$

Using the same CRF as before (with method 1, 0.163), the Annual Capital Recovery Costs may then be estimated as follows:

$$Annual\ Capital\ Recovery\ Costs = (45{,}000 + 180{,}000)\frac{AU\$}{year} \times CRF$$
$$= 36{,}675\ AU\$/year \tag{83}$$

The annual capital recovery costs are then 36,675 AU$/year.

The electric motor used is 18 kW. The energy consumption cost is 11,353 AU$/year.

$$Total\ Cost\ of\ dehulling\ process = \frac{\frac{(36{,}675 + 11{,}353)AU\$}{year}}{5400\frac{kg}{day} \times 365 days/year} \tag{84}$$
$$= 0.04 AU\$/kg$$

2. Capital Cost of Soaking Tank (Scale-up)_

$$Cost\ of\ large\ tank = AU\$2145\ (\frac{(5.4 + 27)\frac{tonnes}{day} \times 1day}{\left(\frac{1{,}100}{1{,}000}\right)\ tonnes})^{0.6} \tag{85}$$
$$= AU\$16{,}327$$

$$PPC = AU\$16{,}327 \times Lang\ factor = AU\$65{,}308 \tag{86}$$

$$Annual\ Capital\ Recovery\ Costs = (16{,}327 + 65{,}308)\frac{AU\$}{year} \times CRF$$
$$= 13{,}307\ AU\$/year \tag{87}$$

$$Total\ Cost\ of\ soaking\ process = \frac{\left(\frac{72AU\$}{day} \times 365days + 13{,}307\right)AU\$}{\frac{year}{5400\frac{kg}{day} \times 365days/year}} \quad (88)$$

$$= 0.02AU\$/kg$$

3. Energy Cost – Boiler

$$Mass\ of\ water = 27tons = \ 2.7 \times 10^7 g \quad (89)$$

$$Energy\ Required = 2.7 \times 10^7 g \times 4.187\ \frac{J}{g\ ℃} * 80℃ = 9 \times 10^9 kJ = 2.5 \times 10^6 kWh = 900GJ \quad (90)$$

According to Australian Energy Regulator, 2023, the cost of natural gas here was taken as an average of AU$10.5 /GJ. The annual natural gas costs from boiler are $AU\$9{,}450/year$. A water cost of 2.6 AU$/ kL was be used here. The cost of water in boiler is 26,280 AU$ /year The total cost of the boiling process includes the cost of the boiler and the natural gas (as shown in following equation 89). The total costs of the boiling process is 0.04AU$/kg.

$$Total\ Cost\ of\ boiling\ \ process = \frac{(80{,}685 + 9450 + 26{,}280)AU\$}{\frac{year}{5400\frac{kg}{day} \times 365days/year}} \quad (91)$$

$$= 0.06AU\$/kg$$